EXPERIMENTAL INVESTIGATION ON THE BEHAVIOR OF RC BEAMS STRENGTHENED BY EXTERNALLY PLACED BFRP SHEETS

A dissertation submitted in the partial fulfilment of the requirements for the award of degree of

MASTERS OF ENGINEERING

IN

STRUCTURAL ENGINEERING

by:

PIYUSH GARG

Roll No. 801524019

UNDER THE SUPERVISION OF

Dr. Prem Pal Bansal

(Associate Professor)

Dr. Sahil Bansal

(Assistant Professor)

DEPARTMENT OF CIVIL ENGINEERING

THAPAR UNIVERSITY, PATIALA-147004, INDIA

DECLARATION

I, Piyush Garg, hereby declare that this dissertation entitled **"Experimental Investigation on the Behavior of RC Beams Strengthen by Externally Placed BFRP sheets"** in fulfilment of the requirement for the award ofDegree of Master of Engineering in Structural Engineering at Thapar University, Patiala, is an authentic record of my work carried out during a period from January 2017 to July 2017 under the supervision of **Dr. Prem Pal Bansal, Assistant Professor,** Department of Civil Engineering, Thapar University, Patiala and **Dr. Sahil Bansal, Assistant Professor,** Department of Civil Engineering, Thapar University, Patiala. This matter presented in this dissertation has not been submitted by me for the award of any other degree of this or any other University.

Piyush

Date: 31/8/2017

Piyush Garg

(Roll No.801524019)

CERTIFICATE

This is to certify that above statement made by the student concerned is correct and true to the best of my knowledge and belief.

Dr. Prem Pal Bansal

Associate Professor

31/8/17

Dr. Sahil Bansal

Assistant Professor

ACKNOWLEDGEMENT

I would like to express my sincere gratitude to my guide **Dr. Prem Pal Bansal, Associate Professor, Civil Engineering Department, Thapar University, Patiala**, and my co-guide **Dr. Sahil Bansal, Assistant Professor, Civil Engineering Department, Thapar University, Patiala** for giving me the opportunity to work with him and also providing excellent guidance and continuous assistance throughout the research work. His constant criticism, advice, assertions, appreciation were very vital and irrevocable, giving me the motivation without which it wouldn't have been possible for me to finish my dissertation. I have received endless support and guidance from him, right from the development of ideas, methodology of work and this presentation. I am thankful to him for his encouragement throughout the work.

I wish to express my gratitude to **Dr. Naveen Kwatra, HOD, Civil Engineering Department, Thapar University, Patiala,** who has been a constant source of inspiration for me throughout this dissertation work.

Special words of appreciation go to **Sh. Ram Sumiran, Sh. Virender** and other laboratory colleagues who helped me in my experimental work. I also sincerely appreciate the support of my friends and colleagues.

I am also thankful to all the staff members of Civil Engineering Department for their full cooperation and help.

At last, I thank my parents, whose love and affectionate blessings have been a constant support and source of inspiration in making this manuscript a reality. I render my gratitude to the almighty who bestowed self-confidence, ability and strength in me to complete this work.

PIYUSH GARG

M.E. STRUCTURAL ENGINEERING

THAPAR UNIVERSITY

ABSTRACT

The concept of using fibers to improve the various properties and characteristics of the concrete is very old. From the last two decades, the use of Fiber Reinforced Polymer (FRP) in civil and structural engineering is going on very large scale. Many researchers or scholars have conducted various experiments for the investigation of behavior of strengthening of beams with FRP for increasing the load carrying capacity in shear as well as in flexure. All new types of innovations of structural engineering are developing by using FRP composites. These innovations depend upon various parameters like the type of fiber using, the arrangement of placing of fiber, the pattern of loading, the type of composite materials and also on the bond behavior between FRP and concrete.

The focus of this research work is to study the behavior of externally placed Basalt Fiber Reinforced Polymer (BFRP) on the load carrying capacity of the RC beams. In the study, RC beams were casted as under-reinforcement beams and strengthened by providing BFRP strips in different orientation such as rectangular strips of BFRP, inclined strips of BFRP and fully U-wrap of BFRP and the effect of the same of behavior of beams were studied. For the validation of the experiment results, theoretical calculations were also made by using various analytical methods as mentioned in literature.

All the beams are of length 2050mm , width 135mm and of 270mm depth and provided with a reinforced of 2-12 mm bars in tension zone and 2-10 mm bars in compression zone. Tests were performed by using four point loading technique and for measuring the displacement, LVDT was placed at mid-point of the beam. After conducting the test, the results shows that the strengthen procedure by using BFRP sheet increase the first crack load by 10% to 46% and the ultimate load carrying capacity of the beams increased up to 36%. The stiffness of the beam strengthened with inclined strips was highest among all the beams. And the results of the analytical studies justified that the results obtained in experiment studies are correct and failure of the beams was according to the expectation.

TABLE OF CONTENTS

LIST OF TABLES

LIST OF FIGURES

CHAPTER-1 INTRODUCTION

1.1 General

Repairing and retrofitting of damaged and under standard civil structures are one of the important and biggest issues that civil engineers facing in present time. In the developed countries such as U.S.A, where approximate most of the development has completed and in the developing countries, where the resources for developing new structures are very limited, the concept of reusing of the old and damage structure by retrofitting them, is growing very fast.

For reusing that old and damage structure, the very first important step is to know about that how much repair is required or how we can retrofit it or how we can strength it. All the three terms i.e. repair, retrofit and strengthening are looking similar in name but have different meaning. If a structure is deficient in function due to several cracks and some structural component is damaged then various composite material is available for repairing it. In those cases, where the performance level of any structure relative to the required level is less then strengthening of that structure to increase its performance level can be done with the addition of the required composite. To increase the seismic facilities, retrofitting i.e. modifications applying on a structure to improve its performance, is available such as the useful nature of composite for the confining of beams or columns.

Initially, steel is used widely for getting the required strengthening and retrofitting of a structure. But in present time, fiber reinforced polymer (FRP) composites is a powerful and available alternate to steel. Since 1980s, civil engineers realized the importance of stiffness, specific gravity, durability, resistance to corrosion and importance of time of completing the structure so it encouraging the use of FRP for repairing, strengthening of structure.

There are generally two types of strengthening methods by using FRP are available and these models are strengthening by externally placed FRP and by near surface mounting i.e. NSM methods. Strengthening can be done by using a sheet or single layer of FRP or by using FRP rods at place of steel rods in RC structures. Instead of this, many scholars has attempted to use fiber as a replacement of steel stirrups for strengthening purpose. For using the FRP as a strengthening material, it is important to identify the various properties like mechanical strength and durability because the strength which is required depends on these properties of FRP. (Sim J. et al., 2005)

Strengthening of RC structures by externally placed FRP is in particular more attractive instead of those methods such as providing additional steel or use of high grade concrete, the cost of which is very high with respect to time. For extending the durability of historical monuments such as Vermont State House and Boston Public Library, with less interference to users, strengthening can be done by FRP composites. Furthermore, manufacturing techniques has revolutionized the technologies of fabrication for the production of FRP composites. These techniques are very useful in manufacturing laminates of good quality having minimum voids

and also having good alignment of fiber by using FRP composites materials. (Hollaway et al., 2008)

Concrete manufactured by using Portland cement is relatively stronger in compression strength as compared to its tensile strength and which makes it brittle. This weakness i.e. less tensile strength will be overcome by the using the steel reinforcement more conventional. Recently, interest in micro-reinforcement of different types as an alternative is increasing with great possibility. This development has gathered around two different types of micro-reinforcement:
1. Discontinuous fibers having random distribution and also of small length and diameter (to produce fiber reinforced concrete).
2. Continuous wire meshes having small diameter for making ferrocement.

For improving the fracture and mechanical properties of concrete, fibers can be include in the concrete and many scholars are investigating the effects of this inclusion of fiber in concrete on the basis of fiber types and contents. Inclusion of fibers in concrete influenced it and effect various properties of it and it is shown in many investigations that the fiber's inclusion in concrete increases the various properties of concrete like strength in tension, strength of flexural, impact strength , abrasion and fatigue resistance, increases its durability capacity, toughness and load taking capacity of RC structures after cracking. But the effect of this inclusion of fibers on concrete's compressive strength is a topic of debate because some scholars have observed the increment in the compressive strength of concrete with the inclusion of fiber while some scholars have observed the decrement in compressive strength but it is noticed that this inclusion has consequential effect on the compressive strength. (Ahmet B. et al., 2015)

1.2 Description of Retrofitting using Fibers

A fiber is a very small isolated reinforcing material manufactured from various materials like steel, basalt, plastic, glass, carbon and natural materials depending on its various shapes and sizes. These fibers can be amalgamated in concrete either by premixing, shotcreting or by using spraying techniques. Different types of fibers, different fabrication methods and different types of its uses are continuously developing. A numerical parameter which is used to describe a fiber is its aspect ratio, which is defined as the length of fiber divided by its corresponding diameter of fiber. (P. Hamelin et al., 2013)

Retrofitting using fiber can be done by using two methods.

1. Fiber Reinforced Concrete
2. Ferrocement

Fiber reinforced concrete (FRC) is a concrete mixture reinforced with continuous or discontinous randomly distribution of small fibers. In the FRC, there are random distribution of small fibers which are dispersed in the concrete, when mixing process is going on and in this way, it improve the various properties of concrete in all directions. These fibers transfer the load to the micro

cracks internally. FRC is successfully using in construction due to its excellent tensile strength, spitting resistance, impact and frost resistance and having good permeability. It also helps in resisting the shock and also helps in increasing the toughness and also resists shrinkage cracking of mortar.

Ferrocement which is also known as thin-shell concrete is a structure of reinforced mortar (lime or cement, aggregate and water) which is placed over the mesh of metal with fibers and steel rods of small diameter spacing closely and the metal which is used commonly is Fe or some other form of steel. It is useful in constructing comparatively having hard surfaces and structures in different forms such as boat's hulls, roof shell, and water tanks. Ferrocement was invented in France and which was also the foundation of reinforced concrete. Ferrocement also uses in different ranges which include sculpture and prefabricated building components. (Fiona Kelly et al., 2015)

Every polymer made from various similar or different monomers. Similarly, Fiber reinforced polymer is made from high strengthened fibers which embedded in a matrix form. Various different types of fibers are available like basalt fiber, carbon fiber, glass fiber etc. These fibers are further discussed in details in next section.

These fibers present in matrix form transfer stress from one fiber to fiber, hence to protect themselves from the environment and also to resist the forces due to abrasion or to resist the widening of cracks. If all fibers in a composite are in one direction then it is known as unidirectional. If it is oriented in different directions then it is multidirectional. The wire mesh reinforcement present in ferrocement improves its brittle properties and spacing in wire mesh increases its ductility property. As compared to reinforcing bars, it has high strength and its behavior is also linearly elastic up to failure.

Sometimes two or more fibers can be used together to obtain a desired property which is not possible while using single fiber. Such as, the modulus and strength of glass fiber can be increased by adding carbon fiber. Similarly, resistance against high temperature and shear strength can also be increased by adding basalt fiber.

To attach this matrix or mesh with concrete various adhesives are used. Some of them are epoxies, urethanes and acrylics. Epoxies have high bond strength and also high temperature strength as compared to acrylics, which has moderate temperature resistance. For applying these adhesives, first remove the cement paste by grinding the surface with the help of disc sander. The dust generated can be removed by air blower and proper care should be taken for doing this procedure. Among the all, epoxies have high mechanical properties i.e.

- High chemical resistance
- Easily attached to various fibers
- Low shrinkage while curing
- No volatile emissions

Fibers can strengthened various structural elements i.e. slabs, beams, columns, shear walls, chimneys, trusses and domes etc.

1.3 Types of Fibers

There are various types of fibers are available and there properties are shown in Table 1.1.

Table 1.1 Properties of Different Types of Fibers (Deniz et al., 2014) (Rizkalla etal., 2015)

Material	Density(g/cm^3)	Tensile Strength(MPa)	Specific Strength (MPa-cm^3/g)	Elastic Modulus (GPa)	Specific Modulus (GPa-cm^3/g)
Steel Rebar	7.85	0.5	0.0667	210	26.7
A-glass	2.46	3.31	1.35	69	28
C-glass	2.46	3.31	1.35	69	28
E-glass	2.60	3.45	1.33	76	29.2
S-2glass	2.49	4.83	1.94	97	39
Silicon	2.16	0.206-0.412	0.095-0.191	-	-
Quartz	2.2	0.3438	0.156	-	-
Carbon fiber (Large)	1.74	3.62	2.08	228	13.1
Carbon fiber (Medium)	1.80	5.10	2.83	241	13.4
Carbon fiber (Small)	1.80	6.21	3.45	297	16.5
Kevlar K-29	1.44	3.62	2.51	41.4	28.8
Kevlar K-149	1.47	3.48	2.37	40	-
Polypropylene	0.91	0.27-0.65	0.297-0.714	38	41.7
Polyacrylonitrile	1.18	0.50-0.91	0.424-0.771	75	63.6
Basalt Fiber	2.65	4.15-4.80	1.57-1.81	100-110	37.3-41.5

1.3.1 Steel Fiber

Steel wire is manufactured with the help of hot and cold working methods. Steel fibers of round shape are manufactured by cutting or splitting the wire, which has diameters in the range from 0.254 to 0.762 mm as shown in Figure 1.1. Sheet fibers of flat shape have cross sections in the range 0.0060 to 0.016 inch in thickness and 0.248 to 0.89 mm in width is manufactured by shearing of sheets. Fibers have also been produced from hot melt extract. Long individual fibers, if not added properly by sifting through a screen, have given trouble in the past by clustering together, often making uniform distribution in the matrix difficult. This problem is now avoided by using fibers that have a low aspect ratio (length over diameter) and have been deformed by crimping. Deformed fibers which are bonding loosely with glue soluble in water to make a bundle are also available. Such fiber bundles separate during the mixing process. Because the

failure of FRC is caused due to pulling out of fibers and for increasing the pullout strength deformed fibers are used and which also increases the mechanical properties of the composite.

Reinforce concrete made with steel fiber is an amalgamated material which is manufactured from concrete mix and steel fibers as a reinforcement. The steel fibers, which are uniformly distributed in the cementations mix .This mixture has various volume fractions, different geometries, random orientations and excellent material properties. (Mazumdar et al., 1977)

Generally steel fiber reinforced concrete is ductile in nature and suited well for those structures which required particularly:-

- High strength for resisting impact and shock loads
- Resist concrete to shrink
- High flexure and tension strength
- Destruction and abrasion resistance
- Resistance to high temperature
- Resistance to earth quake

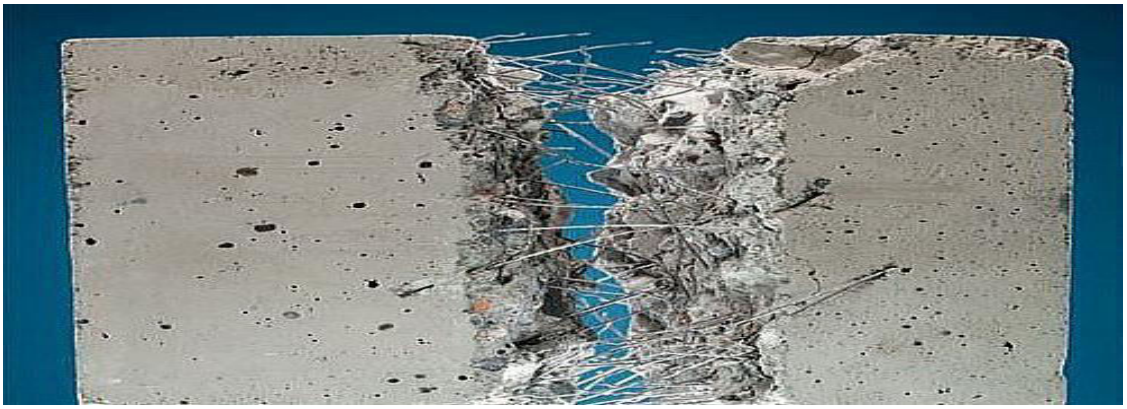

Figure 1.1 Steel fiber (Compositesworld.com)

The efficiency of the fiber distribution depends on the geometry of the fiber, the fiber content, the mixing and compaction techniques, the size and shape of the aggregates and the mix proportions.

Steel reinforced concrete (SRC) can be used in highway pavement, runways of airports, rebellious concrete and lining of tunnel by spraying FRC.

1.3.2 Polymeric Fiber

RC structures manufactured by using SRC normally suffer the problem of corrosion of the steel, due to which failure of those structures occurs. Regular maintenance and repairing is required for improving the durability of those RC structures. There are various different ways to diminish the failure of the RC structures manufactured by SRC. The convention method is to bond the

polymer fiber composites with the structure adhesively as shown in Figure 1.2. This composite helps in increasing the toughness and strength in tension zone and also improve the cracking and deformation physiognomies of the resultant composite. But use of this method also adds another layer, which is disposed to degradation.

These FRC also have a problem to ache from degradation when it is exposed to nautical environment because of surface scorching. As a result of that, the adhesive bond strength is reduced and because of that de-lamination of the composite occurs.

To improve the properties i.e. homogeneity of the concrete, uniform distribution of fibers in the concrete is the right choice. It also helps in reducing absorption of water, provides higher impact resistance, heightened flexural strength and strength of concrete in tension zone. Bureau of Indian Standards (BIS) and Indian Road Congress has recognized the use of polymer fibers with concrete. (Thaumaturgo et al., 2005)

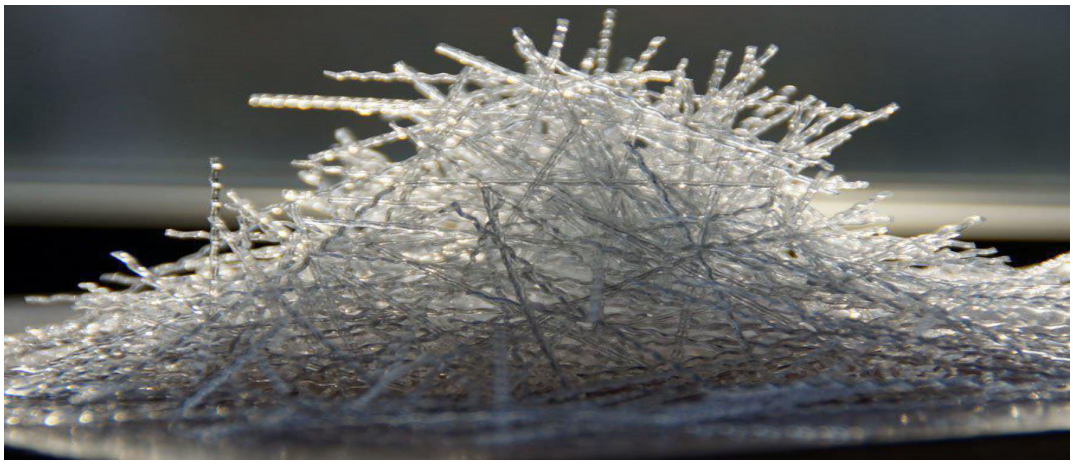

Figure 1.2 Polymer Fiber (Bautech.eu)

Plastic fibers such as nylon and polypropylene have high tensile strength, 561.0-867.0 N/mm^2, but their low modulus precludes any reinforcing effort. However, their elongation (15-25%) enables the composite to absorb 10 to 25 times energy than unreinforced mortar and concrete. In applications requiring high energy absorption plastic fibers have a special advantage.

1.3.3 Glass Fiber

Glass fiber produced in three basic forms, namely- ravings, strands and woven or hewed strand mat. The individual filament vary from 10 to 20 micron and are coated with sizing to protect the fiber from surface abrasion as well as to bind them into a strand as shown in Figure 1.3.

Glass fiber–reinforced concrete is (GFRC) fundamentally a composition of concrete which composites of material like cement, aggregates, water, and plasticizers, in which glass fibers of small length are dispersed. Inclusion of glass fibers in composites result in improvement of tensile and impact strength of the material. GFRC was using from a period of more than 30 years

in structural elements but it was not so widespread at that time, mostly in non-structural ones, e.g. facing panels used in fluting for sanitation network systems, enhancing non-recoverable formwork, and other products. (Mini K. M. et al., 2017)

On the initial stage of the GFRC development, out of the most significant problems, the main problem was the toughness of the glass fiber, because alkalinity of the mortar made it more brittle with the passing of time. But after some experiments, momentous improvement have been made, and in present time, this problem is well-nigh solved because of new types of alkali-resistant glass fibers and by the use of mortar additives, it prevents the process of embrittlement of GFRC**.**

With the spray up process it is possible to incorporate higher volume (6%) and length (2 inches) of fibers with a low water-cement ratio matrix (0.4) and obtain a superior composite. In this process, both the chopped glass fibers and the cement slurry are sprayed with pressurized air onto a surface. If the process is done in a factory then the excess water can be removed by applying suction.

Figure 1.3 Glass Fiber (Textilelearner.in)

Applications of glass-fiber- reinforced concrete or mortar include a variety of precast products, curtain walls and surface bonded masonry construction.

1.3.4 Natural Fiber

Organic fibers include synthetics such as polypropylene or natural fibers such as sisal as shown in Figure 1.4. Organic fibers are lighter in weight and also more chemically inactive than steel and glass fibers. They also may be more economical, especially if they are natural. However these fibers produce lower bond and a lower modulus of elasticity than mineral or metallic fibers; consequently, when they are used in proportions similar to the other types of fibers they do not improve concrete strength properties as much. (Parameswaran et al. 2001)

The natural fibers are basically of four types:

1. Bast or Stem fiber (jute, flax, san etc.)
2. Leaf fiber (Sisan, henqueen)
3. Fruit fiber (coir)
4. Wood fiber (bamboo, reeds)

The natural fiber is used as reinforcing medium not only in cement matrices but also in soil cement construction, it provides a wide range of flexibility in its use because they are not only easily available but also cheap in price. But natural fiber has low elastic of modulus and also absorbs high water, susceptibility to fungal and very prone to insect attack, minimum alkali resistance from the cement concrete are the commonly disadvantages of using natural fibers.

Figure 1.4 Natural Fiber (Chaircone.com)

1.3.5 Carbon Fiber

Carbon fiber also known as graphite fiber is consisting of fibers having diameters of 5–10 micro meters and consists generally of carbon atoms as shown in Figure 1.5. To manufacture carbon fiber, the atoms of carbon are bonded together to form crystals that are more or less aligned parallel to the long axis of the fiber as the crystal alignment gives the fiber high strength-to-volume ratio (making it strong for its size). Several thousand carbon fibers are bundled together to form a tow, which may be used by itself or woven into a fabric.

The properties of carbon fibers, such as high stiffness, high tensile strength, low weight, high chemical resistance, high temperature tolerance and low thermal expansion, make them very popular in aerospace, civil engineering, military, and motorsports, along with other competition

sports. However, they are relatively expensive when compared to similar fibers, such as glass fibers or plastic fibers. Carbon fibers are usually combined with other materials to form a composite. When combined with a plastic resin and wound or molded it forms carbon fiber reinforced polymer (often referred to as carbon fiber) which has a very high strength to weight ratio, and is extremely rigid although somewhat brittle. (Sobuz et al., 2011)

Carbon fiber composites have shown 20% reduction in strength over a period of one year, when cured continuously in water at 50^{o}C. With about 4% volume of fraction of continuously unidirectional aligned fibers. Carbon fiber composites have about 1.5 times the modulus of elasticity. At low fiber fractions, the fracture toughness of fiber is low and not much higher than that of the matrix and is considerably lower than that of the glass fiber composites. (Sobuz et al., 2011)

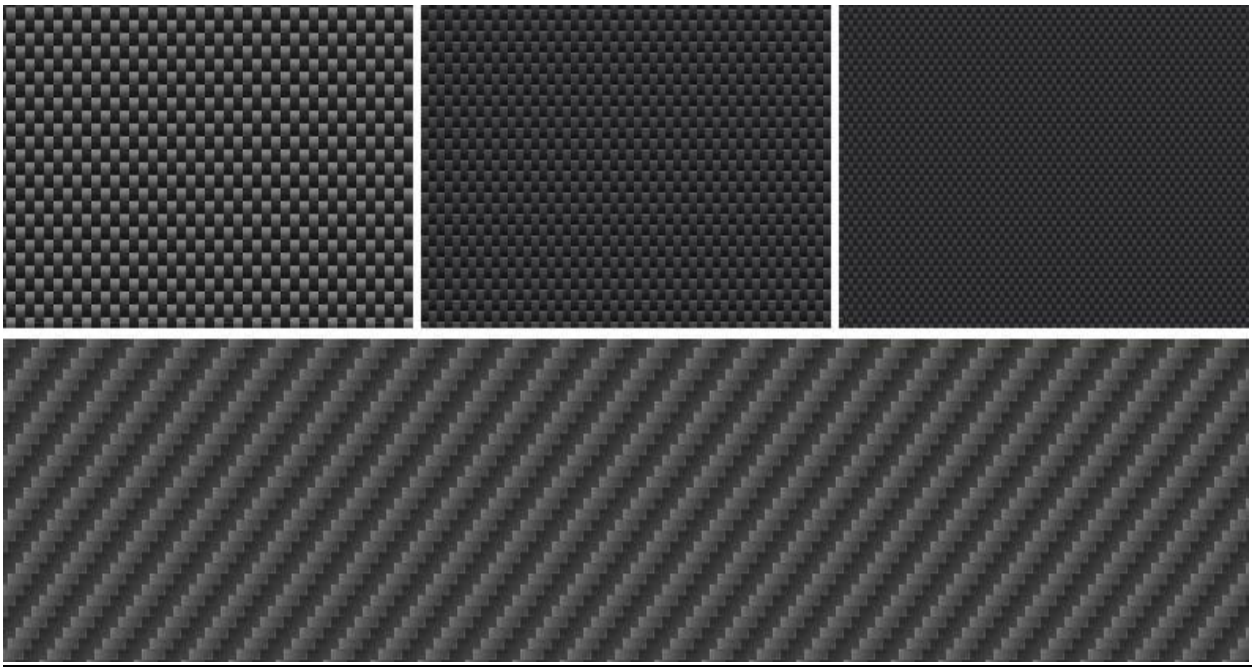

Figure 1.5 Carbon Fiber (Compositestoday.com)

1.4 Basalt Fiber

Basalt Fiber as shown in Figure 1.6 is a new type of inorganic fiber manufactured by the extrusion of melted basalt rock. The Basalt fiber is somewhat more economical because no any other additives present in it. It is known that the tensile strength of basalt fiber is superior to E-glass fiber, and has greater failure strain than the carbon fiber and also has good resistance to chemical attack, impact load and fire with less poisonous hazes. Because of that, Basalt Fiber has a potential to be an appropriate replacement for glass, steel and carbon fibers in many construction applications. Earlier studies showed that the effect of addition of basalt fiber significantly increases the tensile strength and also reduces the brittleness, and increases the toughness, deformation resistance and modulus of rupture of concrete. (Ahmet et al., 2015)

Figure 1.6 Basalt Fiber (Basalt.today)

It was examined experimentally that the use of basalt fiber enhances various mechanical and flexural properties and also increases durability. In concrete bridge deck slabs, the use of basalt improves corrosion resistance and can also be uses as reinforcement in geopolymeric concrete. The basalt fiber also helps in confinement of concrete bonded with cement mortar, which removes various problems related to epoxy based fiber reinforced polymer (FRP) laminates. Basalt fiber can also be used as composite such as for the confinement of columns hybrid glass-basalt FRP laminates performs superior than glass fiber reinforced polymer (GFRP) laminates and also helps in increases resistance to corrosion in sea water. It also helps in delaying the process of debonding, by using NSM basalt bars with externally bonded reinforcement. Basalt fibers can be considered as a suitable alternative to glass in underwater applications. The beams strengthened with basalt FRP also perform superior in comparison to glass FRP when these beams were exposed to elevated temperatures as shown in Table 1.2. Basalt textile-reinforced mortar layers also helps in increases the shear capacity of RC beams. The composite of Steel wire with basalt fiber reinforced polymer was used to extend the fatigue life of steel beams. (Kelly et al 2015)

Basalt fibers manufactured from basalt rocks with the help of melting process. Firstly, the basalt rocks divided into small particles so that fibers can be easily produced from it. In addition, there are no preservatives present in basalt fibers, due to which the cost of this is very less and which makes an additional advantage of it. From these advantages, it is highly expected that the basalt fiber has a great application for a structural strengthening material.

Basalt fiber also has admirable resistance to alkali, and provides superior properties to glass, and available at a lower cost than carbon or aramid fibers. As basalt fiber found in volcanic rocks, it is a natural material and because of that it has a melting point of about 1400°C, and available all over the world different chemical compositions. It is mostly used in construction, and has various applications in highway engineering and is also used to cast moulded parts. The density of basalt

fiber is roughly 5% of glass fiber. The basalt fibers also have elastic tensile modulus (82-110GPa) greater than E-glass fibers (70- 75GPa). The low elongation, effortlessly elastic up until rupture, which results in fabrics having high levels of dimensional stability that provide valuable suppleness and good fatigue resistance. (Hui Li et al., 2015)

Table 1.2 Comparison Between Thermal Properties of Fibers (Hui Li et al., 2015)

Properties	Asbestos	Basalt	Glass	Carbon
Thermal resistance, ^{o}C	500	700	460	300
Melting temperature, ^{o}C	1550	1450	1060	1000
Breaking load for the yarn of 500 tex, N				
at 20 ^{o}C	12	145	100	155
at 400 ^{o}C	104	75	52	60
at 500 ^{o}C	0.5	12.2	10	11
Density, g/cm³	2.5	2.8	2.5	1.75

Table 1.3 Technical Specifications of the Basalt Fiber (Taylor et al., 2016) (Zhu et al., 2016)

Density by area	233 g/m^3
Side length of cell	25 mm
Average thickness	
- Uniaxial tension	0.0424 mm
- Biaxial tension	0.0848 mm
Working temperature rage	-260 to +800^{o}C

Basalt fiber	
Ultimate tensile strength	2100 - 5000 MPa
Tensile elastic modulus	89 GPa
Ultimate tensile strain	3.145%
Density	2.75 g/cm^3

Basalt Textile	
Design thickness	0.0349 mm
Opening size	25 x 25 mm
Weight of the dry sheet	233 g/mm^2
Ultimate tensile load	4040 N
Ultimate tensile strength	1160 MPa
Ultimate tensile strain	1.82%
Young modulus in tensile	67 GPa

Furthermore, basalt fibers also have good acidic resistances, exceeding those of E-glass and different other mineral and synthetic fibers. They also have brilliant resistance to alkalis, while they are marginally less stable than glass in strong acids. Basalt fiber also loss weight loss in boiling water. The inert basic material provides good resistances to UV-light and biologic contamination. Basalt fiber absorbs less humidity and it is less than 0.1% at 65% relative air humidity. Basalt fibers have excellent bonding ability to a broad range of binders, coating compounds and matrix materials in composite applications. The technical specifications of the basalt fiber are shown in Table 1.3.

1.4.1 Evolution of Basalt Fiber

Basalt is a form of igneous rock and created by the cooling of lava at the surface of a planet. It is a most common rock in the Earth's crust. The characteristics of basalt rock vary due to different sources of lava, rate of cooling, and historical exposure to the elements. Basalt deposits having uniform chemical makeup provides fibers of high quality.

There are eruptions of lava of enormous quantity from the center of the Earth from last millions of years. When this lava comes in contact to atmosphere then due to cooling process, it creates the first continent of the planet i.e. the Pangaea. With time, new eruptions and still unknown phenomenal had divided the first continent in the today's structure.

The sphere is a thin layer presented in Earth mantle, when this thin lava comes in contact with superficies it create the basalt Rock, many great canyons and natural sculptures are present on Earth made in basalt by the nature.. The chemical composition of basalt rock is shown in Table 1.4.

Table 1.4 Chemical Composition of Basalt Rock (Young Moon et al., 2005)

Chemical Compound	% weight of basalt
SiO_2	49.58
TiO_2	2.08
Al_2O_3	14.48
Fe_2O_3	4.42
FeO	9.43
K_2O	1.89
Na_2O	2.10
MgO	5.10
CaO	8.50
MnO	0.17

Despite the fact, basalt of high quality can be found easily in the nature; volcanoes keep on throwing tons of lava which strengthened the concept of Advanced Basalt Fiber as a high technology and green composite.

Paul Dhe made the first attempt to manufacture basalt fiber in the United States in 1923 and he was granted U.S. Patent no. 1,462,446. After World War II, different products from basalt fiber were manufactured by researchers in the USA, Europe and the Soviet Union especially for military and aerospace used. Since 1995, the use of basalt fibers has been increasing in civilian applications. The first patent revealing the technique of manufacturing basalt fiber is by a French scientist in the US field in the year 1923 and afterwards the research was started in the United States of Soviet Russia (USSR).

The technology of manufacturing of basalt continues fibers (BCF) was conducted in the USSR; it had a status of closed scientific programs. Because of that, they had no contacts with scientists and engineers from abroad. These efforts of developments are for defense and aerospace applications. In 1956-61, the first samples of BCF were received at scientific research institute in Ukraine of USSR, but the initial industrial equipment was very expensive and consumes very large energy. After disassembling of USSR in 1990's .this technique was made available to others. To lower the cost and commercial use, many efforts are taken. (Benmokrane et al., 2016)

1.4.2 Advantages of Basalt Fiber

1. The basalt fiber reinforced concrete increases the impact strength by about 20 times of reinforced concrete. (Zhong et al., 2013)
2. Three-dimensional concrete reinforcement is provided by basalt fiber while rebar provides only two-dimensional reinforcement. (San-Jose et al., 2014)
3. Basalt fiber is not responsible for galvanic corrosion, while usual rebar is an electrical conductor and also provides the cathode effect. (Urbanski et al., 2015)
4. It also reduces construction time due to no need of installing wire mesh. (Rizkalla et al., 2015)
5. It also reduces the thickness of the concrete layer by half amount.
6. It mixed easily with the concrete. (Rizkalla et al., 2015)
7. The basalt fiber reinforced concrete also increases the fatigue strength by 35%.
8. It also reduces the width of cracks.
9. Basalt fiber reinforced concrete reduces the thickness of concrete cover in reservoirs and underground water channels.
10. It also reduces the maintenance and repairing cost due to its last long life. (Zhong et al., 2013)
11. The melting point of basalt fiber is 1450^{o}C because of that it can't lose its strength at higher temperature. (Hui Li et al., 2015)

12. Basalt fiber is environment friendly and is easily available because of naturally occurring material.
13. It can mill easily with the help of milling equipment. There is no problem of stretch and pull as polymer.
14. Increased frost resistance (up to 35%)
15. It also increases the endurance of concrete (up to 70%)
16. The use of basalt fiber in concrete decreased damages of corners and edges (up to 90%).

1.4.3 Disadvantages of Basalt Fiber

1. The compressive and tensile strength of basalt fiber reinforced concrete is 10-15% and 5-10% less than that of carbon fiber reinforced concrete respectively.
2. The use of basalt fiber in concrete decreases its workability.

1.5 Advantages of Fiber Reinforced Polymer

1. For the same cross sectional area fiber reinforced polymer has three times the ultimate strength of steel.

2. The density and weight of FRP is 20% and 10% of the steel having same cross sectional area.

3. Due to less in weight, it is easy to handle and also to transport FRP.

4. It is difficult to use more than one layer of steel at a particular point, while it is easy to use more than one layer of FRP for strengthening of a particular point.

5. Surface preparation for attaching FRP with concrete is very simple as compared to steel where grit blasting is required.

6. As the thickness of the FRP sheets is very less so it decrease the depth of the strengthening system, which provides extra space i.e. extra headroom space.

7. FRP sheets have high resistance to corrosion as compared to steel or any other sheets. So it can be used in every environment where use of steel is not possible.

8. FRP sheets are also low conductor of heat, so for longer period it is more effective.

9. Water absorption of FRP sheets are negligible so there are no chances of freeze or thaw damage.

10. It is not only easy to use FRP but it also reduces the construction time.

11. FRP sheets also reduce the maintenance cost because FRP sheets don't requires any type of maintenance so reduces the overall cost of the project.

1.6 Disadvantages of Fiber Reinforced Polymer

1. The price of FRP sheets is very high on comparing it with steel sheets having the equivalent load carrying capacity.

2. FRP sheets can easily damage as compared to steel by knife, axe etc. so it can't kept open where it is accessible to public.

1.7 Applications of Fiber Reinforced Polymer

1. FRP sheets can use as a strengthening material for beams by using u-wrap of sheets or wet lay-up sheets. Smith and Teng et al., 2002, had found out that FRP was effective in strengthening of beams in flexural.

2. FRP are also useful in recovering the strength of slab and also increases its stiffness.

3. In case of columns, FRP are very useful in anchoring the columns with the adjacent beams with an U-anchor system.

4. FRP laminates can also be useful for the strengthening of beams and columns in shear by bonding it with the sides of the members.

1.8 Analytical Methods of Calculating Shear Strength of FRP

There are many analytical or mathematical methods or models for calculating the shear strength of the RC beams strengthened with fiber reinforced polymers. Various researchers have given different methods or have done different theories on these models for calculating the shear capacity. Different codes of different countries also providing the whole concept of these models and these models are given below:

1. ACI 440 model of America provides a complete guidance for the designing and calculating the shear strength of the FRP strengthened specimens. (Colotii et al., 2016)

2. CAN/CSA S806 is Canadian code for the designing and construction of RC specimens strengthened with Fiber Reinforced Polymer. The equations of this code were based on another Canadian code i.e. CAN/CSA A23.3. (Acun et al., 2013)

3. CAN/CSA S6-06 is another Canadian code for the designing of highway bridges and also provides procedure of strengthening of RC structures with FRP. (Acun et al., 2013)

4. Fib.TG 9.3 is the European code for the use and designing of RC structures bonded with FRP externally. (Triantafillou et al., 2000)

5. JSCE also recommends the strengthening of RC structures with continuous FRP but there methodology depends on the performance criteria. (Acun et al., 2013)

6. ISIS is the manual for strengthening of RC structures with FRP provided by Intelligent Society of Canada. (Acun et al., 2013)

7. The technical report number 55 of the British society of Concrete also provides the guidelines for the RC structures strengthened with FRPs. (Acun et al., 2013)

8. NCHRP 68 is also another report on designing of RC girders in shear strengthened with FRP composites. (Acun et al., 2013)

All these analytical models are based on various parameters which included stiffness of fiber, properties of different materials used in concrete and FRP, types of application of FRP, bond strength between concrete and FRP, development length and different failure modes. As the parameters on which these codes depends are very high but the procedure mentioned in these codes are very simple to use.

1.9 Objectives of Thesis

The main objectives of this thesis are:

1. To investigate the behavior of RC beams strengthen by externally placed BFRP sheets.

2. To investigate the effect of different arrangements of placement of BFRP sheets on the RC beams.

3. To validate the results obtained by conducting experiments with the results from analytical methods.

1.10 Orientation or Outline of the Thesis

This thesis is described in the following five chapters:

Chapter-1 Introduction presents the brief introduction about the retrofitting using fiber, fiber reinforced polymer, types of fibers, advantages and disadvantages of basalt fiber, advantages and disadvantages of fiber reinforced polymer and its applications.

Chapter-2 Literature Review presents the information about the research work already done by different scholars and their methods of not only applying the loads and also the type of FRP they used and in which manner they have applied that and from that what they achieved.

Chapter-3 Experimental Program presents the information about the materials used for the casting purpose of the specimens. It also provides the information about the design of beams and how it casted and how much curing period is set up for the curing of the beams so that fully satisfied results will achieved and how curing was done.

Chapter-4 Results and Discussions presents the information about the strengthening behavior of the BFRP sheet under different arrangements on the first crack load, ultimate load carrying capacity and the stiffness of the beams and also presents the information about the comparison of experimental results with the results obtained from analytical methods for justification of the results.

Chapter-5 Conclusions presents the brief information about the various conclusions and the different effects of BFRP on the strengthening of beams.

CHAPTER-2 LITERATURE REVIEW

2.1 Introduction

This section explains the existing work of some researchers in strengthening of RC specimens by using externally bonded FRPs. The strengthening of beam can be done in two faces, first is strengthening of beam in shear and second one is strengthening of beam in flexure. Beams can be strengthened in shear by externally bonded FRPs either along the entire section of the specimen or along the sides and soffit of the beams i.e. U-jacketing or along the sides of the beam i.e. side bonding. Many scholars or researchers have studied this strengthening behavior of FRP in beams. Their findings and results are highlighted in the following section.

2.2 Finding of Researchers

Gao Ma et al., (2017) had studied the seismic analysis of predamaged reinforced concrete columns strengthened by using basalt fiber reinforced polymer. They had choosed two levels of damaging i.e. damage at moderate level and severe damage to the R.C. columns by cyclic loading. While the retrofitting process, the displacement and axial load were kept constant. These specimens were tested again at room temperature after providing required epoxy and mortar curing. The energy and ductility dissipation capacities of retrofitted predamaged RC columns with fiber reinforced polymer were improved greatly after BFRP wrapping. The flexural strength of the moderate predamaged RC column was restored fully while it was partially restored for the severe predamaged columns.

Hamelin et al.,[2013] had investigated a hybrid solution for repairing and strengthening of RC beams. Five RC beams 15cm wide and 25cm depth has a length of 2300mm and clear span of 2000mm were casted. The reinforcement steel was 2-12mm rebars at bottom and 2-8mm rebars at top and for shear strengtheneing 28-6mm rebars were provided. For this investigation, three beams were loaded before strengthening and load was applied until longitudinal steel was not yielded. The load was controlled with the help of strain gauge. Then these beams were strengthened by textile reinforced polymer. The test details is shown in the Figure 2.1. These beams were tested by using four point loading and load was applying at an interval of 600mm. The load cell used to measure the load had a capacity of 200KN and displacement was measured with the help of a LVDT placed at the center. They observed that axial stiffness of reinforcement manages the overall behavior of repaired and retrofitted beams and they found that increase in stiffness increases the stress transfer between the internal and external reinforcement.

Mahaidi et al., (2006) had investigated the strengthening of RC beams in both shear and flexure by using CFRPs straps. Six RC beams having 140mm width, 260mm depth and rebars are shown in Figure 2.2. They kept one reference beam for comparison while the other beams were strengthened with CFRP sheets either for strengthening in flexural or for shear strengthening or for both. Two beams were tested in four points loading with over- all length of 2300mm and shear span of 700mm and all other beams were tested in three point bending as shown in Figure

2.3. Load was applying on the beams by using Instron universal testing having a capacity of 250 KN with a loading rate of 0.5mm per minute. They found that CFRP straps increases the shear strength of the beam and debonding failure was prevented by providing extra anchorage for CFRP sheets. The CFRP straps also decreases the interface slip between sheets. They also noticed that 95% of flexural was observed when CFRP straps anchored to CFRP sheets.

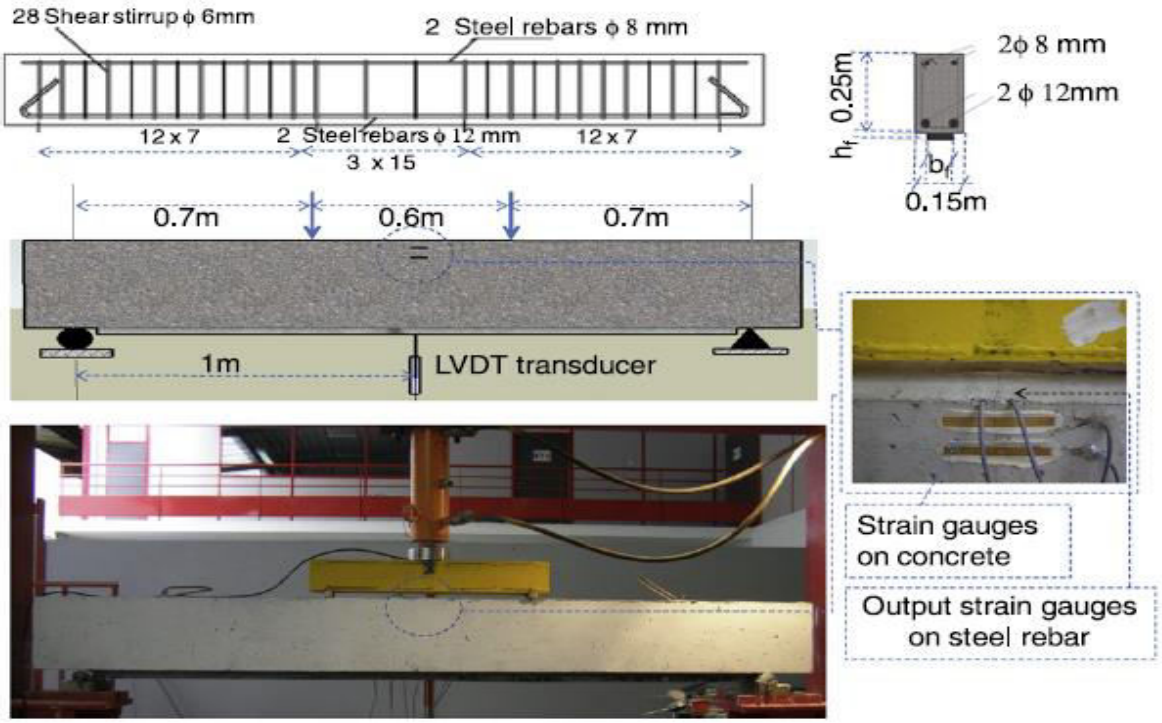

Figure 2.1 Test setup and sensors for the analysis of beams [Hamelin et al.,(2013)]

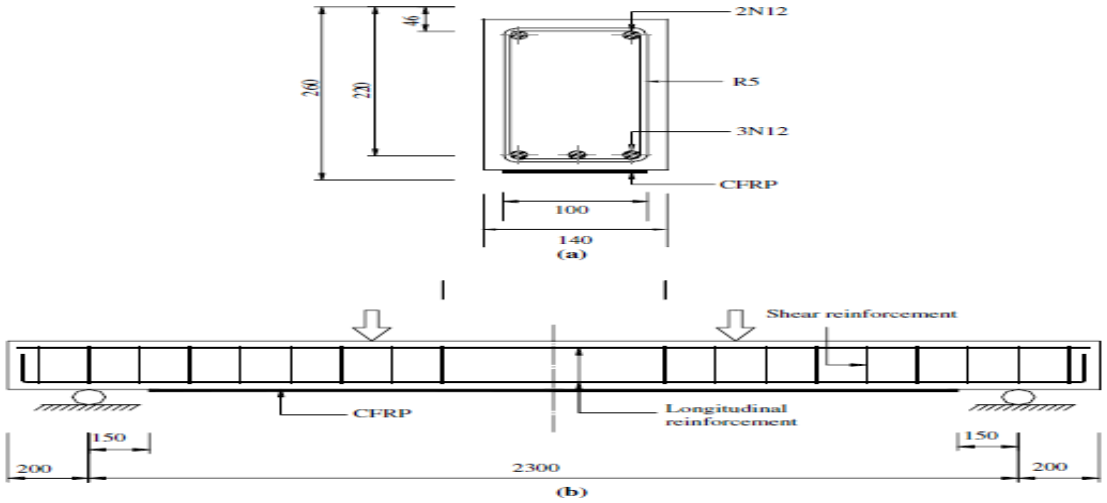

Figure 2.2 Four point bending test set up of beams [Mahaidi et al., (2006)]

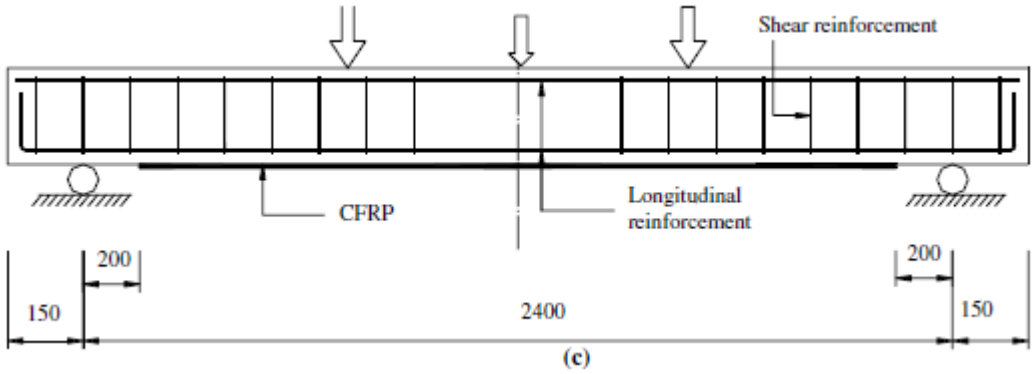

Figure 2.3 Typical Details for Beams and Their Test Setups [Mahaidi et al., (2006)]

strength was observed when CFRP straps anchored to CFRP sheets and only 15% of increase was noticed when only CFRP sheets were used. The main failure mode was the ductile flexural failure due to the yielding of steel.

Leung et al.,(2017) had studied the effect of shear span–depth ratio on the strengthening of RC beams in shear by using U-wrap FRP strips. They had casted twelve beams out of which six are normal beams and six are shear strengthened beams, having a/d ratio from 1 to 3.5. The beams were of length 2000 to 2400mm and the setup is shown in Figure 2.4. Short beams were prepared for a/d < 2.5 while long were for a/d > 2.5. 4-28mm bars were provided in bottom and 2-32mm bars were provided in top and shear stirrups of 12mm bars at 85mm spacing on one side and 6.5mm bars at 160mm spacing on other side so that the beam should fail in shear. Four point loading was applied on all the beams and load was controlled by a hydraulic machine with a displacement control rate of 0.01mm/sec.

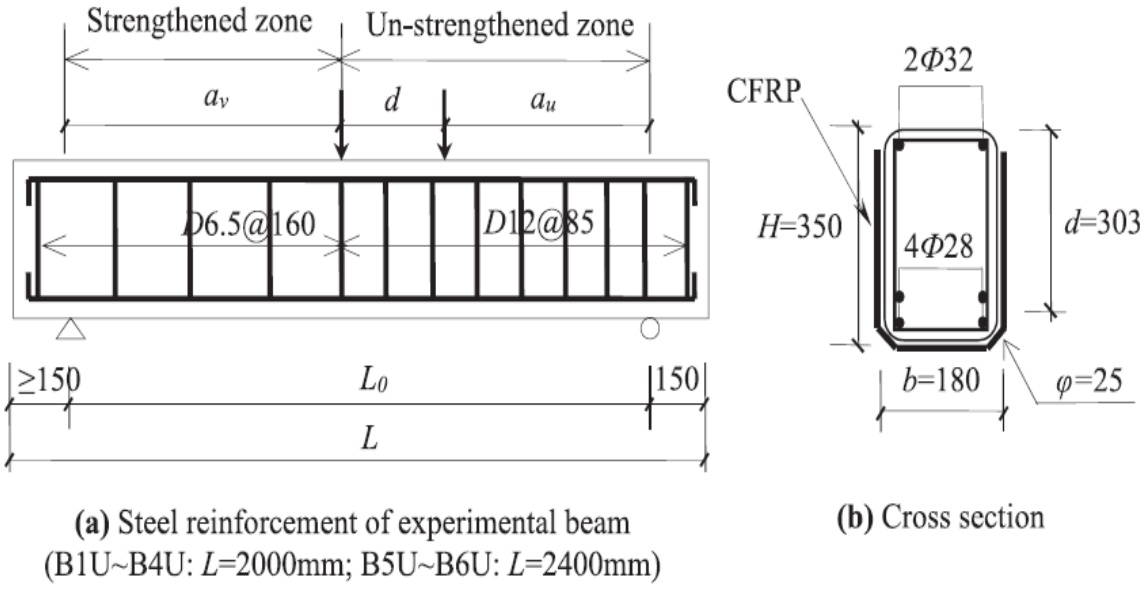

Figure 2.4 RC Beams Strengthened With U-wrap CFRPs [Leung et al.,(2017)]

They noticed that all the beams strengthen in shear were fail in shear and failure pattern was equal to that of the control ones but the shear capacity of strengthened beams were higher than that of the control beams. The FRP shear strengthened beams were affected by shear span/depth ratio and this affection shown by a parabolic shape with increasing a/d ratio from 1 to 3.5, so they concluded that FRP strips were more effective for medium a/d ratio as compared to high a/d ratio and least for low a/d ratios. Failure of FRP in debonding either happenes instantly or without warning and also there were sudden drops in curve of deflection vs shear force of the beam and FRP strips either debonded partially or fully.

Yazdanbakhsh et al., (2016) also studied the effect of FRP on the strengthening of RC beams but they used recycled concrete aggregates. They investigated that the shear capacity of FRP strengthened RC beams with recycled concrete aggregates was higher than that of the RC beams with natural aggregate. For this, they casted beams having cross section of 100 X 150mm and 914mm length and three point loading was used to apply load on the beams with a clear span of 813mm. They applied 100mm wide FRP fabric on the soffit of the beam and FRP straps of 50mm wide at a spacing of 125mm was laid down. Displacement was measured by using two strain gauges close to the mid span of beam and two strain gauges also connected in longitudinal direction for flexural strengthening. Their investigation that the shear capacity of FRP strengthened RC beams with recycled concrete aggregates was higher than that of the RC beams with natural aggregate, was because failure in FRP strengthened beams were due to debonding of flexural strips. And the flexural strips combined with shear strips provided a better confinement when there where increase in stress due to widening of shear cracks.

Hadi et al., (2003) had also done a research on retrofitting of RC beams failure in shear by using FRP. Sixteen beams with area of cross section of 100 X 150mm and having a length of 1.2m each as shown in Figure 2.5. Then the retrofitting was done by using various FRPs and these beams were again tested for getting the desired results. All the beams were subjected to four point loading with a loading rate of 0.05mm/sec and four strain gauges were used to measure the displacement. When the test was conducted, they noticed that beams were not achieving its fully flexural capacity and weak in shear. So for getting this, FRP sheets were wrapped and extended 50mm from shear span. They noticed that helical reinforcement increases the load carrying capacity and also flexural strength and also helical reinforcement had no effect on the shear failure of beams. As the layers of applied FRP increases, flexural strength also increases. The beams strengthened with CFRP had 31% strength as compared to GFRP. The shear capacity of beams retrofitted by GFRP was 17% more than that of original ones.

Benmokrane et al., (2016) had tested the basalt fiber polymer bars in concrete for increasing its load carrying capacity. Six concrete beams with BFRP bars as reinforcement were casted. Each beam was 200mm in width, 300mm in depth and 3100mm in length as shown in Figure 2.6. BFRP bars were of size 10, 12 and 16mm having surfaces coated with sand. All the beams tested under four point loading with a clear span of 2700mm and shear span of 1100mm. The loading

rate for applying load was 1.2mm/min. LVDTs were placed at the crack location of first three cracks to measure the crack width electronically.

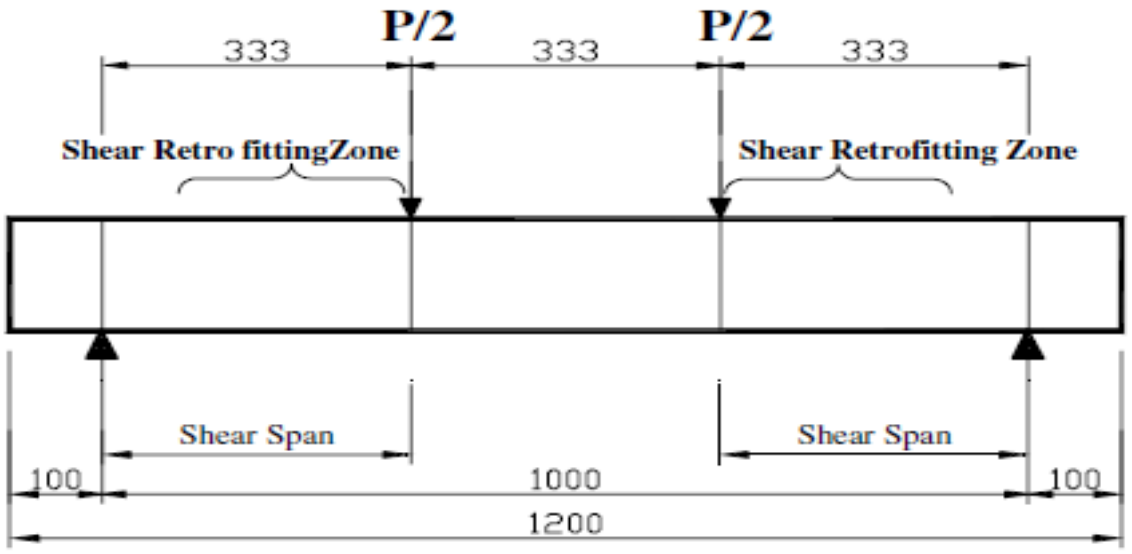

Figure 2.5 Shear Strengthening Configuration [Hadi et al., (2003)]

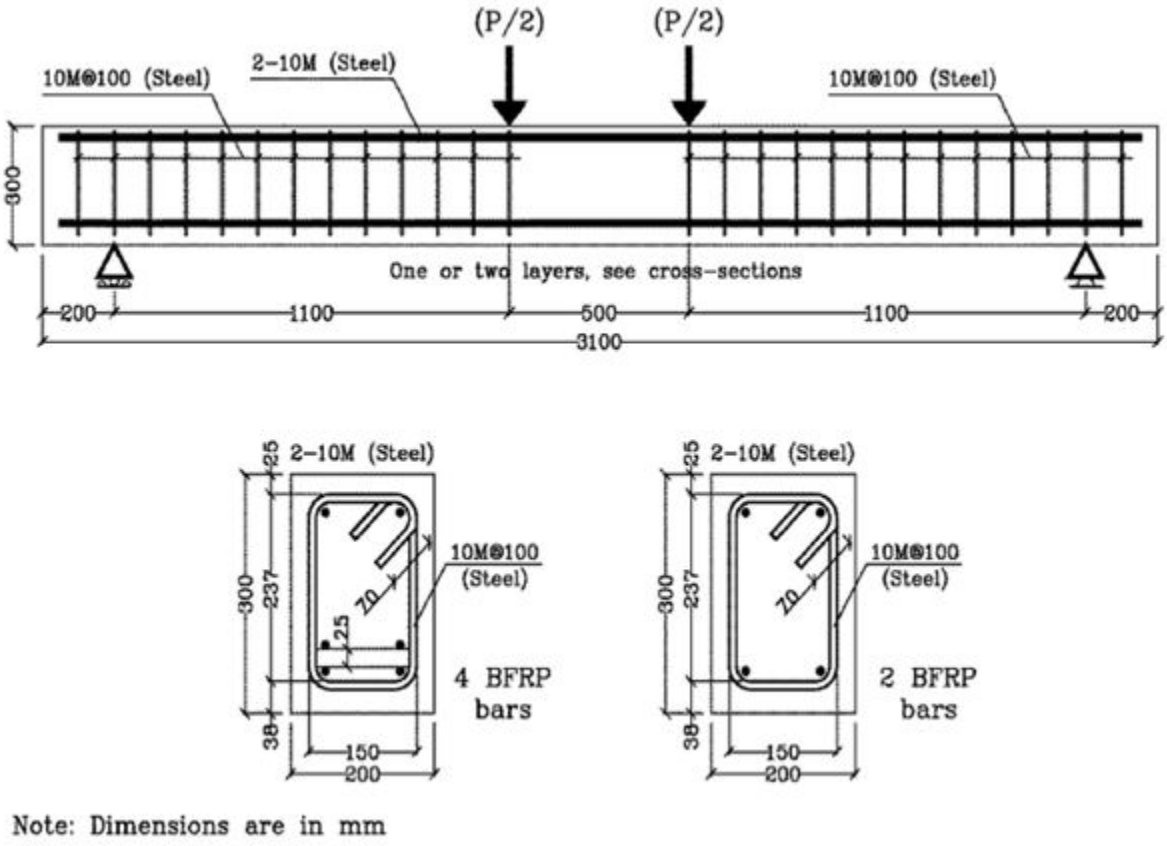

Figure 2.6 Reinforcement Details of Tested Beams. [Benmokrane et al., (2016)]

The deflection of beam subjected to flexural moment was divided into two stages. In first, no cracking occurs and in second, where applied moment increases cracking moment then the cracks propogates due to which stiffness reduces. The reinforcement ratio hadn't affected the pre-cracking response and cracking load of all the beams. After crack occurs, increment in stiffness and decrease in reinforcement strain was proportional to reinforcement ratio. Beams with low reinforcement showed large increment in strains and deflection at cracking. Deep crack occurs due to this increment in strains. And vice versa, the high reinforcement ratio decreases the strain at the same load. Hence, it showed that as the axial stiffness increases there was decrement in deflection and strain and lower in crack, which meant better performance.

Shameli et al., (2013) had conducted an experiment for analyzed the flexural strength of reinforced concrete beams by using external bonding technique by combing the NSM and EBROG wet layup procedure. In this, CFRP was laid on the grove surfaces which show that this EBROG method not only increases the load carrying capacity of reinforced concrete beams by 3% with one layer, 38% with two layer and 56% with three layer of FRP but this also eliminated the premature bonding of FRP sheets.

Shafiq et al., (2016) had studied the performance of BFRP and PVA reinforced beams which were subjected to flexural action. Twenty one reinforced beams were casted to perform this study. Area of cross section of each beam was 100 X 200mm with 1.5m in length. Three types of binders were used to make the reinforced concrete. In first, 100% cement was used and in second and third one, 10% silica fume and 10% metakaolin respectively with 90% of cement was used. All the twenty beams were categorized in three groups and out of seven beams, first one was the control beam. For completing the flexural beams, three point loading was used to apply the load on all the beams. UTM with a capacity of 500KN was used and loading rate was set at 0.001mm/sec. The test results of the experiment conducted shows that BFRP increased the flexural strength of the RC beams as compared to the beams casted with PVA fibers. But use of BFRP in structures was questionable because it didn't contribute in the post flexural behavior. They also noticed that the replacement of cement with silica fume and metakaolin had increased the flexural strength of RC beams when it compared with the RC beams having 100% cement content. Finally, they concluded that addition of both PVA and BFRP increased the strain capacity of RC beams.

Shen et al., (2016) had also investigated the use of basalt fiber reinforced polymer in RC elements. They did this investigation on RC shear walls instead of RC beams. Six RC shear walls with thickness of 120mm, height of 1600mm and length of 1000mm and having aspect ratio of 1.6 were casted. Two types of boundary elements were used. In first 110 X 150mm boundary element having an orthogonal grid of 8mm bars was used and in second 225 X 120mm Boundary element having an orthogonal grid of 10mm bars was used. Confinement was provided with the help of closed stirrups of 8mm placed at a spacing of 150mm c/c. Out of six beams, one was a controlled specimen while in next three beams BFRP strips of 200mm width were applied diagonally forming a X pattern and in next two beams three layers of BFRP strips of width

120mm and 1780mm in length were applied followed by two layers at 90 ^{o}. A constant axial load of 350KN was applied and maintained on the wall throughout the whole test. The load was applied in two phases, in first loading speed was 50KN/min with 30KN as a level till it reached 150KN i.e. force phase and in second loading speed was 18mm/min with 4.0mm as a level i.e. displacement control. In force one, only cycle was applied but in displacement control phase three cycles were applied. And in both the phase lateral load and displacement were note down for the analysis of results. The displacement was measured with the help of LVDTs. When all the tests were conducted, they declared that strengthen of RC elements with BFRPs was a good technique and BFRPs strips increases the seismic performance of RC elements under cyclic loading. They had noticed that ductility was good in the RC elements in which three layers of BFRPs strips were provided when it was compared with the ductility of RC beams having diagonally placed BFRPs strips. But the stiffness of all the specimens were greater than the controlled one and also the energy dissipations capacities and damping coefficients were also larger than the control specimen. At last they concluded that the technique of strengthening of RC elements with BFRPs was very effective.

Sobuz et al., (2011) also studied the strengthen effect of CFRP laminates on the flexural behavior of RC beams and epoxy was used to attach the CFRP with the bottom of the beams. Five beams were casted for this study having CFRP of different configurations. Four point loading was used for applying the load on the beams having a clear span of 1900mm. One of these beams were referred as control one for comparison. The other left four beams were strengthened by CFRP by changing its levels. This study shown that use of CFRP sheets on the tension faces of beams increases the stiffness and load carrying capacity of the reinforced concrete beams. Hence, it was observed that for strengthening in flexural U-wrapped of CFRP laminates was very effective.

Sim et al., (2005) also studied the effect of strengthen of RC structures by basalt fiber The basalt fiber had the tensile strength of 1000 N/mm^2, which was 30% and 60% of the carbon and glass fiber respectively. For the evaluation of flexural strengthening, the basalt fiber strengthening improved the yielding and the ultimate strength of the beam specimen up to 27% on the basis of number of layers applied. Results show that, two layers of the basalt fiber sheets provide a better strength.

Concrete beams of length 2400mm, width of150 mm, and 250 mm high with a clear span of 2000 mm were casted and every beam had one third of an equivalent steel ratio. D10 stirrups were used at 100 mm spacing to avoid shear failure. Figure 2.7 shows the details of beams. After casting, the basalt fiber sheet was placed except for the beam which was used for reference. Figure 2.8 shows the procedure of strengthening of each step. The specimens were tested under a bending load and the displacements were measured by using LVDTs at the bottom and strain gauges on the rebars. For avoiding the shear failure, the shear span to depth (a/d) ratio was 3.5. Different variables were the number of the layers of fiber, and the strengthening length, 0.8 and 1.0 L.

Figure 2.7 shows the fractured beam specimens. In all beams, first cracks developed at around 15 kN. The longitudinal rebar yielded at 46 kN in reference beam, and with a continuous increase in deflection, the reference beam failed at 60 kN in flexural with a crushing of concrete in a compressive zone. The strengthened beams, exhibited a typical failure mode of the strengthened beam specimens, as shown in Figure 2.8. With three layers of the basalt sheets length of 0.8l, the failure of the beam was due to debonding between the basalt sheet and concrete, see Figure 2.9.

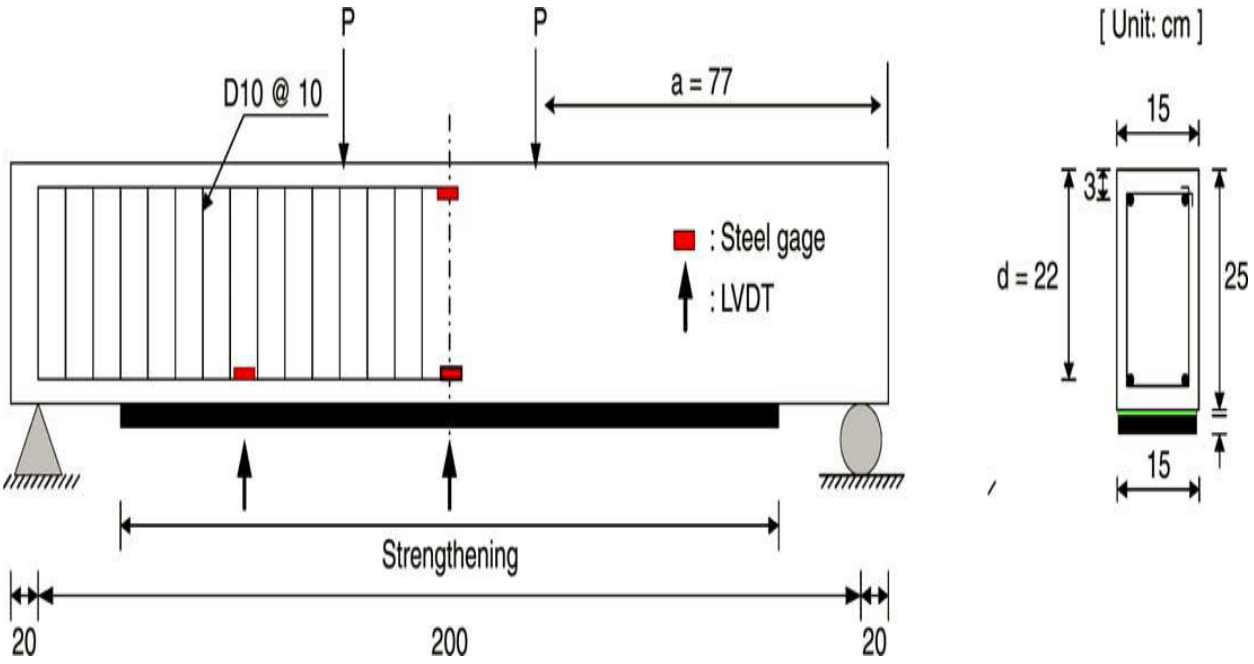

Figure 2.7 Specimen geometry and location of measuring devices [Sim et al., (2005)]

Figure 2.8 Strengthening procedure for basalt fiber sheet [Sim et al., (2005)]

Figure 2.9 Failure modes of strengthened beams [Sim et al., (2005)]

With the increment in number of layers the yielding and ultimate strength were increased, especially for two and three layers. With one layer of the basalt sheet, increment in yielding strength was 15% but no increase in the ultimate strength was noticed. With two layers the yielding and the ultimate strength were increased by 26 and 27%, and with three layers increment was16 and 29%. Increment in the number of the layer also increased the post-yielding stiffness. With the yielding of rebar, the steel rebar and the basalt sheets sustain the applied load, and when rebar yields load was further carried by the strengthening material. Because of which, it is noticed that that there was increment in stiffness of the strengthening material with the increment in layer.

Urbanski et al., (2015) analyzed the effect of BFRP on the deflection of RC beams. Three RC beams with 8mm BFRP bars as bottom reinforcement for flexural and three RC beams with normal steel bars were casted. All the beams were of 80mm width, 140mm in height and 1200mm in length. The middle portion of the beams was without stirrups and there was also no top reinforcement. A cover of 20mm was provided in bottom. An extensometer was used to measure the strains in all the beams. Four point loading was used for applying the load on all the beams. Load was applied in three cycles. In first cycle, load was applied upto 10KN and then released to 5KN. In second cycle, load was again applied upto 20N and then released to 5KN. And in final cycle, load was applied till failure. When the test was conducted, there was no rupture of BFRP bars subjected to flexural due to which fully tensile strength hadn't reached. And the failure of the beam was happened due to the shear in support zone so there was no failure due to high strength and ductility. The results show that the beams having BFRP bars had linear load-strain curve while there was yielding of reinforcement in beams reinforced with steel. The load carrying capacity of all the beams was almost equivalent but the mode of failure was different in both types of beams. In beams reinforced with BFRP bars, the mode of failure was shear in the support zone while the mode of failure in beams reinforced with normal steel was due to crash in concrete in compression zone. The amount of deflection in beams reinforced with

BFRP bars was greater than the beams reinforced with normal steel bars because the modulus of elasticity of beams with BFRP bars was lesser than the modulus of elasticity of beams with beams reinforced with normal steel bars. This study shows that BFRPs bars can be used in various concrete structures.

Islam et al., (2005) had also studied the effect of FRP system on the strengthening of RC deep beams in shear. Six similar beams were casted and tests were performed on them for this investigation. Out of these six beams, one beam was referred as a control beam for comparison purpose. And all the other beams were tested when they were strengthened with CFRP wraps. This studied had shown that strengthen of beams with CFRP wraps slower down the diagonal cracks and the load carrying capacity of the beams also increases. This shows that orientation of FRP is more effective when it compared with the other concrete in which different materials will used. And the increment of 40% in shear strength was observed in this investigation.

V. Fiore et al., (2015) had studied the behavior of externally wrapped basalt fiber on the compression of RC cylinders. In this study, basalt fiber reinforced polymer was bonded with concrete with the help of epoxy resin. Basalt fibers were applied in two forms either fully or partially wrapping. Then all the tests were conducted in compression. And for comparison point of view few cylinders were wrapped with carbon fiber reinforced polymer and tested in compression. The loading was also applied in two ways either monotonic or cyclic. 26 cylinders having cross section area of 150 X 300mm were casted. The compression tests were conducted after 7 and 28 days in UTM having a capacity of 5000KN and load was applied at a rate of 0.2mm/min and displacement was measured with the help of LVDTs, placed at an angle of 120^{o}. This study shows that BFRP increases in confinement of RC specimens with a little increase in strain and also strain softening behavior exhibited.

Banerjee et al., (2007) had conducted an experiment for the increment of shear strength in RC beams with external reinforcement of fiber reinforced polymer. Nine beams were casted and tested for this experiment. All the nine beams were classified in three different classes i.e. unstrengthened, repaired and retrofitted. Three types of systems were used for repair and retrofitting technique i.e. E-glass with epoxy, carbon wet layup with epoxy and carbon strips with epoxy. This study had shown that there was enhancement in the strength of strengthened and repaired beams when they were compared with unstrengthened and pre cracked beams. The shear behavior of reinforced concrete beams strengthened with FRP in shear was evaluated with the help of influencing factor by using various analytical models which also include ACI 440 model. This comparison shows that the shear failure of beam was very much depend upon the aspect ratio i.e. shear span/depth ratio and it also effect the shear strength of the beams.

Fenfang Yin et al., (2015) had studied the effect of strain rate on the bond length of BFRP sheets bonded with concrete. The strength depends upon the bond between the FRP and the concrete and this bond is further depends upon the length of bond between FRP sheets and concrete. This study presented the investigation conducted on the dynamic behavior of bond

length between BFRP sheets and concrete at different strain rate levels. Dynamic tests were conducted for the evaluation of the effect of strain rates on the effectiveness of the bond length between BFRP and concrete. Specimens casted for this study were of cross section 100 X 100mm and of length 510mm. BFRP sheets were applied in layers on the opposite sides of elements. A hydraulic testing machine was used for conducting the test and two transducers were used for measuring the displacement having a range of 10mm and load was measured with the help of a load cell and a load rate of 3.5KN/min was kept fixed and dynamic loads were applied at a rate of 0.07, 0.7, 7 and 70mm/sec. All the set up was controlled automatically with the help of a computer. This dynamic tests show that there was a increment in modulus of elasticity of BFRP as increase in strain rate. BFRP stiffness and strength of concrete affect the bond length between BFRP and concrete. As the strain rate increases, decrement was noted in the bond length of BFRP and concrete. It concluded that strain rate has a negative effect on the bond strength between BFRP and reinforced concrete.

2.3 Researcher's Findings on Different Analytical Models

In the latest studies, various experiments or investigation was conducted for the implementation of various mathematical or analytical models in different design codes and on the basis of which various different guidelines for the strengthening system of RC structures with externally placed FRPs were published or mentioned. There are various complications in this task of modeling which require active study and the mechanism of resistance is also complex and which need more accurate prediction.

Computation of the shear strength of the RC structures strengthened with externally placed or bonded FRP is very necessary for the justification of the experimental results and also for comparison. The shear strength of the RC beam strengthened with FRP can expressed as

$$V_u = V_c + V_s + V_f$$

Where,

V_u is the shear strength of the RC beam strengthened with FRP

V_c is the contribution of concrete in shear strength

V_s is the contribution of steel in shear strength

V_f is the contribution of FRP in shear strength

As the work of estimation of contribution of shear strength of the concrete and steel is very complex due to their heterogeneous nature and also due to their complex mechanisms of transferring shear. Many scholars have proposed various numerical models based on these mechanisms. Various parameters which effect the contribution of the shear strength of the

concrete are compressive strength of concrete, shear span to depth ratio, depth of the beam, steel reinforcement and different axial forces etc.

The contribution of the shear strength of the steel is computed on the basis of an assumption that shear crack intersect the steel at failure. There are various parameters which effect the contribution of the shear strength of the steel and these factors are area of reinforcement, yielding strength of the steel, spacing between the stirrups and effective of the RC beam etc.

The contribution of the shear strength of the FRP also depends on various different factors and these factors are thickness of fiber sheet, bonding mechanism between FRP and concrete, technique of application of FRP on concrete. The various different models for the computation of this shear strength are discussed in the following section.

2.3.1 ACI 440 Model

ACI 440 model is the method mentioned in American code i.e. ACI 440 and on the basis of which, the method of computing of contribution of shear strength of the FRP is presented and given as:

$$V_{frp} = \frac{Afrp\ .\ ffrp,e\ .\ (cos\alpha + sin\alpha).\ df}{sfrp}$$

Where,

$$A_{frp} = 2.n.t_{frp}.w_{frp}$$

$$f_{frp,e} = \epsilon_{frp,e}\ .\ E_{frp}$$

n is number of FRP layers/strips applied

$$\epsilon_{frp,e} = \begin{cases} 0.004 \ \leq\ 0.75\ .\ \epsilon\ frp,u & \text{(for full wrapping)} \\ kv\ .\ \epsilon\ frp,u \ \leq\ 0.004 & (U-\text{jacketing and Side bonding}) \end{cases}$$

$$k_v = \frac{k1\ .k2\ .Le}{11{,}900\ .frp,u} \leq 0.75$$

$$L_e = \frac{23{,}300}{(n\ .\ tfrp\ .Efrp)^{0.58}} \qquad \text{(N,mm)}$$

$$k_1 = \left(\frac{fc}{27}\right)^{\frac{2}{3}}$$

$$k_2 = \begin{cases} \frac{df-Le}{df} & (\text{For U}-\text{jacketing}) \\ \frac{df-2\ .\ Le}{df} & (\text{For side bonding}) \end{cases}$$

2.3.2 Triantafillou's Model

The load carrying capacity of the FRP bonded externally is depends on the different failure modes i.e. either by FRP debonding or by tensile fracture of FRP. But it is very difficult to find out which failure mode will occur because this mode depends on various different factors i.e. bond between concrete and fiber, young modulus of FRP and concrete, thickness of the FRP sheet/ strips, availability of the anchorage length and how FRP attached with concrete etc. On the basis of which Triantafillou has proposed a different approach i.e. semi-qualitative for the determination of the contribution of the shear strength of the FRP bonded externally and the contribution of the shear strength was given as:

$$V_{frp} = 0.9 \,.\, d \,.\, b_w \,.\, \rho_{frp} \,.\, E_{frp,e} \,.\, \epsilon_{frp,e} \,.\, (1 + \cot\alpha) \,.\, \sin\alpha$$

Where,

$$\rho frp = \frac{2 \,.tfrp}{bw} \,.\, \frac{wfrp}{sfrp}$$

$$\epsilon_{frp,e} = \begin{cases} 0.7 \left(\frac{(fc)^{\frac{2}{3}}}{Efrp \,.\rho frp} \right)^{0.30} . \epsilon frp, u \,; & \text{for fully wrapping} \\ \min \left[0.65 \,. \left(\frac{fc^{\frac{2}{3}}}{Efrp \,.\rho frp} \right)^{0.56} . 10^{-3}, 0.17 \,. \left(\frac{fc^{\frac{2}{3}}}{Efrp \,.\rho frp} \right)^{0.30} . \epsilon frp \right]; & \text{for U} - \text{jacketing} \\ 0.048 \,. \left(\frac{fc^{\frac{2}{3}}}{Efrp \,.\rho frp} \right)^{0.47} ; & \text{for fully wrapped aramidic FRP} \end{cases}$$

2.3.3 Cheng-Teng's Model

In this model, Chen-Teng proposed that the distribution of strain in FRP is not uniform because crack width varies around the whole beam. With the process of retrofitting, the process of failure starts with the higher stress point and due to which ultimate strength of the FRP is not achieved. The contribution of the shear strength of the FRP is given as:

$$Vfrp = 2. \, f_{frp,e} \,.\, w_{frp} \,.\, t_{frp} \,.\, \frac{dfrp,e \,.\, (cot\Phi + cot\alpha)}{sfrp} \,.\, \sin\alpha$$

Where,

$$d_{frp,e} = z_t - z_b$$

$$z_t = \max (0.1 \,.\, d, d_{frp,t}) - 0.1 \,.\, d$$

$$z_b = (d - (h - d_{frp})) - 0.1 \,.\, d$$

The effective stress that is carried by FRP is

$$f_{frp,e} = D_{frp} \cdot \sigma_{frp,max}$$

and

$$D_{frp} = \begin{cases} \frac{2}{\pi.\Lambda} \cdot \frac{1-\cos(\frac{\pi}{2} \cdot \Lambda)}{\sin(\frac{\pi}{2} \cdot \Lambda)} ; for\ \Lambda \leq 1 \\ 1 - \frac{\pi-2}{\pi \cdot \Lambda} ; \qquad for\ \Lambda > 1 \end{cases}$$

$$\sigma_{frp,max} = \min \begin{cases} ffrp,u \\ 0.427 \cdot \beta w \cdot \beta l \cdot \sqrt{\frac{Efrp \cdot \sqrt{fc}}{tfrp}} \end{cases} \quad (Nmm)$$

where

$$\beta_l = \begin{cases} 1 ; if\ \Lambda \geq 1 \\ \sin\left(\frac{\pi}{2} \cdot \Lambda\right) ; \Lambda < 1 \end{cases}$$

$$\beta_w = \sqrt{\frac{2-\frac{sfrp}{sfrp \cdot sin\beta}}{1+\frac{sfrp}{sfrp \cdot sin\beta}}}$$

$$\Lambda = \frac{Lmax}{Le}$$

$$L_e = \sqrt{\frac{Efrp \cdot tfrp}{\sqrt{fc}}} \qquad (Nmm)$$

2.3.4 Monti-Liotta's Model

Monti-Liotta also proposed a mathematical model of equations for calculating the contribution of shear strength of the FRP which is used for the strengthening purpose of the RC beams. This model depends on the resisting mechanism proposed by Moersch. By using this method, the contribution of shear strength of the FRP for fully wrapping is given as:

$$V_{frp} = 0.9 \cdot d \cdot f_{fed} \cdot 2 \cdot t_{frp} \cdot \left(\frac{wfrp}{sfrp}\right) \cdot (\cot\Phi + \cot\beta) \cdot \sin\beta$$

The contribution of the shear strength of the FRP for side bonding is given as:

$$V_{frp} = 0.9 \cdot d \cdot f_{fed} \cdot 2 \cdot t_{frp} \cdot \frac{sin\beta}{sin\Phi} \cdot \frac{wfrp}{sfrp}$$

Where,

$$f_{fed} = \begin{cases} ffdd \,.\, \frac{zrid,eq}{z} \,.\, \left(1 - 0.6 \,.\, \sqrt{\frac{Leq}{zrid,eq}}\right)^2 & (for\ side\ bonding) \\ ffdd \,.\, \left(1 - \frac{1}{3} \,.\, \frac{Le \,.\, sin\beta}{z}\right) & (for\ U - jacketing) \\ ffdd \,.\left(1 - \frac{1}{3} \,.\, \frac{Le \,.\, sin\beta}{z}\right) + \frac{1}{2} \,.(nR \,.\, ffrp,u - ffdd).\left(1 - \frac{Le \,.sin\beta}{z}\right) & (for\ wrapping) \end{cases}$$

Where,

$$f_{fdd} = \sqrt{0.6 \,.\, \frac{Efrp \,.\, fctm \,.\, kb}{tfrp}} \qquad \text{(Nmm)}$$

$$L_e = 0.6 \,.\, \sqrt{\frac{Efrp \,.\, tfrp}{\sqrt{fctm \,.\, kb}}} \qquad \text{(Nmm)}$$

$$k_b = \begin{cases} \sqrt{\frac{1.5}{1+(\frac{wfrp}{100})}} & (for\ sheets) \\ \sqrt{\frac{1.5 \,.\, (2-\frac{wfrp}{sfrp})}{1+(\frac{wfrp}{100})}} & (for\ strips) \end{cases}$$

$z_{rid,eq} = z_{rid} + L_{eq}$

$z_{rid} = z - L_e \,.\, \sin\beta$

$z = 0.9 \,.\, d$

$L_{eq} = \frac{u1}{\epsilon fdd} \,.\, sin\beta$

$u_1 = 0.33 \,.\, k_b$ (mm)

$n_R = 0.2 + 1.6 \frac{rc}{bw}$

and

$\frac{rc}{bw}$ can either be greater than or equal to 0 and smaller or equal to 0.5

2.3.5 General Nomenclature and Different Notations

In this section, different notations and nomenclature used in this study are mentioned

d = effective depth of the beam

b = width of the beam

D = Total depth of the beam

a = shear span of the beam

a/d = shear span to depth ratio

A_{sb} = area of longitudinal steel in the tension side of the beam

A_{st} = area of longitudinal steel in the compression side of the beam

A_{sv} = area of transverse steel

ρ_{st} = longitudinal steel to cross section ratio

ρ_{sv} = transverse steel to cross section ratio

Φ = crack angle

w_{frp} = width of the FRP reinforcement

s_{frp} = center to center spacing of the FRP reinforcement

t_{frp} = thickness of the FRP sheet/strip

d_f = effective depth of the FRP

β = angle of FRP fiber orientation w.r.t the beam axis

A_{frp} = area of the FRP sheet/strip

ρ_{frp} = ratio of FRP reinforcement

L_a = available bond length of the FRP sheet/strip

f_y = yield strength of longitudinal steel

f_{yv} = yield strength of transverse steel

f_c = compressive strength of the concrete

E_{frp} = modulus of elasticity of the FRP

$f_{frp,u}$ = ultimate tensile strength of the FRP sheet/strip

$\epsilon_{frp,u}$ = ultimate strain in the FRP sheet/strip

$f_{frp,e}$ = effective tensile strength of the FRP sheet/strip

$\epsilon_{frp,e}$ = effective ultimate strain in the FRP sheet/strip

L_e = effective bond length of the FRP sheet/strip

n = number of layers of the FRP sheet/strip

$d_{frp,e}$ = effective height of the FRP bonded on both sides

z_t = coordinate of the top edge of the FRP

z_b = coordinate of the lower edge of the FRP

$d_{frp,t}$ = distance from the beam compression side to the top edge of the FRP

d_{frp} = distance from the beam compression side to the lower edge of the FRP

$\sigma_{frp,max}$ = maximum stress in the FRP

D_{frp} = stress distribution factor for FRP

β_L = bond length coefficient

β_w = strip width coefficient

L_{max} = maximum bond length

f_{fed} = FRP effective bond strength

f_{fdd} = debonding strength of the FRP sheet/strip

r_c = cornet rounding radius

f_{ctm} = tensile strength of the concrete

k_b = covering scale/coefficient

Chapter-3 Experimental Program

3.1 General

The aim of this experimental program is to strengthen the beam fail in shear with basalt fiber. The basic tests carried out on various materials used for casting of beams are discussed in this chapter and a brief description of mix design of concrete and its curing period is also discussed. And further experimental setup and test on the specimens are discussed.

3.2 Materials Used

The properties of materials used in this dissertation were determined in laboratory according to the prescribed methods by IS codes. Materials used for development of control concrete were Cement, Coarse Aggregates, Fine Aggregates and Water. The main aim for studying properties of materials used is to verify the acceptance of material as per codes and for the development of required mix proportion for concrete. The description materials and their calculated properties used in this work are discussed in following sections.

3.2.1 Cement

Cement is a material that binds fine aggregates with coarse aggregates and is responsible for holding together of concrete. It is a fine powder which mainly controls strength and hardness properties in concrete. Several types of Cement are available but most widely used is the Portland cement. According to (Nawy, 2009) Portland Cement is formed out of mixture of rocks of clay and limestone as raw materials for cement production is found them like calcium carbonate ($CaCO_3$), Iron Oxide (Fe_2O_3) and Silicon dioxide (SiO_2).

Firstly, these rocks are crushed and blended. Now they are heated in a kiln to clinker. This clinker is left for cooling and then grounded to get a fine powder. At the final grinding stage, addition of small amounts of gypsum is done to produce dry powder (Portland Cement). The Cement used in our dissertation work is Ordinary Portland Cement of Grade 43 and of brand Ultratech Cement. This cement complies with the requirements of IS : 269-2015 for OPC 43 grade. The various properties of cement are shown in Table 3.1.

3.2.2 Fine Aggregates

Fine aggregates are usually less than 4.75 mm in size. Sand is mostly used as fine aggregate which mainly contains small rounded and angular particles of silica. Fine aggregates mainly act as filler in voids of coarse aggregates and reduce the chances of concrete to shrink or crack.

Fine aggregates are mainly of three types: Natural sand which is obtained from disintegration of rocks naturally, Crushed stone sand which is obtained from crushing hard stones & Crushed Gravel Sand which is obtained from crushing natural gravel.

In our dissertation work, fine aggregates were procured from local supplier in Patiala which confirms to Grading zone II confirming to IS 383: 1970. Properties of fine aggregate used for formation of concrete are shown in Table 3.2. The set of sieves through which fine aggregate was sieved to obtain sieve analysis in shown in Table 3.3 The fine aggregate belonged to Zone-II.

Table 3.1 Physical Properties of Cement

S.No.	**Physical Requirements**	**Test Results**	**Requirements Of IS:269-2015**	
1.	Fineness (m^2/kg) (IS 4031 Part-1)	254	255	Min
2.	Standard Consistency (%)	26.0	-	-
3.	Setting Time (minutes)			
a.	Initial	160	30	Min
b.	Final	225	600	Max
4.	Soundness			
a.	Le-Chat Expansion (mm)	0.5	10	Max
b.	Autoclave Expansion (%)	0.012	0.8	Max
5.	Specific Gravity	3.161		
6.	Compressive Strength (MPa)			
a.	72 +/- 1hr.(3 days)	32.5	23	Min
b.	168 +/- 2 hr.(7 days)	42.9	33	Min

Table 3.2 Properties of Fine aggregate

S. No.	Characteristics	Value
1.	Type	Medium Sand
2.	Specific Gravity	2.63
3.	Total water absorption	5.5%
4.	Grading Zone	II
5.	Fineness Modulus	2.78
6.	Bulk Density of Loose Sand	1.46
7.	Bulk Density of Compacted Sand	1.64

Table 3.3 Sieve Analysis of Fine Aggregate

S.No.	I.S. Sieve	Weight Retained on Sieve (gm)	Cumulative Weight Retained (gm)	Cumulative % Retained
1.	4.75mm	13	13	1.3
2.	2.36mm	1	4	1.4
3.	1.18mm	380	394	39.9
4.	0.6mm	164	558	56.8
5.	0.3mm	262	820	83.5
6.	0.15mm	115	935	95.5
7.	Pan	40	975	100
	Total	975		278.4

3.2.3 Coarse Aggregate

Aggregates which are retained over IS sieve of 4.75 mm size are called coarse aggregates. In concrete mix, 60% to 80% is occupied by aggregates. High content of aggregates affects properties in both fresh and hard concrete. Main role of aggregates is to provide a solid hardened mass of concrete. These aggregates act as a filler material in concrete. Also, aggregates helps in reducing cost of concrete by replacing cement which is a costly ingredient.

The coarse aggregates used in this work are obtained from local supplier in Patiala. In this dissertation only 10mm aggregates were used.

Coarse aggregates are mainly of two types: Crushed and Uncrushed gravels. Crushed gravels are made by crushing of gravel and hard stone whereas stones obtained from disintegrating of rocks naturally or partially crushed stones forms latter type. The aggregates were tested as per Indian Standard IS:383-1970. Properties of fine aggregate used for formation of concrete is shown in Table 3.4.The set of sieves through which coarse aggregate were sieved to obtain sieve analysis in shown in Table 3.5.

Table 3.4 Properties of Coarse Aggregate

S.No.	Properties	Value
1.	Type	Well graded Aggregate
2.	Maximum Size	10mm
3.	Specific Gravity	2.7
4.	Total Water Absorption	1.95%
5.	Fineness Modulus	6.51

3.2.4 Water

Water which is useful for drinking can be used in concrete. Water available from lakes, streams is suitable for casting. If water contains sewage waste or it is from any industries then it should be avoided. In this experiment, tap water is used.

Quality of water using in concrete controls many properties such as workability, permeability, compressive strength, shrinkage and cracking. Water–cement ratio is the ratio of weight of water to weight of cement in concrete mix. A high water-cement ratio improves workability and produces wet and fairly weak concrete thus reduces strength of concrete which is prone to shrinkage and cracking whereas low water-cement ratio produces very stiff and strong concrete. In this design, w/c ratio was taken as 0.5. The water used in mixing of concrete was potable water.

Table 3.5 Sieve Analysis of Coarse Aggregate (Tested in Lab)

I.S. Sieve	Weight Retained on Sieve (gm)	Cumulative Weight Retained (gm)	Cumulative % Retained
80mm	0	0	0
40mm	0	0	0
20mm	9	9	0.18
10mm	2907	2916	58.43
4.75mm	1803	4719	94.56
Pan	271	4990	-
Total	4990	Sum	651.56

Fineness Modulus of Coarse Aggregate = 651.56/100 = 6.51

3.2.5 Steel Reinforcement

HYSD bars of 12mm of grade-500 of Tata Tiscon steel confirming to IS:1786-1985 are used as main longitudinal steel. 12mm and 10mm bars are used as compression reinforcement. And 6mm steel bars are used as stirrups. Mechanical properties of reinforcement used are shown in Table 3.6.

Table 3.6 Mechanical Properties of Reinforcement

Mechanical Property	Min. Req. as per IS: 1786 (Fe 500)	Calculated (Fe 500)
Yield Strength, MPa	500	520
Ultimate Tensile Strength, MPa	545	601.1

3.2.6 Retrofitting Material

Basalt Fiber Rock Geomesh with opening size of 10 X 10 mm opening size and 0.7-0.8mm thickness and 300-2000mm wide as shown in Figure 3.1 were used for retrofitting of beams. The geomesh was manufactured by Hydro Design Management Co. Pvt. Ltd. The strength of the net is as good as metal reinforcement, however, it is 2.6 times lighter, thus simplifying transportation and handling in construction. Rock fiber Geo Mesh is more durable than metallic and glass fiber reinforcement. The Properties of fiber are shown in Table 3.7.

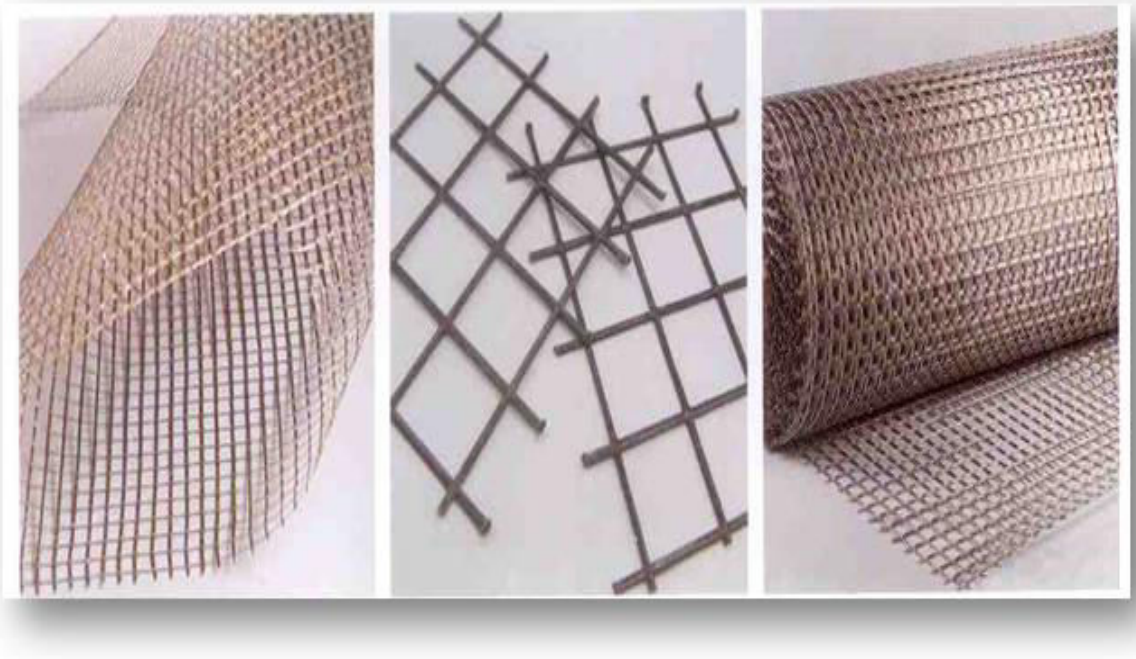

Figure 3.1 Basalt Fiber Used in the Experiment

Table 3.7 Properties of Basalt Fiber (Provided by Manufacturer)

S.No.	Physical Properties	Value
1.	Specific Surface Weight	350 g/m^2
2.	Maximum Load	3500 N/5cms
3.	Density	2640 kg/mm^3
4.	Moisture Content	0.1%
5.	Melting Point	1350^oC

3.3 Mix Design and Proportions

Concrete mix was prepared using OPC 43 grade cement, fine aggregate, and crushed stone aggregate with maximum size of 10 mm. A design mix of M25 as per IS guidelines was prepared. The ratio of cement : sand : aggregate was taken as 1:1.76:2.96. Total aggregates were taken as 75 percent of total concrete volume. Since only 10 mm aggregates was used hence coarse aggregates was 60 percent of total aggregates and fine aggregates was 40 percent of total aggregates. Water absorption of coarse aggregates and fine aggregates was 1.95% and 5.5% respectively. This amount of water was added while preparing mix.. Mix proportion of prepared control concrete is shown in Table 3.8.

Table 3.8 Mix proportion of M25 Grade Concrete

Concrete Grade	**Ingredients**			
	Cement(kg/m^3)	**Water(kg/m^3)**	**CA(10mm) (kg/m^3)**	**FA (kg/m^3)**
M25	390	186	1156	690

The compressive strength test results of cubes and split tensile strength of cylinders prepared with this design mix are shown in Table 3.9 and Table 3.10.

Table 3.9 Compressive Strength Test Results of Design Mix

S.No.	Particulars	Compressive Strength (MPa) 7 days	Compressive Strength (MPa) 28 days
1.	Average Value of 3 Cubes	24	36

Table 3.10 Split Tensile Strength Test Results of Design Mix

S.No.	Particulars	Tensile Strength (MPa) 7 days	Tensile Strength (MPa) 28 days
1.	Average Value of 3 Cylinders	3.7	5.25

3.4 Design of Beams

The designing of the beams was according to the under reinforced section, casted with concrete having grade of M25 and steel used was Fe-500 and area of cross section of all the beams was 135 X 230 mm and having a length of 2050mm. Two bars of 12mm diameter were provided as tension reinforcement in the zone of tension and two bars of 10mm diameter were provided as compression reinforcement in the zone of compression. Two legged 6mm diameter stirrups were provided at a spacing of 150mm c/c. The important details of the beam are shown in Figure 3.2.

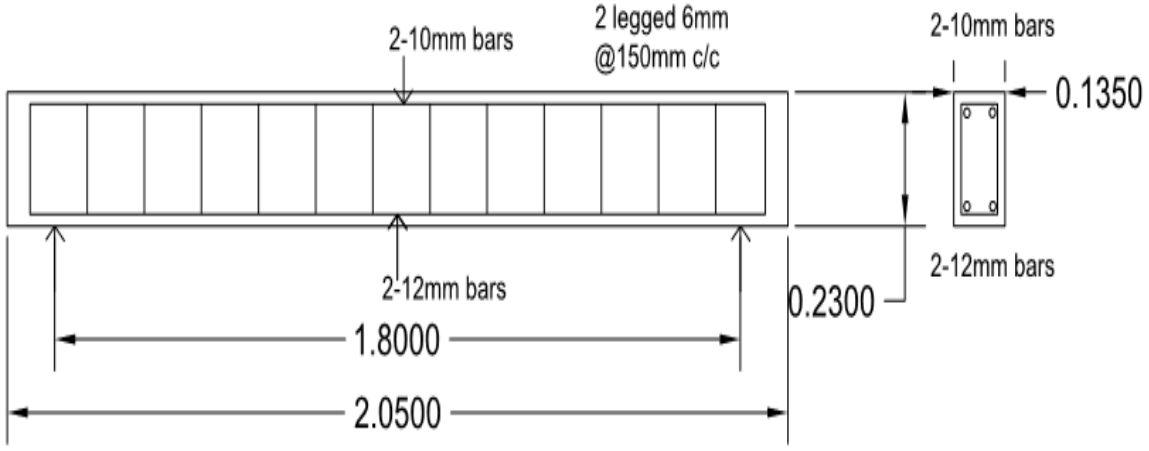

Figure 3.2 Details of RC Specimens

3.5 Casting and Curing

For the Casting, all the moulds i.e. of cubes, cylinders and beams were cleaned and oiled properly. All the moulds were tightened securely before casting. Necessary care was taken so that there is no gaps left from which there is no possibility of leakage of slurry. Proper procedure had been taken for batching, mixing and casting operations. The Concrete mix was prepared with the help of rotating mixer with proper care so that there would be no loss of amount of materials. First of all, coarse aggregates and fine aggregates were weighted with an accuracy of 0.5gms. Initially, the mixer was washed with water so that no material will be stuck with it. Then, the coarse aggregate was first put in the rotating mixer followed by fine aggregates. Then, the 25% water was poured in the mixer and mixer was started for the proper mixing of aggregates. Then the cement was poured in three amounts followed by 25% amount of water with each amount of cement so that proper care should be taken. Then the mix was poured on a water tight platform for use for casting. The Process of casting is shown in Figure 3.3.Casting was completed in two steps:

Figure 3.3 Casting of RC Beams

1. Casting of 6 cubes of size 150 X 150 X 150 mm and 6 cylinders of size 150 X 300mm for the checking that design mix will give the required strength.
2. Casting of beams of size 135 X 230 X 2050 mm with 3 cubes and 3 cylinders for every 4 beams.

Clean and oiled cube and cylinder moulds were then placed on vibrating table and filled in three layers so that there will be no voids. Vibrations were stopped as the cement slurry comes on the top surface of the mould.

The moulds of beams were first clean and then oiling was done so that removing will be easy after the casting. The vibrating was done with the help of a needle vibrator because it was not possible to place it on the vibrating table. After that demoulding was done with proper care so that no edges were broken. The cubes and cylinders were kept in curing tank for the respective time period of 7 and 28 days. The samples of beams were covered with gunny bags and curing was done for the 28 days.

3.6 Strengthening Procedure

The strengthening of the beams was done with the help of basalt fiber reinforced polymer. For bonding the sheets with the casted beam, a procedure was followed. First of all, the top surface of the beam was grinded with the help of a grinder for removing all the invisible voids and the weak layers from the surface and for exposing the aggregates that was provided in the concrete so that proper adhesion will be there between the concrete and the respective laminates. The dust particles formed due to the grinding process was removed with help of an air blower for getting the smooth surface. The process of grinding was shown in the Figure 3.4.

Figure 3.4 The process of grinding

Before applying the epoxy on the grinded surface, all the required sheets of BFRP were cut in the desired length. The epoxy which was used for bonding the laminates was Dr. Fixit 211 epoxy bonding agent. It comes in two parts and for making the epoxy, these two parts were mixed completely and properly for getting a homogeneous mixture and which was very smooth in applying. Then this epoxy was applied on the grinded surface with the help of a brush and applied in such a manner that the overall adhesive thickness of this epoxy was remains constant and there will be no gaps or voids present on the surface because if there will be gaps then it resist the bonding process and the desired results will not be achieved. After that the BFRP sheet was placed with the help of a roller on the top of the epoxy coat and the roller was used for removing the undesirable voids or entrapped air bubbles.

While applying the BFRP sheets on the concrete, a constant pressure was maintained so that proper bond between the concrete and the laminates will achieve with the help of epoxy and for also removing the excess epoxy from the surface. Room temperature was maintained during the whole process. All the specimens then further cured for one week at room temperature.

3.7 Experimental Setup

The beams were tested after 28 days of casting. All the beams were tested as simply supported beams subjected to two point loading subjected to L/3 distance from each end, where L is the effective span i.e. 1.80m. The shear span to effective depth ratio (a/d) was equal to 2.6.

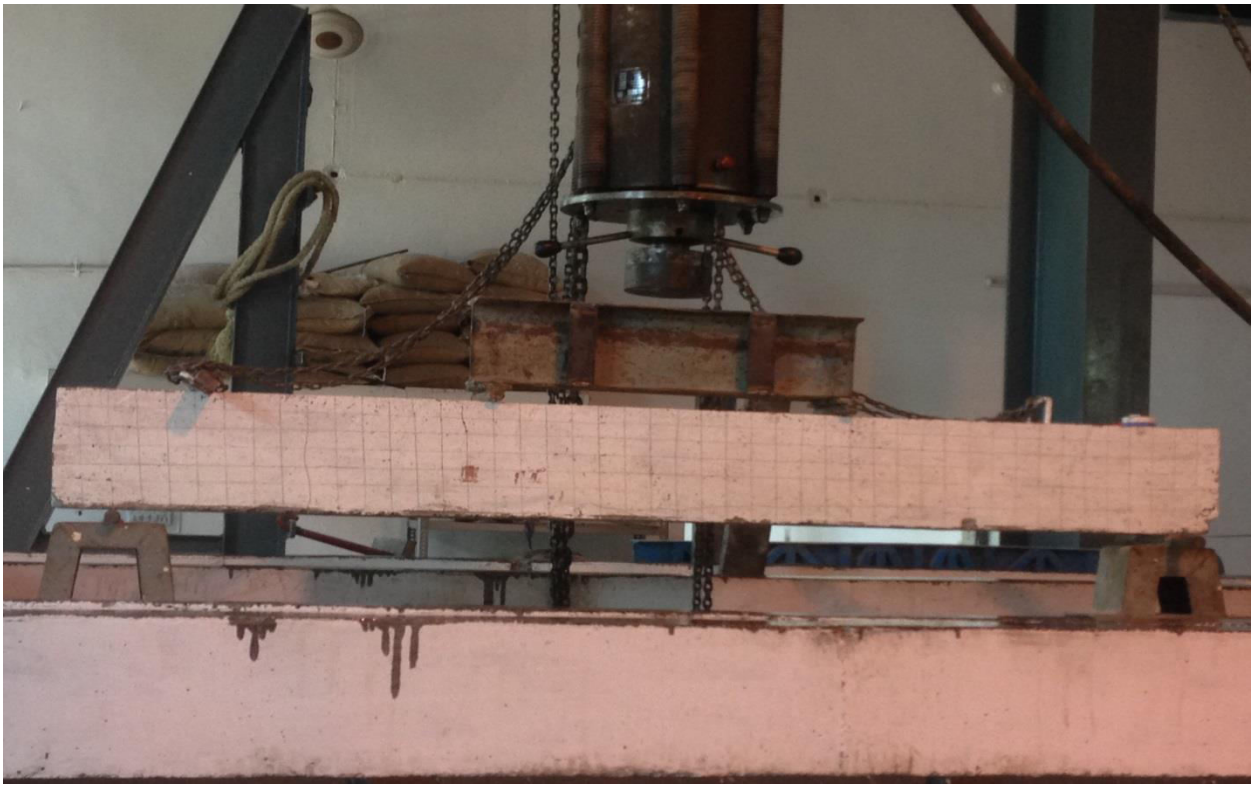

Figure 3.5 Test Setup and its details

This setup gives constant moment and zero shear in the section between the loads and constant maximum shear force between support and load. The moment was linearly varying between supports and load. The testing procedure for the entire beam specimens was same. The tests were performed using the setup as shown in the Figure 3.5.

All the testing was carried out at the loading frame having capacity of 5000KN. The tests were carried out using displacement control and the applied loads were monitored with the help of a software named as Max which provides both the load value and displacement value. One LVDT was placed at a distance L/2 to measure the deflection. The reading was taken at regular intervals of load. During loading, the specimen was visually inspected and cracks were marked. For the clear visibility of cracks, the surfaces were painted with white distemper prior to testing.

3.8 Arrangements of Beams

The experimental program consists of four simply supported RC beams having same dimensions of 135 X 230 X 2050 mm. The amount of reinforcement provided in all the beams was same. . Two bars of 12mm diameter were provided as tension reinforcement in the zone of tension and two bars of 10mm diameter were provided as compression reinforcement in the zone of compression. Two legged 6mm diameter stirrups were provided at a spacing of 120mm c/c. The explanation of the strengthened beams with BFRP with different arrangements was shown in the Table 3.11.

Table 3.11 Arrangements of Different Beams

Label on beam	Arrangements of beams	BFRP reinforcement in shear
RB-01	Reference/Control beams	-
SB-01	Beam strengthened with arrangement - 1	200mm wide U-strips at 100mm c/c spacing
SB-02	Beam strengthened with arrangement – 2	Complete U-wrap
SB-03	Beam strengthened with arrangement – 3	200mm wide inclined strips at 100mm c/c spacing

3.8.1 Referred and Controlled Beam

One controlled beams (CB-01) having no external reinforcement of BFRP was used as reference beams. The reinforcement provided in these beams was same as that of the other strengthened beams. The reinforcement was provided in such a manner that the beams will fail in shear. The arrangements of control beams were shown in Figure 3.6.

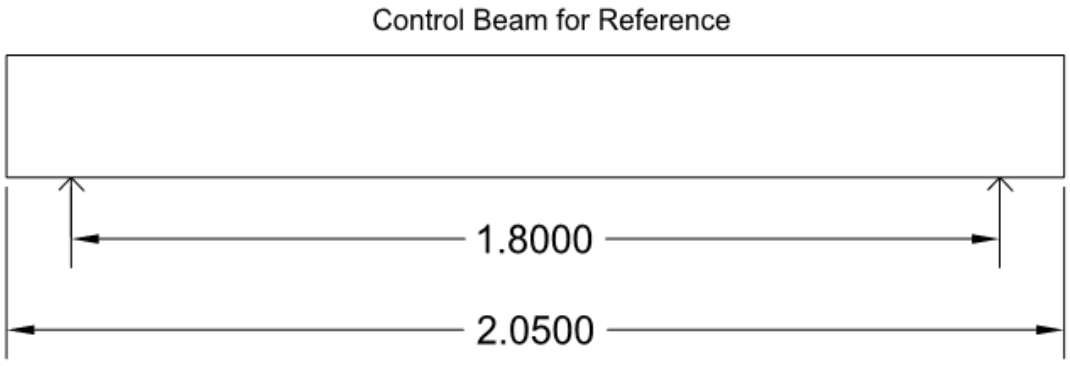

Figure 3.6 Details of the Control Beam

3.8.2 Strengthening of Beam with Arrangement – 1

One beam SB-01 was strengthened with this arrangement. In this arrangement, BFRP was applied in the form of U-strips having a width of 200mm and provided at a spacing of 100mm c/c as shown in Figure 3.7. The strips provided in two layers for decreasing the mesh size. This arrangement was used increasing the shear capacity of the beams. The arrangement of these beams was shown in Figure 3.8.

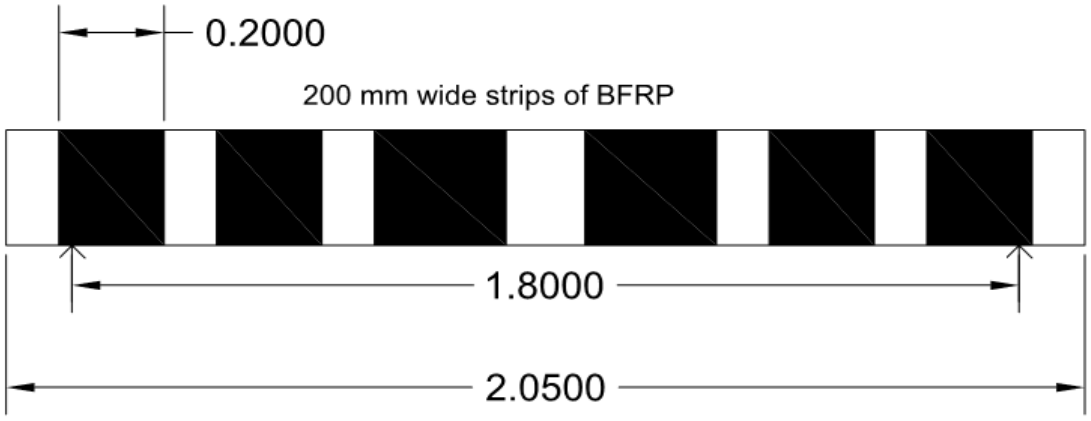

Figure 3.7 Details of Beam Strengthened with Arrangement-I

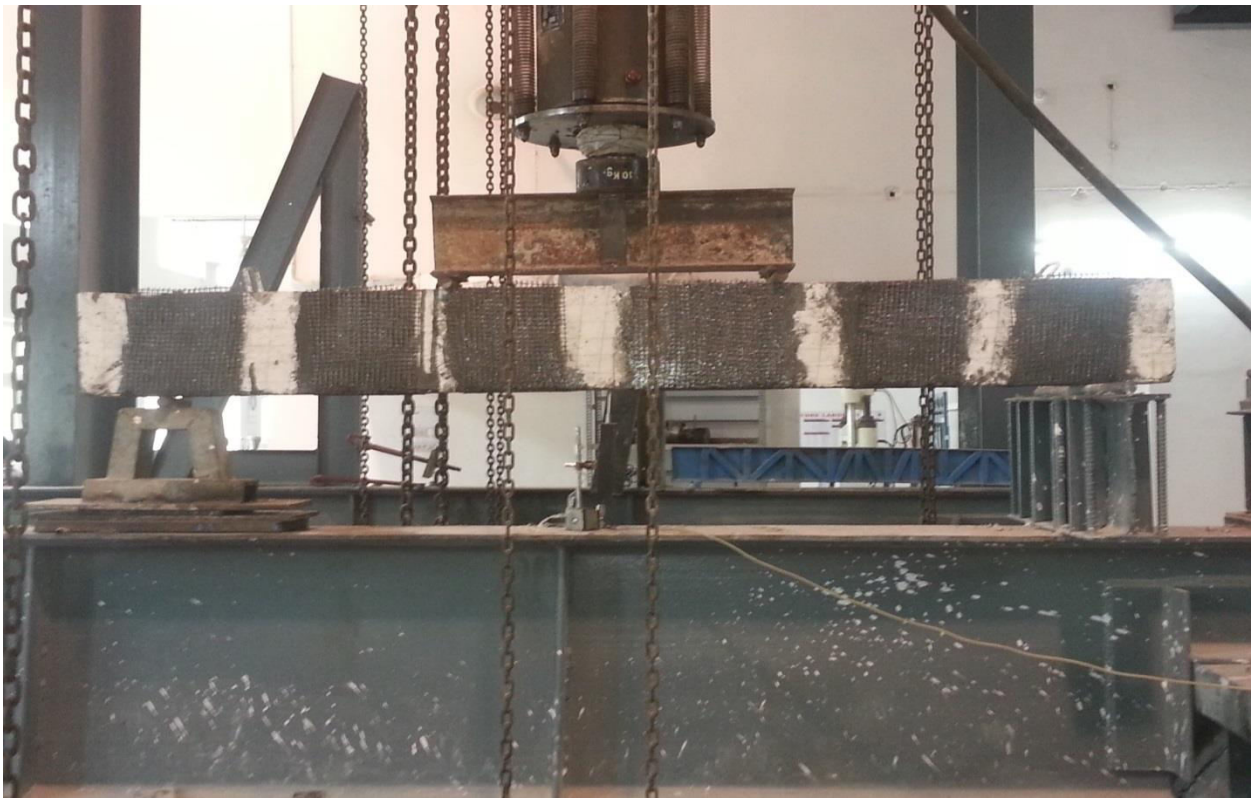

Figure 3.8 Test Setup for Beam Strengthened with Arrangement-I

3.8.2 Strengthening of Beam with Arrangement – II

One beam SB-02 was strengthened with this arrangement. In this arrangement, BFRP was applied in the form of U-wrap for covering the whole beam for increasing the shear capacity. Two layers were also provided in this arrangement for decreasing the mesh size. The arrangement of these beams was shown in Figure 3.9 and Figure 3.10.

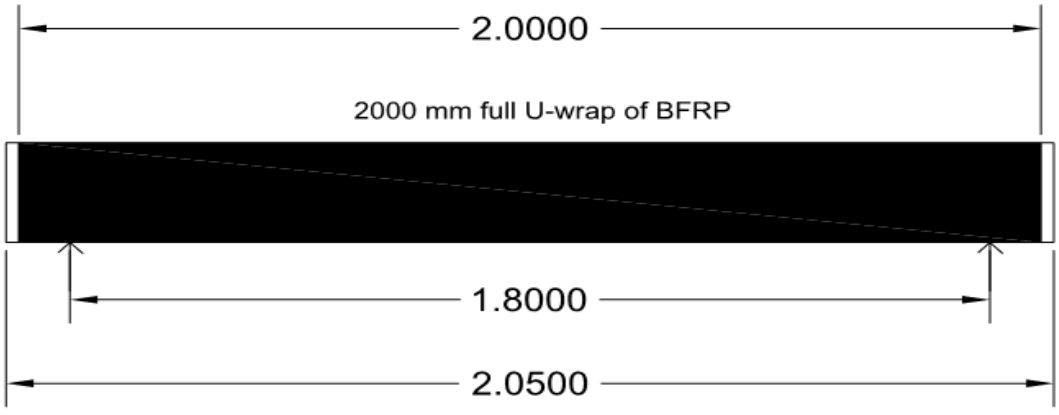

Figure 3.9 Details of Beam Strengthened with Arrangement-II

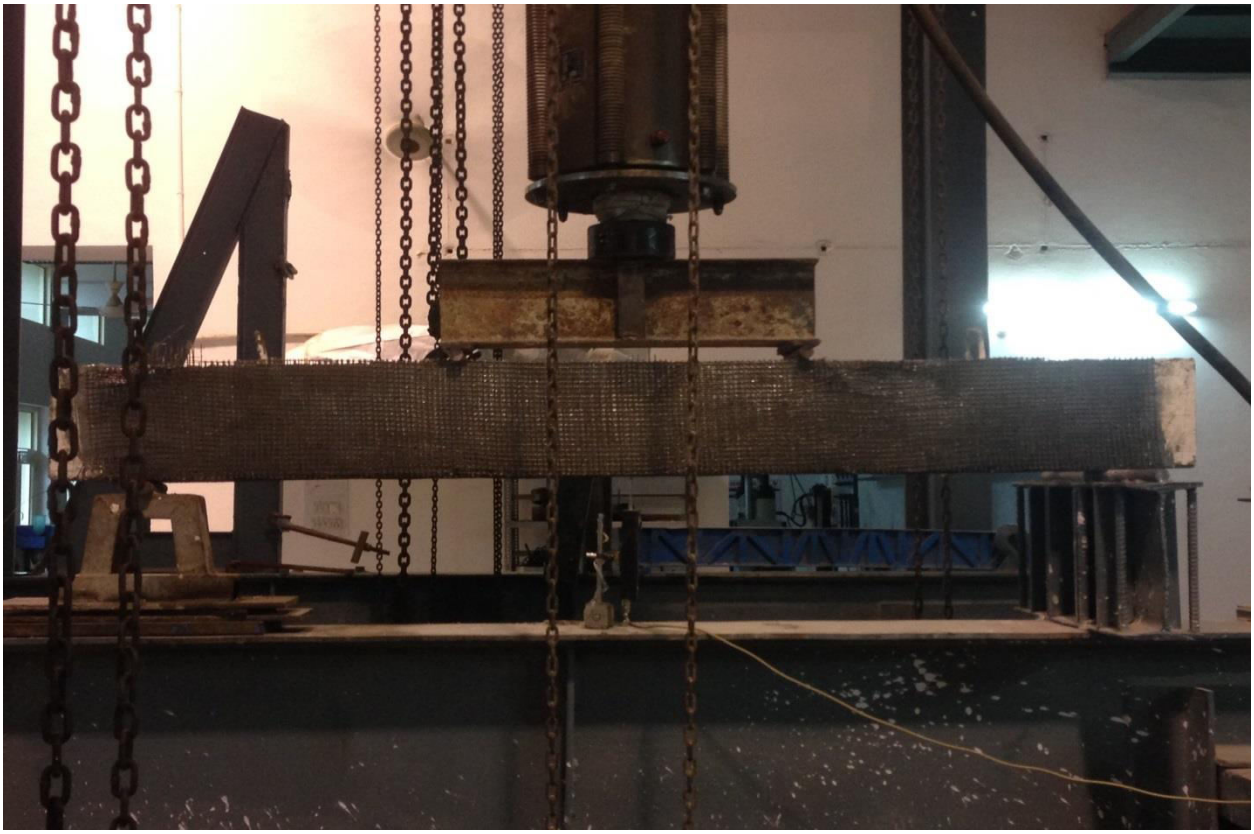

Figure 3.10 Test Setup for Beam Strengthened with Arrangement-II

3.8.3 Strengthening of Beam with Arrangement – III

One beam SB-03 was strengthened with this arrangement. In this arrangement, inclined BFRP strips were provided because shear cracks were also follow the inclined pattern. The inclined BFRP strips were provided at an angle of 45^{o} with the bottom of the beam. The strips were of width 200mm and provided at a spacing of 100mm c/c. This arrangement was shown in Figure 3.11 and Figure 3.12.

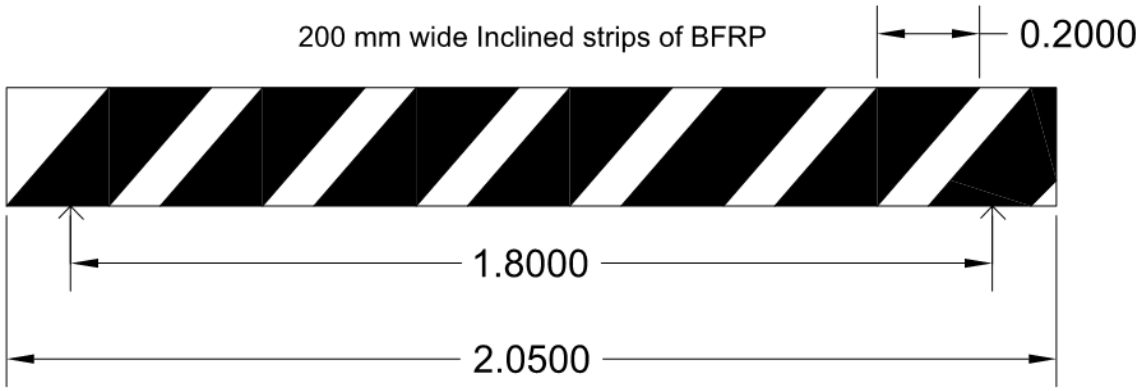

Figure 3.11 Details of Beam Strengthened with Arrangement-III

Figure 3.12 Test Setup for Beam Strengthened with Arrangement-III

CHAPTER-4 RESULTS AND DISCUSSIONS

4.1 INTRODUCTION

In this present work, BFRP strips were used for the strengthening purpose of RC beams. Four RC beams were casted for this study and tests were conducted by using four point loading up to the full failure level. One of the four beams was a control beam, which was used as a reference beam for comparison. While BFRP strips was used as external reinforcement in all the other beams for the strengthening purpose and having different arrangements.

Results of all the beams are presented in this chapter. These results include effect of BFRP strips on the load carrying capacity of beams after strengthening and stiffness of beams. In last, comparison of all the beams was conducted for contrasting them.

4.2 EXPERIMENTAL RESULTS

In this section, the results of the experiments are discussed and presented. All the results are classified into various topics and these topics are load - displacement curves, the various cracks pattern and the deformation behavior of all the beams with their mode of failure.

4.2.1 Experiment Result of Controlled/Referenced Beam

For conducting this experiment, a test setup was made. In this test setup, a frame was made for applying the two points load. Then the beam was placed and the load was applied with the help of hydraulic jack and the values of the displacement were note down with the help of LVDT placed under the central point i.e. mid-point of the beam.

After maintaining all the necessary arrangements, load was applied. When the load was applied, there was very little increment in the displacement as the value of load increases. But as the value of load crosses 10kN, there was more increment in displacement proportional to the load value because there was loss of stiffness after the first crack appears in the beam. The value of load where first crack appeared was 15.2kN. The load-displacement curve was shown in Figure 4.2 and the respective data of load-displacement is shown in Table 4.1.

The yield load of the beam was calculated with the help of procedure which is mention below (Khalifa et al., (1998) and all the procedure was shown in Figure 4.1.

1. First draw a line i.e. line.1 at a point $0.5P_u$ on Y-axis, where P_u is the ultimate load.
2. Then draw a line i.e. line.2 passing from the origin and point where the line drawn in step-1 met the load v/s displacement curve.
3. Then draw a straight line i.e. line.3 between the point i.e. ultimate load of the beam on Y-axis and the point where this line met the load v/s displacement curve.
4. Then from the point i.e. the intersecting point of the lines drawn in step-2 and step-3, draw a straight line i.e. line.4 passing from the X-axis.

5. Then from the point, where the line drawn in step-4 met the load v/s displacement curve, draw a line i.e. line.5 passing from Y-axis.
6. The point where the line.5 met the Y-axis is the value of yield load.

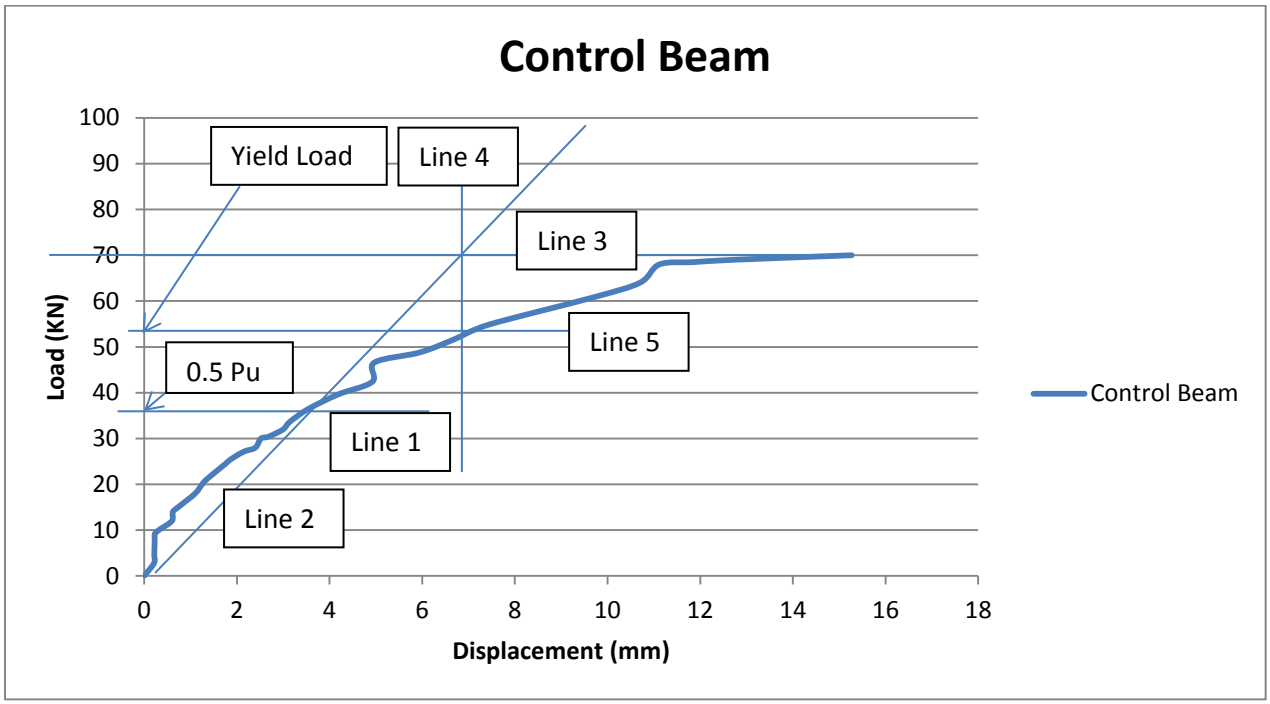

Figure 4.1 Showing the Procedure of Calculating Yield Load

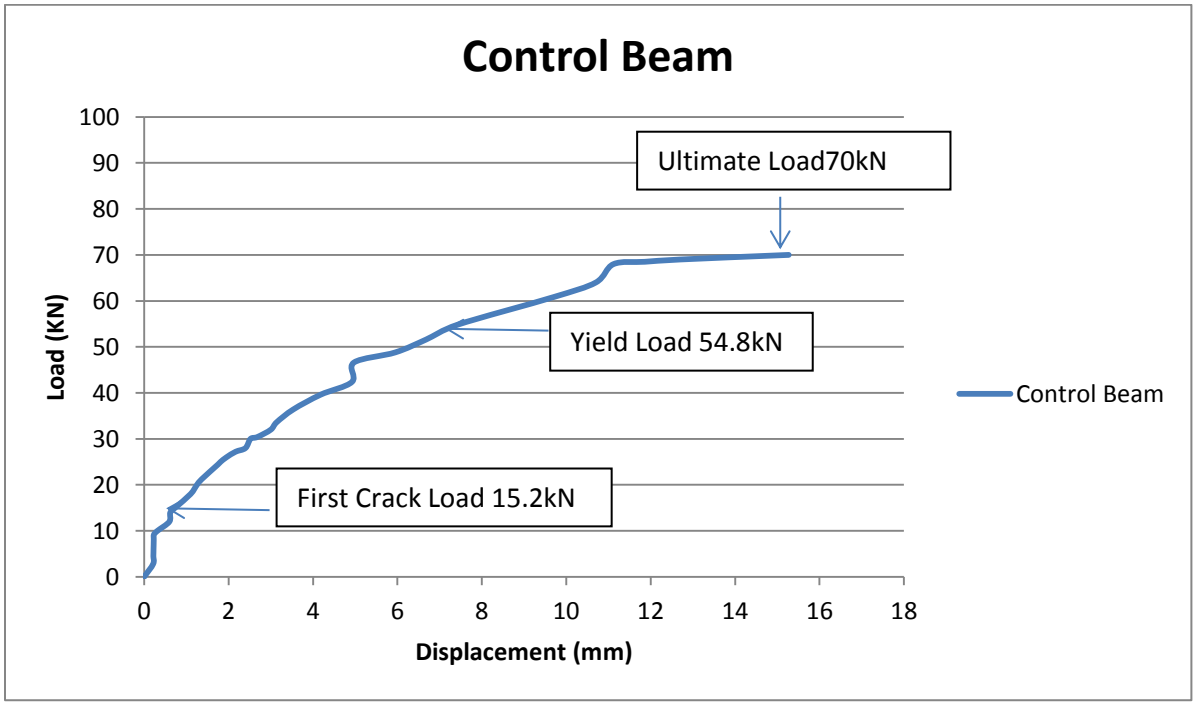

Figure 4.2 Load v/s Displacement Curve of Controlled Beam

Table 4.1 Load vs Displacement data of Referenced Beam

Load (kN)	Mid-Point Displacement (mm)	Load (kN)	Displacement (mm)
0	0	25	1.81
2.8	0.213	30	2.52
4.5	0.218	33.6	3.138
6	0.222	39.6	4.179
8	0.227	42.4	4.925
9.2	0.231	46.6	4.97
10	0.314	48.8	5.95
12	0.597	54.8	7.42
15.2	0.62	64	10.7
18	1.1	68	11.86
20	1.25	70	15.27

Figure 4.3 Failure and Crack Pattern in Referenced Beam

From this procedure, the value of yield load was calculated, which was 54.8kN and the corresponding displacement was 7.42mm. Initially, cracks was starting visible near the center and then with further increment of load, the cracks were propagated from center towards the support and at last the beam fail in shear at a load value of 70kN with a corresponding value of displacement of 15.27mm. Initially, the cracks developed at an angle of 90^{o} with the beam but as the load increases, the crack pattern also followed an inclined pattern due to the shear failure, as shown in the figure. The failure pattern of the controlled beam is shown in Figure 4.3.

4.2.2 Experiment Result of Beam Strengthened with Rectangular Strips of Basalt FRP

In this arrangement, the strengthening of beam was done with two layers of 200mm BFRP sheet each at a spacing of 100mmc/c at the all three faces except the top face, where the load was applied and no other type of external shear reinforcement was provided. The load v/s displacement curve is shown in Figure 4.4 and the respective data of load v/s displacement is shown in Table 4.2.

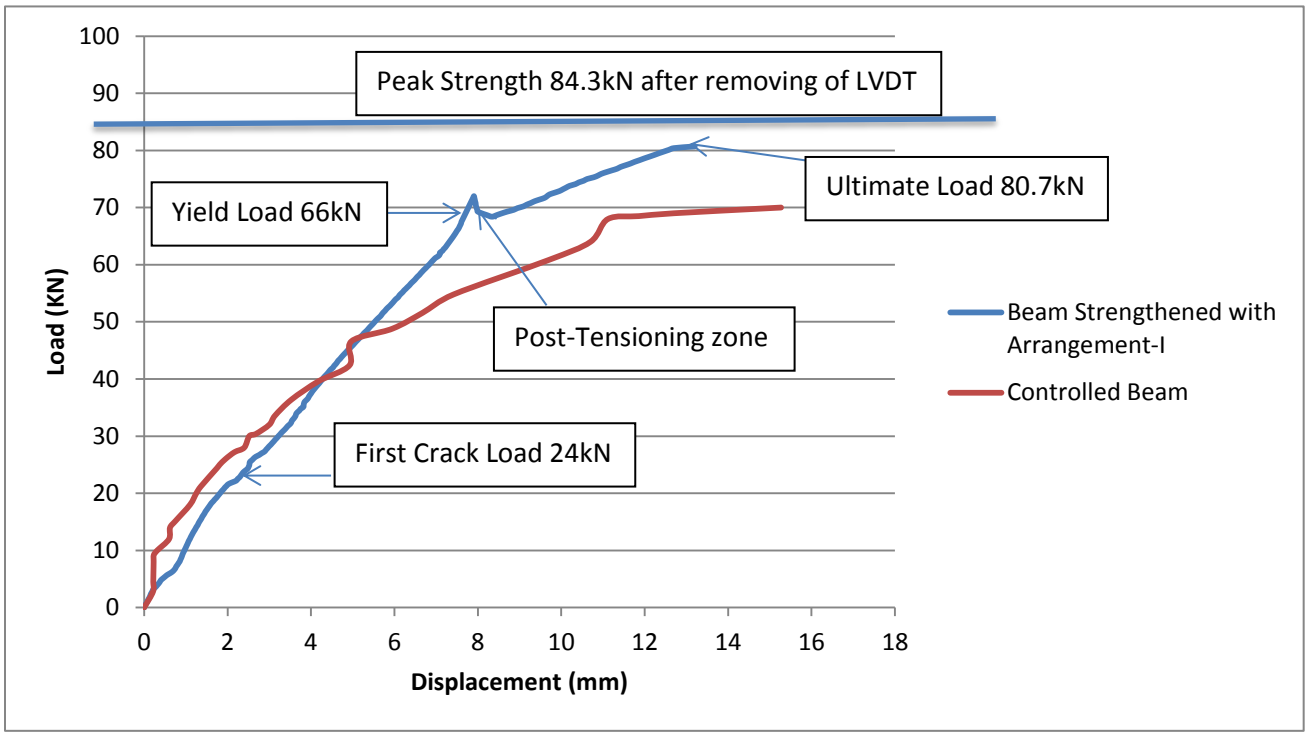

Figure 4.4 Load v/s Displacement curve of Beam Strengthened with Arrangement-I

Firstly, all the necessary arrangements were made similar to that of the controlled beam for conducting the testing. Then the load was applied with the help of hydraulic jack and displacement was measured by LVDT placed on the mid-point of the beam.

Initially, as the load was applied, there was gradually increment of displacement and slope was also not as steep as that of controlled beam because the BFRP maintained the stiffness of the

beam which slows down the rate of increment of graph. As the beam was strengthened with BFRP for increasing its load carrying capacity, the value of first crack load was increased as compared with the controlled beam. The first crack was appeared at the load value of 24kN and the corresponding displacement was 2.108mm. The maximum load that the beam carried was 80.7kN and the displacement at this point was 13.2mm, but the peak strength of this beam was 84.3kN and because of removal of LVDT earlier, the value of displacement at this point was not available. The load at which steel starts yield was 66 kN and the respective displacement at this point was 7.506mm.

Table 4.2 Load v/s Displacement Data of Beam Strengthened with Arrangement-I

Load (kN)	Mid-Point Displacement (mm)	Load (kN)	Displacement (mm)
0	0	35	3.818
2	0.146	40	4.268
4	0.31	45	4.878
6	0.62	50	5.54
8	0.854	55	6.154
10	0.958	60	6.832
12	1.096	65	7.426
14	1.252	70	7.766
16	1.394	72	7.906
18	1.586	70	7.97
20	1.83	70	9.09
22	2.108	72	9.66
24	2.43	74	10.34
26	2.626	78	11.76
28	2.958	80	12.46
30	3.218	80.7	13.2

Initially, as the load increases the value of displacement also increases but at the load value of 72 KN, there was decrement in load but there was no decrement in the value of displacement because this was the post-tensioning zone of beam which shows in the curve. The value of load was decreases from 72 to 70 KN then further increase from 70 to 80.7 KN. The maximum load that the beam was carried or the value of load at which the beam fail was 84.3 KN. There was 15% increment in load carrying capacity of RC beam strengthened with BFRP rectangular strips as compared with the load carrying capacity of controlled beam.

As shown in Fig.31, the beam was failed in flexure as compared to controlled beam, which fail in shear because BFRP has the property of increasing the shear capacity of the RC specimens. It shows that, as the BFRP sheets was placed over the RC beam, it increases its load carrying capacity and also increases the shear strength of the beam strengthened with this arrangement and there was crushing of concrete after fully yielding of steel so full capacity was achieved. As the beam failed in flexure, there was also some shear cracks as moved from center towards support. There was no cracks where the BFRP sheets was present but all the cracks were adjacent to the BFRP sheets, which shows that the no cracks propagates the BFRP sheets because the cracks always propagates from that portion of the beam which was weak in strength and the presence of BFRP sheets increased the strength of RC beam so no cracks propagated from BFRP. The failure pattern of this beam is shown in Figure 4.5.

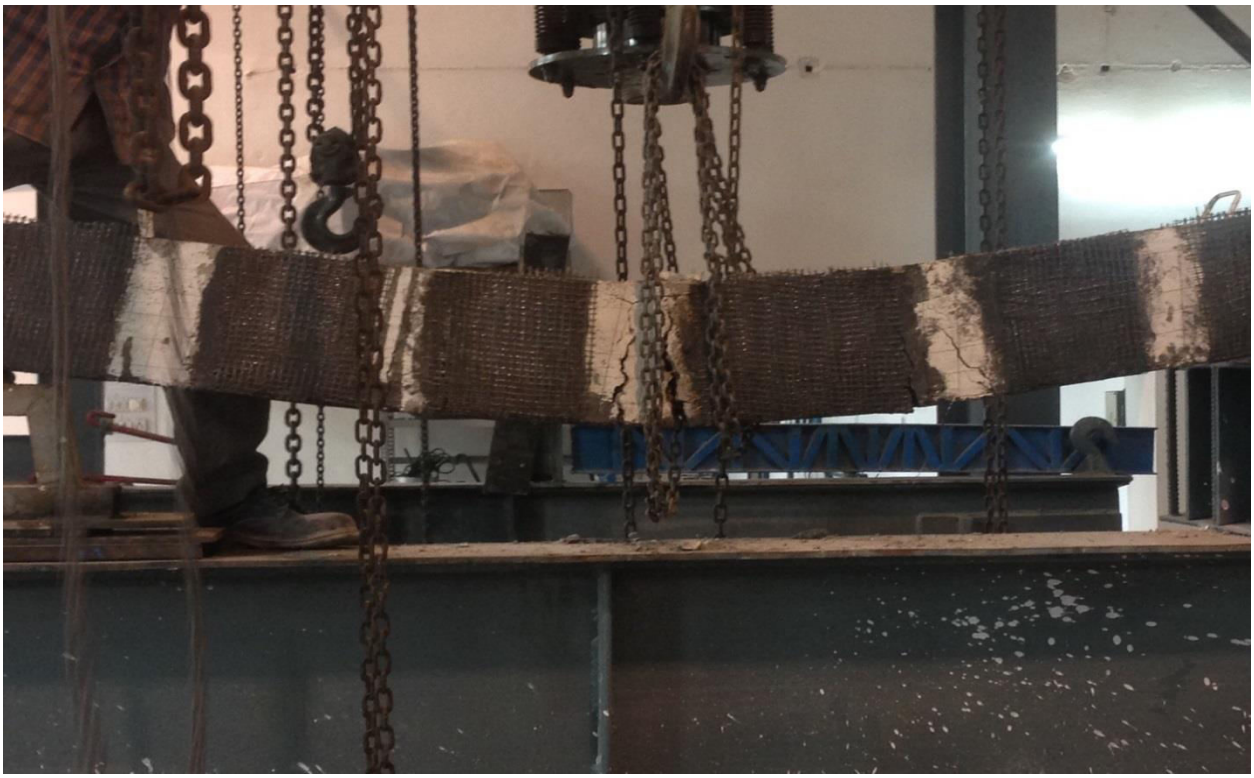

Figure 4.5 Failure and Crack Pattern of Beam Strengthened with BFRP Rectangular Strips

4.2.3 Experiment Result of Beam Strengthened with U-wrap of Basalt FRP

In this arrangement, the strengthening of beam was done with two layers of 2000 mm BFRP sheet each at the all three faces except the top face, where the load was applied and no other type of external shear reinforcement was provided. The load v/s displacement curve is shown in Figure 4.6 and the respective data of load v/s displacement is shown in Table 4.3.

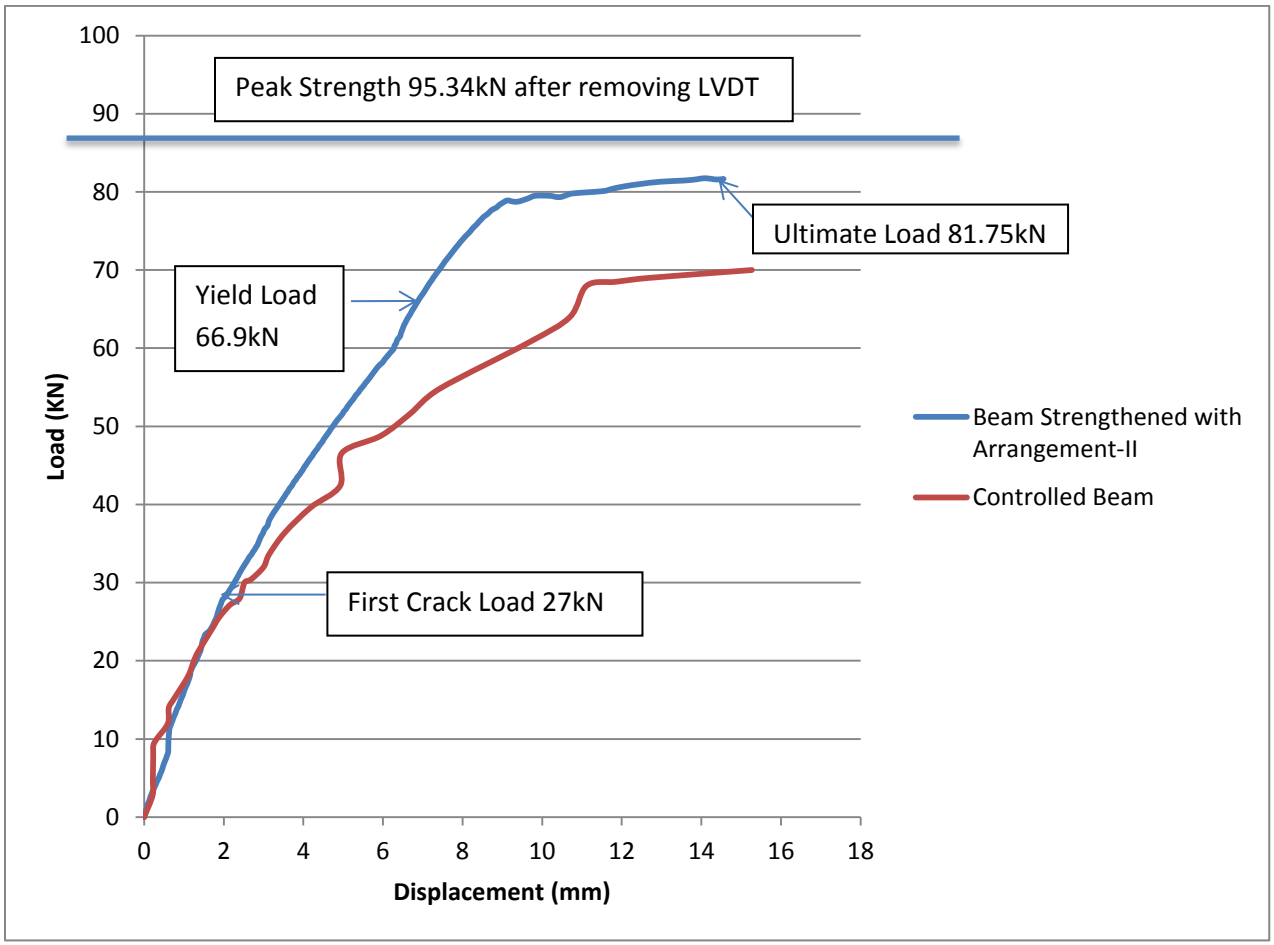

Figure 4.6 Load v/s Displacement curve of Beam Strengthened with Arrangement-II

Firstly, all the necessary arrangements were made similar to that of the controlled beam for conducting the testing. Then the load was applied with the help of hydraulic jack and displacement was measured by LVDT placed on the mid-point of the beam.

Initially, as the load was applied, there was gradually increment of displacement and slope was also not as steep as that of controlled beam because the BFRP maintained the stiffness of the beam which slows down the rate of increment of graph. But as the first cracks appears on the beam, it decreases the stiffness but due to presence of BFRP this decrement was very less so very little effect was observed on the rate of the graph. The value of load at which first crack occurred was 27kN and the respective value of displacement was 1.906 mm.

Table 4.3 Load v/s Displacement Data of Beam Strengthened with Arrangement-II

Load (kN)	Mid-Point Displacement (mm)	Load (kN)	Displacement (mm)
0	0	38	3.128
2	0.128	40	3.378
4	0.266	42	3.646
6	0.444	44	3.938
8	0.592	46	4.174
10	0.61	48	4.474
12	0.682	50	4.754
14	0.852	55	5.512
16	0.988	60	6.276
18	1.146	70	7.394
20	1.31	75	8.202
22	1.444	78	8.852
24	1.666	79	9.664
26	1.846	79.5	9.828
28	1.978	79.35	10.474
30	2.266	79.5	10.568
32	2.5	80	11.536
34	2.728	81	12.456
36	2.944	81.75	14.09

The maximum load that the beam carried was 81.75 kN and the displacement at this point was 14.09 mm. But the peak strength of the beam was 95.34kN and due to removal of LVDT, the value of displacement at this point was not available. The load at which steel starts yield was 66.9kN and the respective displacement at this point was 6.994mm. As we compared with the controlled beam, there was less displacement in beam strengthened with fully u-wrap of BFRP as compared with controlled beam because the beam was fully covered with BFRP sheets and this cover was not easy to break and hence the displacement was less. Due to which, the rate of increase of displacement with load is slow when it compared with referenced beam.

As shown in figure, the beam was failed in flexure as compared to controlled beam, which fail in shear. It shows that, as the BFRP sheets was placed over the RC beam it increases its load carrying capacity and the shear strength of the beam strengthened with this arrangement also increases and there was crushing of concrete after fully yielding of steel so fully capacity was achieved. As the beam failed in flexure, there was few shear cracks as moved from center towards support. The load carrying capacity of the RC beam was increased by 18% as compared to controlled beam. The failure pattern is shown in Figure 4.7.

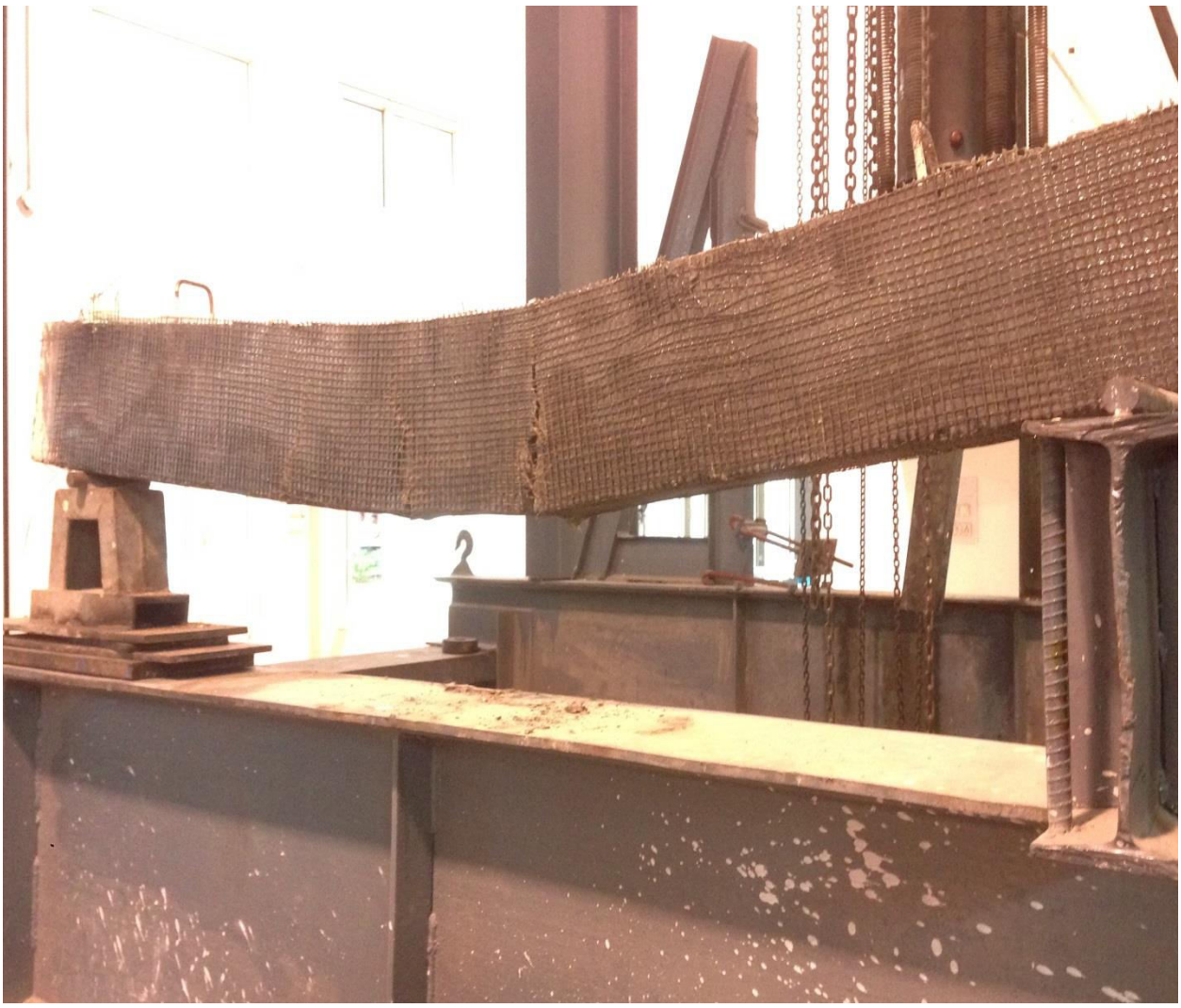

Figure 4.7 Failure and Crack Pattern of Beam Strengthened with Fully BFRP U-wrap

4.2.4 Experiment Result of Beam Strengthened with Inclined Strips of Basalt FRP

In this arrangement, the strengthening of beam was done with two layers of 200 mm inclined strips of BFRP sheet each at a spacing of 100 mm c/c at the all three faces except the top face, where the load was applied and no other type of external shear reinforcement was provided. The layers of BFRP was applied in such a manner that from one side the support will cover with the

BFRP sheet while the other side will have no cover of BFRP sheet. This arrangement was suggested for calculating the proper effect of BFRP on the shear capacity of the beam. The data of load v/s displacement is shown in Table 4.4 and the respective load v/s displacement curve is shown in Figure 4.8.

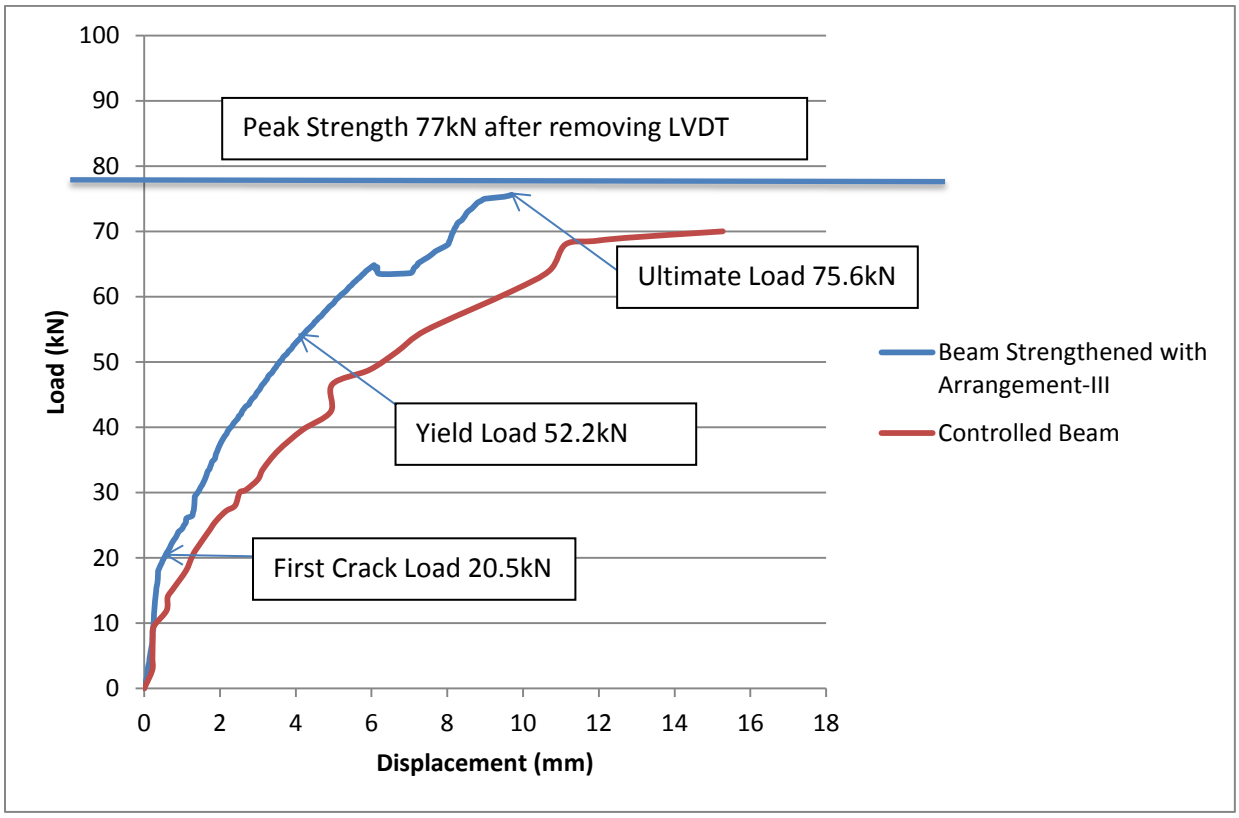

Figure 4.8 Load v/s Displacement curve of Beam Strengthened with Arrangement-III

Firstly, all the necessary arrangements were made similar to that of the controlled beam for conducting the testing. Then the load was applied with the help of hydraulic jack and displacement was measured by LVDT placed on the mid-point of the beam.

Initially, as the load was applying, there was more increment in load as compared to the displacement because the stiffness of the beam was very high and this increment in load was going on until the first crack appears. As the first crack appears, there was loss of stiffness and the displacement started increasing at a high rate. The value of load at which the first crack appears was 20.5kN and the corresponding displacement was 0.580mm. The maximum load that the beam carried was 75.6kN and the displacement at this point was 9.7 mm.

Initially, as the value of load increases there was increment in displacement but after 64.8 KN value of load there was decrement in load but no decrement in displacement was noted and this decrement in load was from 64.8 KN to 64.5 KN and then further the value of load started

increasing. And at last, it achieved the maximum value of 75.6 KN and the beam fail at this value of load.

Table 4.4 Load v/s Displacement Data of Beam Strengthened with Arrangement-III

Load (kN)	Mid-Point Displacement (mm)	Load (kN)	Displacement (mm)
0	0	28	1.32
2	0.082	30	1.412
4	0.128	35	1.856
6	0.184	40	2.268
8	0.218	45	2.946
10	0.25	50	3.586
12	0.26	55	4.302
14	0.3	60	5.152
16	0.34	64.8	6.076
18	0.368	63.9	7.088
20	0.536	64.5	7.144
22	0.702	66	7.48
24	0.908	70	8.176
26	1.124	75.6	9.7

As we compared with the controlled beam, there was less displacement in beam strengthened with inclined strips of BFRP sheet as compared with the controlled beam because the presence of the inclined strips increased the stiffness and due to which, the rate of increase of displacement with load is slow when it compared with referenced beam. The rate of increase of load is very high as compared to all other beams and this beam has the lowest displacement from all the other beams. The displacement was approximate 35% less with respect to the controlled beam. But this

displacement has no negative effect on the load carrying capacity of the beam. The maximum load that the beam carried was 75.6 while the controlled beam carried the load of 70kN.

The crack pattern of this beam was divided into three parts and all these parts are shown in the Figure 4.9 to Figure 4.12. As the fiber arrangement was different in this beam was different on both the ends so the crack pattern also varies depending on this arrangement

Figure 4.9 Failure and Crack Pattern of Beam Strengthened with no Inclined Strips on Face A

Figure 4.10 Failure Pattern of Beam Strengthen with Inclined Strips on support on Face B

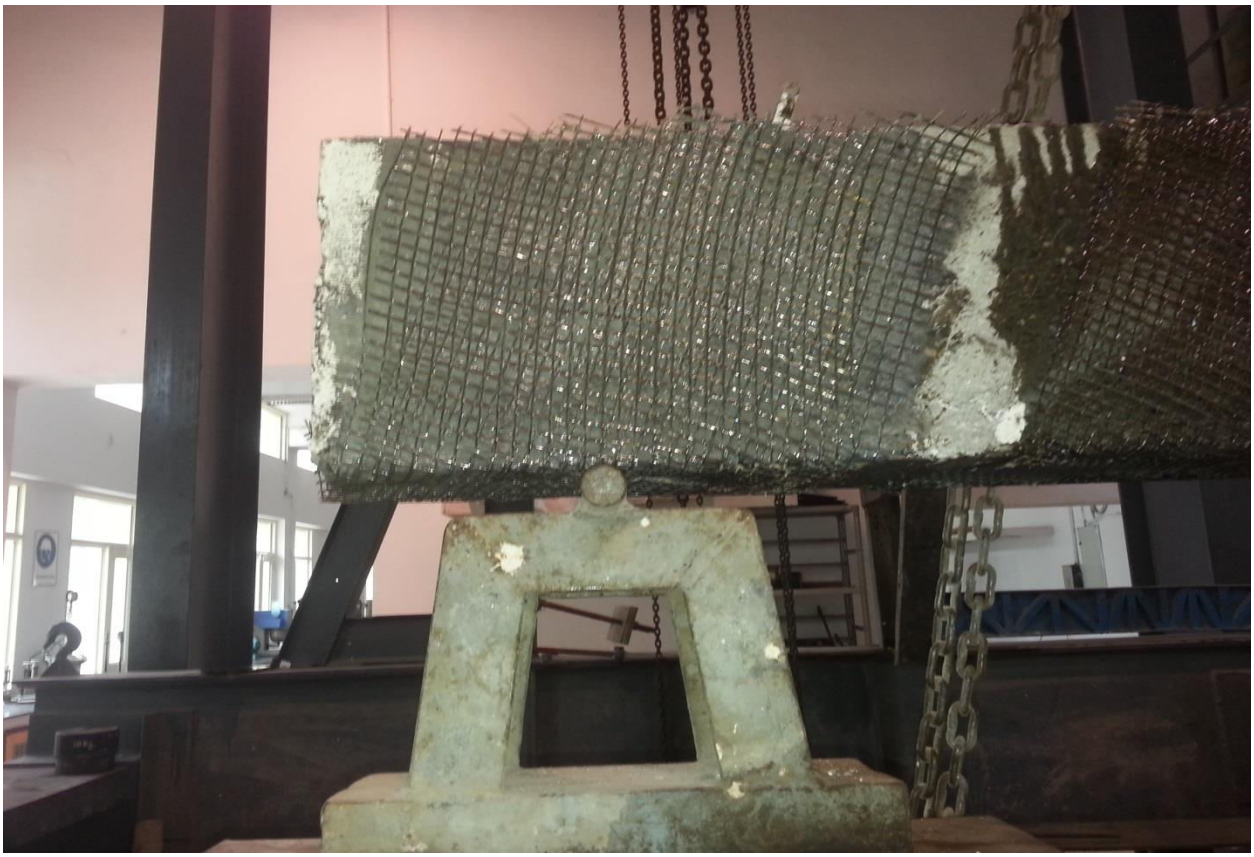

Figure 4.11 Failure Pattern of Beam Strengthened with Inclined Strips on the support

Figure 4.12 Failure and Crack Pattern of Beam Strengthened with Inclined Strips on center

As shown in Figure 4.9, the inclined strips of BFRP sheets were applied on the beam but there was no BFRP on one side of support at Face A. As in controlled beam which was not strengthened with BFRP strips so it failed in shear. Similarly, in this beam where no BFRP strips were on support, the beam failed in shear and not achieving its fully capacity. In Figure 4.10, which shows the Face B of the beam, where BFRP was on the support but as on Face A there was no BFRP so the cracks on Face B were lesser in size as compared to the cracks on Face A.

As the beam failed in shear, so the beam was not capable of achieving its flexural strength so there was no cracks in the mid span of the beam. And on the support, where BFRP sheet was on the both sides of the beam, there were no cracks on this support.

So, it concluded from this test that BFRP increases the shear capacity of the beam but at the places where no BFRP was applied was weak in shear. Hence, the beam was not achieving its flexural strength and failed in shear.

4.2.5 Comparison of Beam Strengthened with Arrangement-I, II and Arrangement-III

In arrangement-I, beam was strengthened with rectangular strips of BFRP sheet of width 200mm placed at a spacing of 100mm c/c and In arrangement-II, beam was strengthened with fully u-wrapping of BFRP sheet and In arrangement-III, beam was strengthened with inclined strips of BFRP sheet of width 200mm and placed at a spacing of 100mm c/c. The load application and displacement measurement and all other arrangements were same in the testing of all types of beams. So that the comparison of these beams will be conducted very easily be.

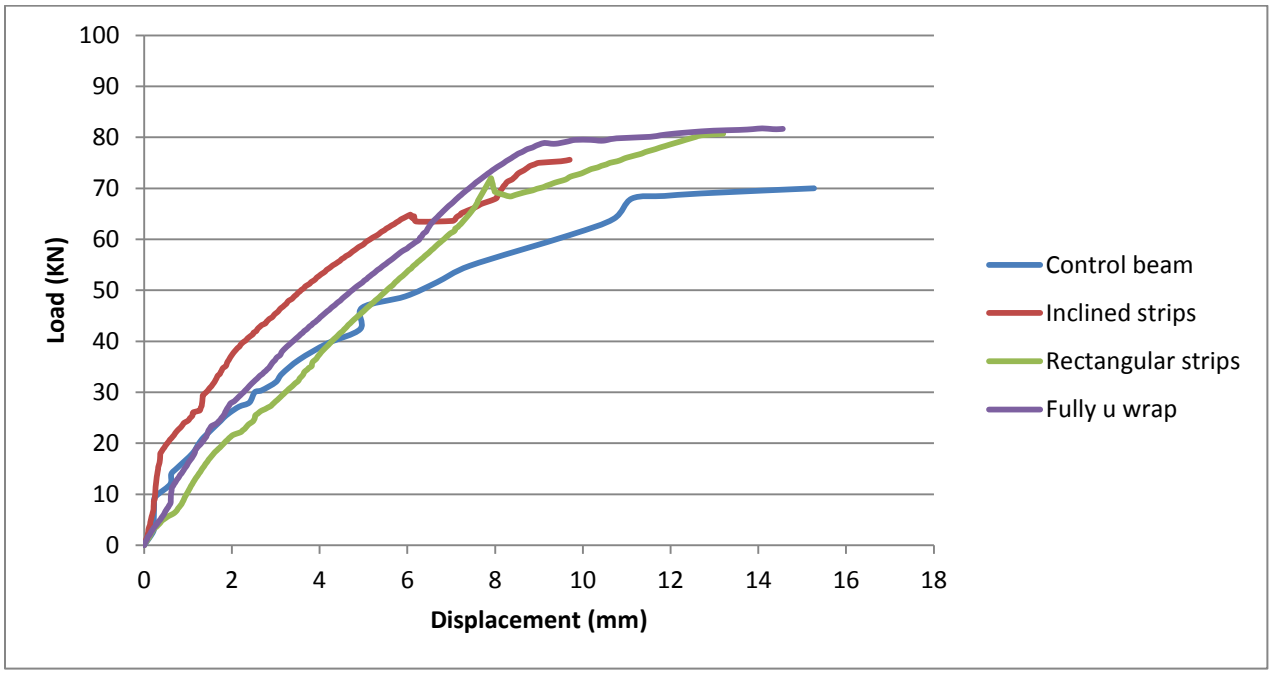

Figure 4.13 Load v/s Displacement Curve of Controlled Beam and with Arrangement-I, II, III

Out of all the beams, the beams with arrangement – I and II failed in flexure while the other two beams i.e. beam strengthened with arrangement-III and controlled beam were failed in shear. The load carrying capacity of beam strengthened with u-wrap was higher among all the beams as shown in Figure 4.13. But the value of displacement of the beam strengthened with inclined strips was less among all the beams because of the stiffness and value of displacement of controlled beam was high among all the beams. All the beams strengthened with BFRP have better load carrying capacity than the controlled beam and also the displacement of all the beams strengthened with BFRP sheet was less than the controlled beam. Among all the beams, the strengthening procedure of fully u-wrap was better because this arrangement not only increases the shear capacity but also increases the flexural capacity of the beam.

4.3 EFFECT OF STRENGTHENING WITH BFRP ON THE LOAD CARRYING CAPACITY OF BEAMS

In this section, first crack load and ultimate load carrying capacity of the controlled beam and the beams strengthened with BFRP with different arrangement will discussed. The results of all the beams were compared with the result of controlled beam.

4.3.1 First Crack Load

The first crack load of all the beams is shown in Figure 4.14. This figure shows that the value of first crack load is highest for beam strengthened with fully u-wrap of BFRP sheet among all the strengthen beams because fully u-wrapping of BFRP sheets has highest capacity among all the arrangements to resist the cracks and it was difficult for cracks to propagate from the fiber. The value of first crack load for this arrangement was 46.8% higher than the value of first crack load of the controlled beam and 12.5% higher than the beam strengthen with rectangular strips and 31.5% higher than the beam strengthen with inclined strips of BFRP.

After the beam strengthened with arrangement-II, beam strengthened with rectangular strips of BFRP sheet has the highest value of first crack load because the presence of BFRP sheets made the beam denser. The value of first crack load was approximately 30% higher than the value of first crack load of controlled beam and 17% higher than the value of first crack load of beam strengthen with inclined strips of BFRP sheets.

The beam strengthened with inclined strips has the minimum increment among all the strengthened beams because this arrangement has little effect on making the beam denser and it was easy for cracks to propagate because one side of support has no covering of basalt fiber reinforced polymer sheets. The value of first crack load was 11% higher than the value of first crack load of the controlled beam. The value of first crack load of the beam strengthen with arrangement-III was 14.5% lesser than the beam strengthen with arrangement-I and 24% lesser than the value of first crack load of the beam strengthen with fully u-wrapping of basalt fiber reinforced polymer sheets.

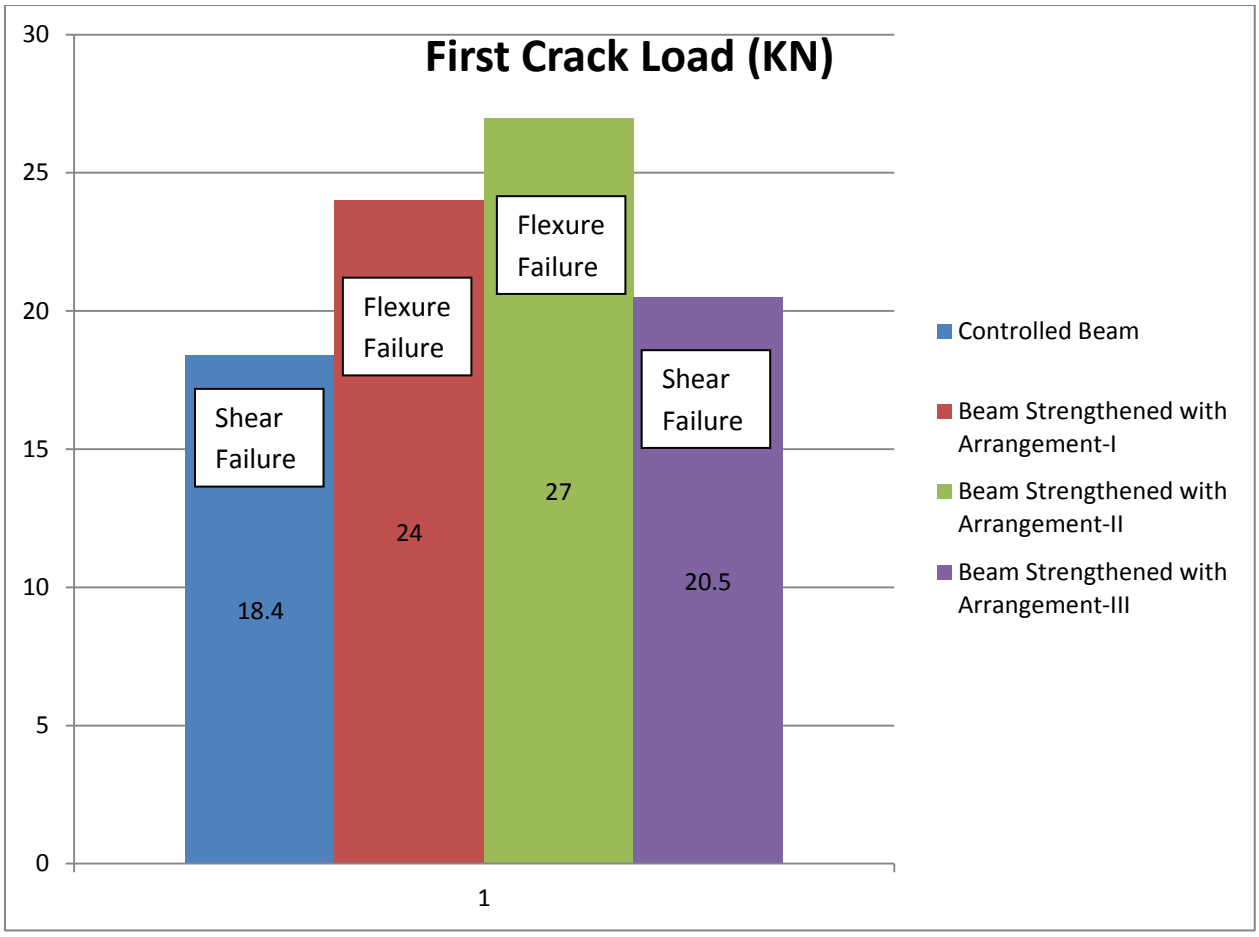

Figure 4.14 First Crack Load of Controlled Beam and Strengthen with Arrangement-I, II, III

4.3.2 Ultimate Load Carrying Capacity

The ultimate load carrying capacity of all the beams is shown in Figure 4.15. This figure shows that the value of ultimate load carrying capacity is highest for beam strengthened with fully u-wrap of BFRP sheet among all the strengthen beams. The value of ultimate load for this arrangement was approximately 18% higher than the value of ultimate load of the controlled beam and 3% higher than the beam strengthen with rectangular strips and 9.33% higher than the beam strengthen with inclined strips of BFRP.

After the beam strengthened with arrangement-II, beam strengthened with rectangular strips of BFRP sheet has the highest value of ultimate load because the presence of BFRP sheets made the beam denser. The value of ultimate load was approximately 14.3% higher than the value of ultimate load of controlled beam and 7% higher than the value of ultimate load of beam strengthen with inclined strips of BFRP sheets.

The beam strengthened with inclined strips has the minimum increment among all the strengthened beams because this arrangement has little effect on making the beam denser and it was easy for cracks to propagate because one side of support has no covering of basalt fiber reinforced polymer sheets. The value of ultimate load was 7.75% higher than the value of ultimate load of the controlled beam. The value of ultimate load of the beam strengthen with arrangement-III was 6.25% lesser than the beam strengthen with arrangement-I and 8.65% lesser than the value of ultimate load of the beam strengthen with fully u-wrapping of basalt fiber reinforced polymer sheets.

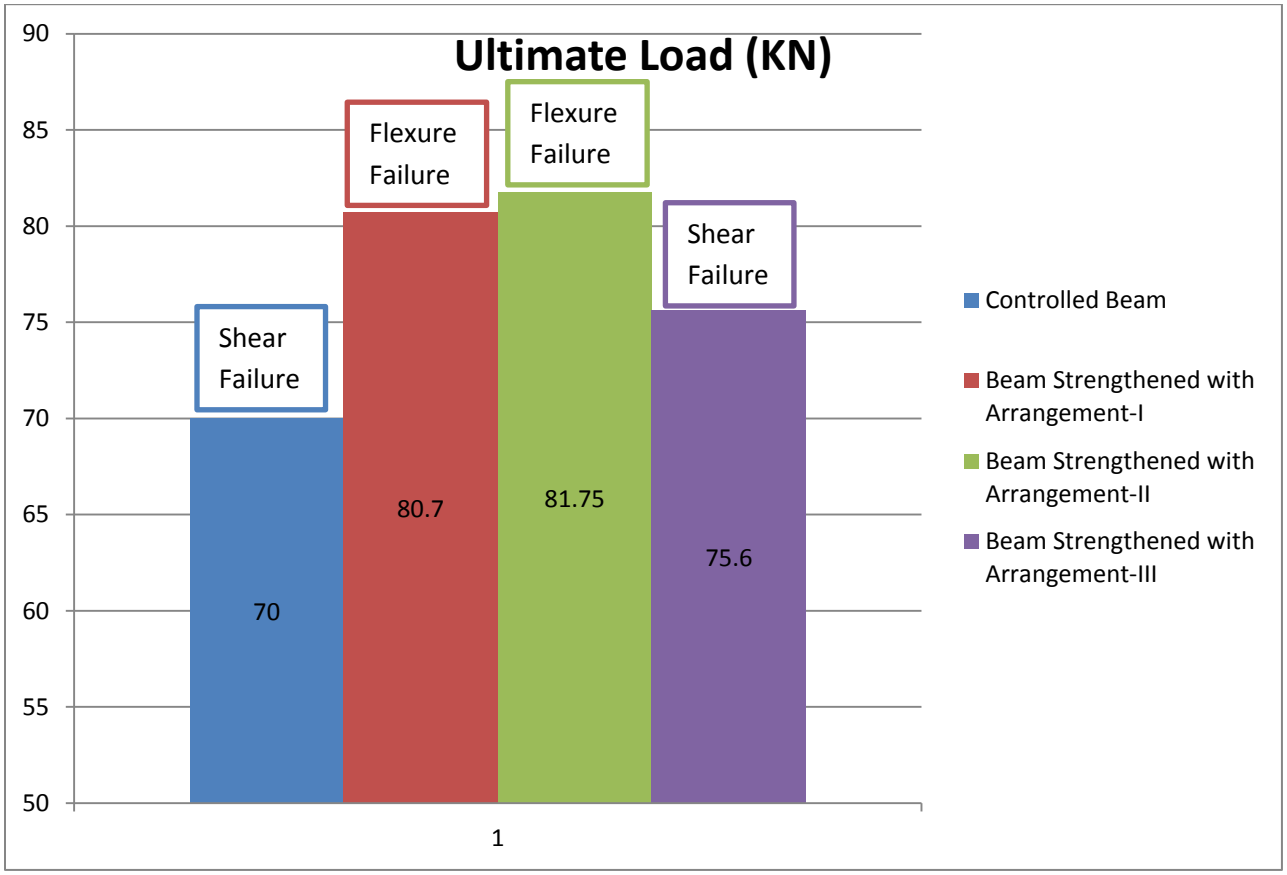

Figure 4.15 Ultimate Load of Controlled Beam and Strengthened with Arrangement-I, II and III

4.3.3 Peak Strength of the Beams

The peak strength of all the beams is shown in Figure 4.16 This figure shows that the value of peak strength is highest for beam strengthened with fully u-wrap of BFRP sheet among all the strengthen beams. The value of peak strength for this arrangement was approximately 36.71% higher than the value of peak strength of the controlled beam and 13% higher than the beam strengthen with rectangular strips and 25% higher than the beam strengthen with inclined strips of BFRP.

After the beam strengthened with arrangement-II, beam strengthened with rectangular strips of BFRP sheet has the highest value of peak strength because the presence of BFRP sheets made the beam denser. The value of peak strength was approximately 21.4% higher than the value of peak strength of controlled beam and 13.33% higher than the value of peak strength of beam strengthen with inclined strips of BFRP sheets.

The beam strengthened with inclined strips has the minimum increment among all the strengthened beams because this arrangement has little effect on making the beam denser and it was easy for cracks to propagate because one side of support has no covering of basalt fiber reinforced polymer sheets. The value of peak strength was 8.57% higher than the value of peak strength of the controlled beam. The value of peak strength of the beam strengthen with arrangement-III was 11.76% lesser than the beam strengthen with arrangement-I and 21% lesser than the value of peak strength of the beam strengthen with fully u-wrapping of basalt fiber reinforced polymer sheets.

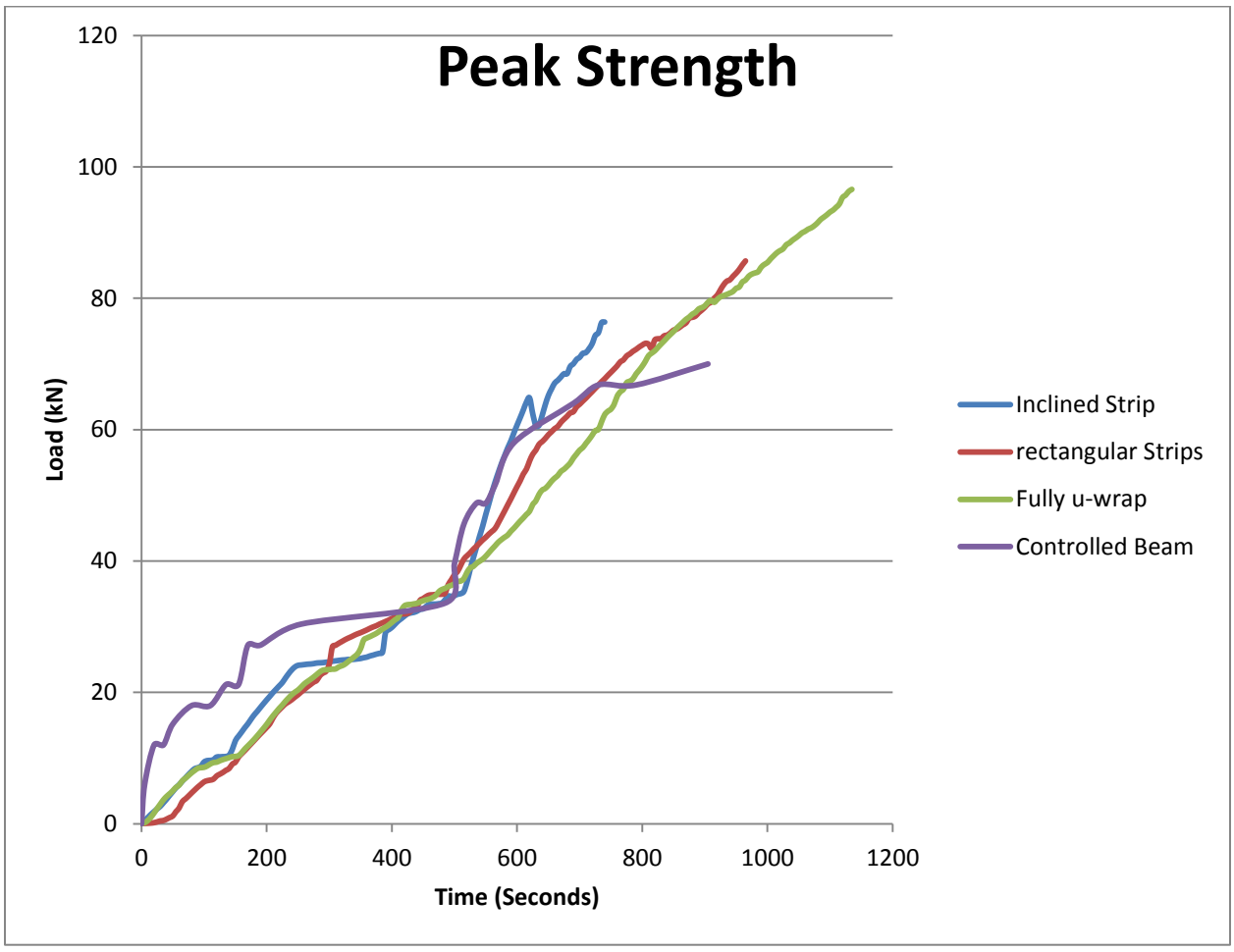

Figure 4.16 Peak Strength of Controlled Beam and Strengthened with Arrangement-I, II and III

4.4 EFFECT OF BFRP STRENGTHENING ON THE STIFFNESS OF BEAM

In this section, the effect of strengthening of beams with BFRP on the stiffness will be discussed. The stiffness of all the beams were calculated at the yielding level of load and it was calculated by dividing the load by the respective displacement. The results of all the strengthening beams were compared with the results of the controlled specimen and the corresponding conclusions were getting.

The Stiffness of all the beams is shown in Figure 4.17. This figure shows that the stiffness of the beam strengthened with inclined strips is highest among all the other beams because the displacement of this beam was lowest among all the other beams and at the yield level of load, this beam has high load to displacement ratio due to which the stiffness of this beam increases by such a large amount. The stiffness of this beam was 70% greater than the stiffness of the controlled beam and 43% greater than the stiffness of the beam strengthen with rectangular strips and 29.7% greater than the beam strengthen with fully u-wrapping of the BFRP sheets.

After the beam strengthened with inclined strips, the stiffness of the beam strengthened with fully u-wrap of BFRP sheet was highest among the remaining beams. The stiffness of this beam was 31.3% greater than the controlled beam and 11% approximate greater than the beam strengthen with rectangular strips.

The beam strengthened with rectangular strips of BFRP has the lowest stiffness among all the strengthened beams. The stiffness of this beam was 20% greater than the controlled beam and 20% less than the beam strengthen with arrangement-II and 30% less than the beam strengthen with arrangement-III.

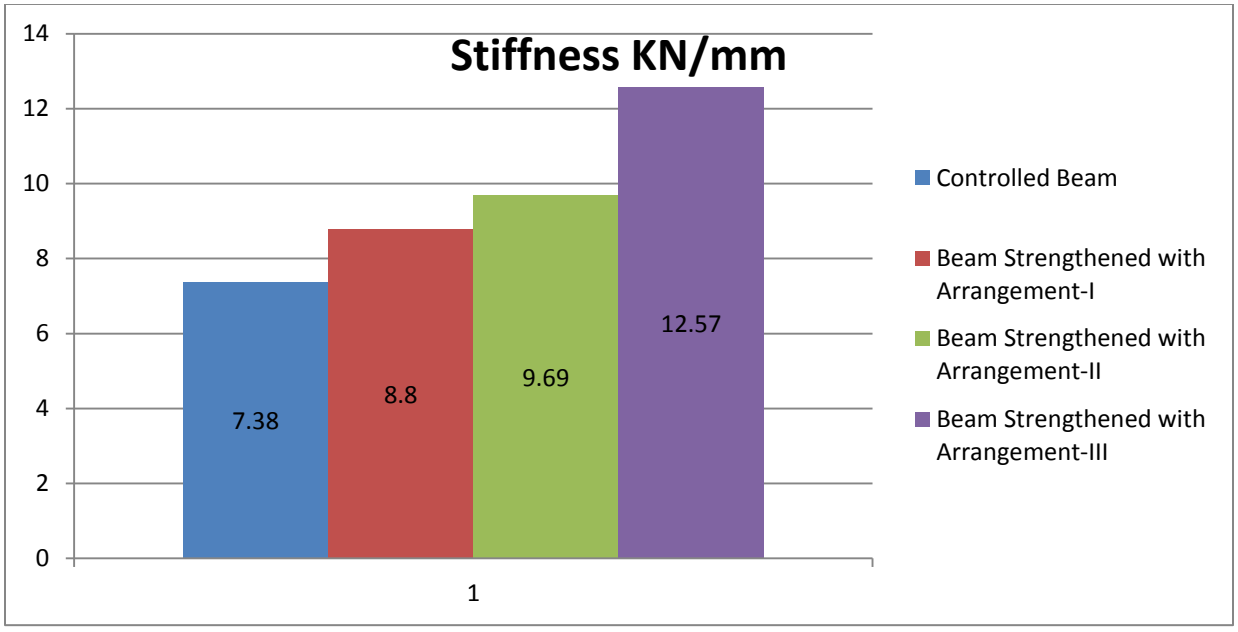

Figure 4.17 Stiffness of Controlled Beam and Strengthened with Arrangement-I, II and III

4.5 Validation of the Experimental Results

In this section, the validation of the experimental results is done by using the analytical approach or mathematical modeling for calculating the load carrying capacity of the RC beams strengthen with externally placed BFRP sheets/strips. Two criteria's are chosen for the validations i.e. shear criteria and flexural criteria. For calculating the shear strength of the RC beam strengthen with externally placed BFRP sheets/strips, firstly calculate the contribution of the shear strength of the beam without the externally placed FRP reinforcement by using ACI model and then the contribution of the shear strength of the externally placed FRP will calculate. To calculate the contribution of the shear strength of the externally placed BFRP, proposed model by Chen-Teng and Chen (2013) is used. For calculating the flexural strength, model proposed by Sallam (2015) is used. At last, the results from this analytical model are compared with the experimental results obtained from the study.

4.5.1 Shear Strength of the Beam

In the latest studies, various experiments or investigation was conducted for the implementation of various mathematical or analytical models in different design codes and on the basis of which various different guidelines for the strengthening system of RC structures with externally placed FRPs were published or mentioned.

Computation of the shear strength of the RC structures strengthened with externally placed or bonded FRP is very necessary for the justification of the experimental results and also for comparison. The shear strength of the RC beam strengthened with FRP can expressed as

$$V_u = V_c + V_s + kV_f$$

Where,

V_u is the shear strength of the RC beam strengthened with FRP

V_c is the contribution of concrete in shear strength

V_s is the contribution of steel in shear strength

V_f is the contribution of FRP in shear strength

k is the shear distribution factor

4.5.1.1 Contribution of Shear strength of the Beam without External FRP

As the work of estimation of contribution of shear strength of the concrete and steel is very complex due to their heterogeneous nature and also due to their complex mechanisms of transferring shear. Many scholars have proposed various numerical models based on these

mechanisms. Various parameters which effect the contribution of the shear strength of the concrete are compressive strength of concrete, shear span to depth ratio, depth of the beam, steel reinforcement and different axial forces etc.

According to ACI, the contribution of the shear strength of the concrete is given as:

$$V_c = C_1 * (1 - 0.35 * a_v/d) * f_t * w * D$$

Where,

C_1 = Constant depend on the grade of concrete

A_v = shear span

d = effective depth of the beam

f_t = tensile strength of the concrete

w = width of the beam

D = total depth of the beam

The contribution of the shear strength of the steel is computed on the basis of an assumption that shear crack intersect the steel at failure. There are various parameters which effect the contribution of the shear strength of the steel and these factors are area of reinforcement, yielding strength of the steel, spacing between the stirrups and effective of the RC beam etc.

According to the ACI, the contribution of the shear strength of the steel is given as:

$$V_s = 0.9 * d * A_s * f_y * (\sin\beta + \cos\beta)/s$$

Where,

d = effective depth of the beam

A_s = area of the stirrups from where crack intersect the steel

f_y = yield strength of steel

β = angle of the inclination of the stirrups w.r.t. the beam axis

s = spacing of the stirrups

Calculations:

$V_c = C_1 * (1 - 0.35 * a_v/d) * f_t * w * D$

$C_1 = 0.72$

$a_v/d = 567/210 = 2.7$

$f_t = 0.27 * (f_c) \wedge (2/3)$

Where,

f_c = Compressive strength of the concrete

f_c = 34 MPa (Calculated experimentally)

$f_t = 0.27 * (34) \wedge (2/3)$

$f_t = 2.83$ N/mm^2

w = 135 mm

D = 230 mm

$V_c = 0.72 * (1 - 0.35 * 2.7) * 4.85 * 135 * 230$

V_c = 12290 N

And

$V_s = 0.9 * d * A_s * f_y * (\sin\beta + \cos\beta)/s$

d = 210 mm

$f_y = 500$ N/mm^2

$A_s = 28.26$ mm^2

$\beta = 90^o$

s = 150 mm c/c

$V_s = 0.9 * 210 * 28.26 * 500 * (\sin 90^o + \cos 90^o)/150$

V_s = 17803.8 N

4.5.1.2 Contribution of Shear strength of the External FRP

Chen-Teng and Chen proposed a model for calculating the contribution of the shear strength of the external FRP in 2013. And they also introduced a factor known as shear distribution for calculating the relation between internal reinforcement i.e. steel and the external reinforcement i.e. FRP. This method is useful in calculating the shear strength in which FRP was placed wither by side bonding or by U-jacketing.

According to Chen-Teng and Chen, the calculation of the contribution of the shear strength of FRP is given as:

$$V_{frp} = 2 * f_{frp,e} * t_f * w_f * (h_f * (\cot\Phi + \cot\beta)/\sin\beta/sf)$$

Where,

$f_{frp,e}$ = effective stress of the FRP

tf = thickness of the FRP = 2 * 0.7 = 1.4 mm

wf = width of the FRP

hf = effective height of the FRP (0.9d) = 0.9 *210 = 189 mm

β = angle between fiber and longitudinal axis of the beam

Φ = angle between crack and longitudinal axis of the beam

sf = spacing between FRP strips

and

$$f_{frp,e} = D_{frp} * \sigma_{frp,max}$$

Where,

D_{frp} = stress distribution factor

$\sigma_{frp,max}$ = maximum stress in FRP

When $L_{max} > L_e$ then,

$$\sigma_{frp,max} = (2 * E_f * G_f/t_f)^{(1/2)}$$

When $L_{max} < L_e$ then,

$$\sigma_{frp,max} = (\text{Sin}((\pi/2)*\Lambda)) * (2 * E_f * G_f/t_f)^{(1/2)}$$

Where, L_{max} is

$$= hf/\text{Sin}\beta \qquad \text{For U-strips}$$

$$= hf/2/\text{Sin}\beta \qquad \text{For side bonding}$$

Where,

$$L_e = (\partial_f * E_f * t_f/\Gamma_f)^{(1/2)}$$

$\lambda = L_{max}/L_e$

$G_f = 0.308 * ((\beta_w)^2) * ((f_t)^(1/2))$

E_f = Elastic Modulus of FRP = 105 GPa (Provided by manufacturer)

$\tau_f = 1.5 * \beta_w * f_t$

$\partial_f = 2 * G_f / \tau_f$

$$\beta_w = \left(\frac{2-\frac{wf}{sf*Sin\beta}}{1+\frac{wf}{sf*Sin\beta}}\right)^{\frac{1}{2}}$$

$f_t = 0.395 * ((f_{cu})^(0.55)) = 3.11$ MPa

$f_{cu} = f_c/0.8 = 42.5$ MPa

And when $\lambda \leq 1$ then,

$D_{frp} = (2/(\pi/2)) * [1 - Cot(\pi\lambda/2)]$

When $\lambda > 1$ then,

$D_{frp} = (1 - (\pi - 2))/(\pi\lambda)$

Calculations:

(1) Beam Strengthen with 200 mm wide BFRP Rectangular Strips

$w_f = 200$ mm

$s_f = 400$ mm

$\beta = 90^o$

$L_{max} = h_f/Sin\beta$

$L_{max} = 189/Sin90^o$

$L_{max} = 189$ mm

$$\beta_w = \left(\frac{2-\frac{wf}{sf*Sin\beta}}{1+\frac{wf}{sf*Sin\beta}}\right)^{\frac{1}{2}}$$

$\beta_w = 1$

$G_f = 0.308 * ((\beta_w)^2) * ((f_t)^(1/2))$

$G_f = 0.308 * ((1)^2) * ((3.11)^(1/2))$

$G_f = 0.54$

$\Gamma_f = 1.5 * \beta_w * f_t$

$\Gamma_f = 4.665$

$\partial_f = 2 * G_f / \Gamma_f$

$\partial_f = 2 * 0.54 / 4.665$

$\partial_f = 0.23$

$L_e = (\partial_f * E_f * t_f/\Gamma_f) ^ (1/2)$

$L_e = (0.23 * 105000 * 1.4/4.665) ^ (1/2)$

$L_e = 85.13$ mm

$\lambda = L_{max}/L_e$

$\lambda = 189/85.13$

$\lambda = 2.22$

As $L_{max} > L_e$

$\sigma_{frp,max} = (Sin((\pi/2)*\lambda)) * (2 * E_f * G_f/t_f)^(1/2)$

$\sigma_{frp,max} = 284.605$ MPa

As $\lambda > 1$

$D_{frp} = (1 - (\pi - 2))/(\pi\lambda)$

$D_{frp} = 0.84$

$f_{frp,e} = D_{frp} * \sigma_{frp,max}$

$f_{frp,e} = 0.84 * 284.605$

$f_{frp,e} = 239.07$ MPa

$V_{frp} = 2 * f_{frp,e} * t_f * w_f * (h_f * (cot\Phi + cot\beta)/sin\beta/sf)$

$V_{frp} = 63257.92$ N

(2) Beam Strengthen with 200 mm wide BFRP Inclined Strips

w_f = 200 mm

s_f = 400 mm

$\beta = 45^o$

$L_{max} = h_f/Sin\beta$

$L_{max} = 189/Sin45^o$

L_{max} = 267.25 mm

$$\beta_w = \left(\frac{2-\frac{wf}{sf*Sin\beta}}{1+\frac{wf}{sf*Sin\beta}}\right)^{\frac{1}{2}}$$

β_w = 0.87

$G_f = 0.308 * ((\beta_w)^2) * ((f_t)^(1/2))$

$G_f = 0.308 * ((0.87)^2) * ((3.11)^(1/2))$

G_f = 0.41

$\tau_f = 1.5 * \beta_w * f_t$

τ_f = 4.06

$\partial_f = 2 * G_f / \tau_f$

$\partial_f = 2 * 0.41 / 4.06$

∂_f = 0.2

$L_e = (\partial_f * E_f * t_f/\tau_f) ^ (1/2)$

$L_e = (0.2 * 105000 * 1.4/4.06) ^ (1/2)$

L_e = 85.1

$\lambda = L_{max}/L_e$

$\lambda = 267.25/85.1$

λ = 3.14

As $L_{max} > L_e$

$\sigma_{frp,max}$ = (Sin((π/2)*ʎ)) * (2 * E_f *G_f/t_f)^(1/2)

$\sigma_{frp,max}$ = 247.99 MPa

As ʎ > 1

D_{frp} = (1 - (π - 2))/(πʎ)

D_{frp} = 0.0.88

$f_{frp,e}$ = D_{frp} * $\sigma_{frp,max}$

$f_{frp,e}$ = 0.89 * 247.99

$f_{frp,e}$ = 218.23 MPa

V_{frp} = 2 * $f_{frp,e}$ * t_f * w_f * (h_f * (cotΦ + cotβ)/sinβ/sf)

V_{frp} = 57743.66 N

(3) Beam Strengthen with 2000 mm wide BFRP full U-wrap

β = 90°

L_{max} = h_f/Sinβ

L_{max} = 189/Sin90°

L_{max} = 189 mm

$$\beta_w = \left(\frac{2-\frac{wf}{sf*Sin\beta}}{1+\frac{wf}{sf*Sin\beta}}\right)^{\frac{1}{2}}$$

β_w = 1.11

G_f = 0.308 * ((β_w)^2) * ((f_t)^(1/2))

G_f = 0.308 * ((1.11)^2) * ((3.11)^(1/2))

G_f = 0.67

ɾ$_f$ = 1.5 * β_w * f_t

ɾ$_f$ = 5.18

∂_f = 2 * G_f / ɾ$_f$

∂_f = 2 * 0.67 / 5.18

$\partial_f = 0.26$

$L_e = (\partial_f * E_f * t_f/r_f) \wedge (1/2)$

$L_e = (0.26 * 105000 * 1.4/5.18) \wedge (1/2)$

$L_e = 85.9$ mm

$\lambda = L_{max}/L_e$

$\lambda = 189/85.9$

$\lambda = 2.2$

As $L_{max} > L_e$

$\sigma_{frp,max} = (Sin((\pi/2)*\lambda)) * (2 * E_f * G_f/t_f)\wedge(1/2)$

$\sigma_{frp,max} = 317.02$ MPa

As $\lambda > 1$

$D_{frp} = (1 - (\pi - 2))/(\pi\lambda)$

$D_{frp} = 0.83$

$f_{frp,e} = D_{frp} * \sigma_{frp,max}$

$f_{frp,e} = 0.83 * 317.02$

$f_{frp,e} = 263.13$ MPa

$V_{frp} = 2 * f_{frp,e} * t_f * w_f * (h_f * (\cot\Phi + \cot\beta)/\sin\beta/sf)$

$V_{frp} = 73105.41$ N

4.5.1.3 Total Shear Strength of the Beam

For calculating the total shear strength of the beam, first interaction between the contribution of the shear strength of the steel and the contribution of the shear strength of the FRP has to be find out. For this interaction, a factor 'k' has to calculate. The expression for 'k' is given as:

$$k = 1 - u * (1 - k_s)$$

Where,

$$u = V_s/V_f$$

$k_s = 0.2$ For U-strips

The shear strength of the RC beam strengthened with FRP can expressed as

$$V_u = V_c + V_s + kV_f$$

(1) Beam Strengthen with 200 mm wide BFRP Rectangular Strips

u = 17803.8/63257.92

u = 0.28

k = 1 – 0.28 * (1 - 0.2)

k = 0.776

V_u = 12290 + 17803.8 + 0.776 * 63257.92

V_u = 79181 N

(2) Beam Strengthen with 200 mm wide BFRP Inclined Strips

u = 17803.8/57743.66

u = 0.3

k = 1 – 0.3 * (1 - 0.2)

k = 0.776

V_u = 12290 + 17803.8 + 0.76 * 57743.66

V_u = 73979 N

(3) Beam Strengthen with 2000 mm wide BFRP full U-wrap

u = 17803.8/73105

u = 0.243

k = 1 – 0.243 * (1 - 0.2)

k = 0.8056

V_u = 12290 + 17803.8 + 0.8056 * 73105

V_u = 88986 N

4.5.2 Flexural Strength of the Beam

In the latest studies, various experiments or investigation was conducted for the implementation of various mathematical or analytical models in different design codes and on the basis of which various different guidelines for the strengthening system of RC structures with externally placed FRPs were published or mentioned. There are various complications in this task of modeling which require active study and the mechanism of resistance is also complex and which need more accurate prediction. The flexural strength of the beam was calculated on the basis of model provided by Sallam et al, 2015.

Computation of the flexure strength of the RC structures strengthened with externally placed or bonded FRP is very necessary for the justification of the experimental results and also for comparison. The flexure strength of the RC beam strengthened with FRP can expressed as

$$V_u = \frac{1.2 * Mr}{Ls}$$

Where,

M_r = Total moment of the section of the beam

$M_r = M_u + M_f$

M_u = Moment due to concrete and steel

M_f = Moment due to fiber

L_s = Shear Span of the beam

According to I.S., the moment due to concrete and steel can also be calculated as:

b = Width of the beam = 135 mm

D = Total depth of the beam = 230 mm

Cover = 20 mm

d = effective depth of the beam = 210 mm

A_{st} = Area of tension steel = 2 * 3.14 * 12 * 12/4 = 226.08 mm^2

Asc = Area of compression steel = 2 * 3.14 * 10 * 10/4 = 157 mm**2**

Grade of concrete = M25

Steel reinforcement = Fe 500

f_{ck} = 25 MPa and f_y = 500 MPa

$f_{cc} = 0.447 * f_{ck}$

$f_{cc} = 0.447 * 25 = 11.175$ MPa

$f_{sc} = 0.87 * f_y$

$f_{sc} = 0.87 * 500 = 435$ MPa

Limiting strain in steel, $\epsilon_{su} = 0.002 + \frac{0.87*fy}{Es}$

$= 0.002 + 0.87 * 500/200000 = 0.004175$

Calculate, the depth of neutral axis for a balanced section,

$$x_{u,max} = \frac{0.0035*d}{0.0055+\frac{0.87*fy}{Es}}$$

$x_{u,max} = (0.0035 * 210)/(0.0055 + 0.002175)$

$x_{u,max} = 95.76$ mm

Let xu, be the depth of the neutral axis and for the equilibrium of the internal forces on the section

$$C_u = T_u$$

$$0.362 * f_{ck} * b * x_u + A_{sc} * (f_{sc} - f_{cc}) = 0.87 * f_y * A_{st}$$

$$0.362 * 25 * 135 * x_u + 157 * (435 - 11.175) = 0.87 * 500 * 226.08$$

$$x_u = 26.03 \text{ mm}$$

Since $x_u < x_{u,max}$, the section is under-reinforced

Strain in tension steel,

$\epsilon_s = 0.0035 * (d - x_u)/x_u$

$\epsilon_s = 0.0035 * (210 - 26.03)/26.03$

$\epsilon_s = 0.0247$

As, $\epsilon_s > \epsilon_{su}$, hence tension steel yields.

The actual strain in compression steel is

$\epsilon_{sc} = 0.0035 * (x_u - d')/x_u$

$\epsilon_{sc} = 0.0035 * (26.03 – 20)/26.03$

$\epsilon_{sc} = 0.0081$

As, $\epsilon_{sc} > \epsilon_{su,}$ hence compression steel also yields.

Then, the moment is calculated as:

$M_u = 0.362 * f_{ck} * x_u * b *(d- 0.416\ x_u) + A_{sc} * (f_{sc} – f_{cc}) * (d – d')$

$M_u = 0.362 * 25 * 95.76 * 135 * (210 - 0.416 * 95.76) + 157 * (435 – 11.175) * (210 – 20)$

$M_u = 32550980$Nmm = 32.55 kNm

Moment due to the fiber is calculated as:

$$M_f = F_f * (d_f – c)$$

Where,

c = Distance from top fiber of the beam to the neutral axis of the section

d_f = Depth of the fiber

And,

$$F_f = \epsilon_f * E_f * A_f$$

$$f_{frp,e} = \epsilon_f * E_f$$

$$E_f = 105000 \text{ MPa}$$

(1) Beam strengthen with 200mm wide rectangular strips

$A_f = 200 * 210$

$A_f = 4200\ mm^2$

$f_{frp,e} = 239.07$

$F_f = 239.07 * 4200 = 100380$ N

$c = 210 – 95.46 = 114.54$ mm

$d_f = 210$ mm

$M_f = 10038 * (210 – 114.54) = 9582270$ Nmm

$M_f = 9.58$ kNm

Total moment = 32.55 + 9.58 = 42.13

Hence, Vu = 1.2 * 42.13/0.57 = 84.69kN

(2) Beam strengthen with 200mm wide inclined strips

A_f = 200 * 210

A_f = 4200 mm^2

$f_{frp,e}$ = 218.23

F_f = 218.23 * 4200 = 91560 N

c = 210 – 95.46 = 114.54 mm

d_f = 210 mm

M_f = 91560 * (210 – 114.54) = 8740310 Nmm

M_f = 8.74 kNm

Total moment = 32.55 + 8.74 = 41.29

Hence, Vu = 1.2 * 41.29/0.57 = 79.69 kN

(3) Beam strengthen with 2000mm wide fully U-wrap

A_f = 2000 * 210

A_f = 42000 mm^2

$f_{frp,e}$ = 263.13

F_f = 263.13 * 42000 = 110514 N

c = 210 – 95.46 = 114.54 mm

d_f = 210 mm

M_f = 110514 * (210 – 114.54) = 10549723 Nmm

M_f = 10.54 kNm

Total moment = 32.55 + 10.54 = 43.09

Hence, Vu = 1.2 * 43.09/0.57 = 90.71 kN

4.5.3 Comparison between Analytical and Experimental Results

For the analytical validation, the results from obtained from the analytical study is compared with the results obtained from the experimental study. The results of this comparison are shown in Table 4.5.

Table 4.5 Comparison of Analytical and Experimental Results of Beam

Beam Label	Load Carrying Capacity of the Beam (kN)			Mode of Failure	Ratio
	Theoretical Results		Experimental Results		
	Shear Criteria	Flexure Criteria			
Control Beam	68.5	72.7	70	Shear	1.02
Beam strengthen with Arrangement-I	79.2	84.69	83.8	Flexure	1.05
Beam strengthen with Arrangement-II	88.98	90.71	95.3	Flexure	1.07
Beam strengthen with Arrangement-III	73.97	79.69	74.7	Shear	1.01

From this Table 4.5, it is found out that the analytical results are correlating with the experimental results of the shear strength, having ratio approximate equal to 1.

CHAPTER-5 CONCLUSIONS

The starting of this thesis was with study of various research papers, which helps in finding the perfect ideology for the strengthening of RC beams with FRP. The main objective of this thesis is to find out the effect of BFRP sheet on the strengthening of the RC beams under shear. The whole investigation is depends upon the different arrangement of the BFRP sheets in which they applied externally on the RC beams. The main focused of this thesis is on the ultimate load carrying capacity of the beams and the crack pattern under failure of all the beams and the stiffness and first crack load of the beams and their comparison. On the basis of which, the following conclusions have drawn:

1. The externally placed BFRP has increases the ultimate load carrying capacity of the RC beams from 8% to 17 % for arrangement-III to arrangement-II respectively.
2. The externally placed BFRP has increases the value of first crack load of the RC beams from 19.55% for inclined strips, 38% for rectangular strips to 48.9% for fully u-wrap of BFRP sheets.
3. The stiffness of the beam strengthened with BFRP sheet also increases as compared with the controlled beam. The stiffness of beam strengthened with inclined strips increased by 20%, 31.3% and 70% for arrangement-I, II and III respectively.
4. The beam strengthened with arrangement-I and II not only increases the shear capacity of the beam but also increases the flexural capacity of the RC beams while the beam strengthened with arrangement-III failed in shear. From this, it is concluded that the inclined strips of the BFRP sheet has very less effect on increasing the shear capacity of the RC beam.
5. Among all the BRFP strengthening techniques, the strengthening of the beam by fully u-wrapping of BFRP sheet is more effective than the other techniques. This technique not only increases the first crack load but also the value of ultimate load carrying capacity also increases.
6. The controlled beam was failed in shear with a sudden drop in the value of load whereas the failure of the strengthen beams is in a gradual pattern except for the beam which was strengthened with the inclined strips of BFRP. This beam also failed in shear followed almost the same pattern as of controlled beam i.e. in shear.

7. The crack width and the value of displacement were decreasing with the use of the BFRP sheets.
8. The beam strengthened with inclined strips has two pattern of cracking i.e. the support covered with BFRP sheet has no crack but the support which has no covering of BFRP sheet failed in shear. There are least cracks on the face where fiber is there and more cracks are on those face where no fiber is there.
9. There was no debonding of the BFRP sheets from the beam which shows that the BFRP has more efficiency on achieving the fully strength of the RC beams.
10. The epoxy is sufficient for placing the BFRP sheet over the grinded surface of the RC beams.

As the BFRP sheet has significant effect on the strengthening of the RC beam but placement of the BFRP sheet plays a major role in achieving the full strength of the beam and also on increasing the stiffness of the beam.

REFERENCES

1. Ahmet B. Kizilkanat, Kabay N., Akyüncü V., Chowdhury S., Abdullah H. Akça, "Mechanical properties and fracture behavior of basalt and glass fiber reinforced concrete: An experimental study". Construction and Building Materials, 100, 2015, 218–224.
2. Al-Amery R. and Al-Mahaidi R., "Coupled flexural-shear retrofitting of RC beams using CFRP straps". Composite Structures, 75, 2006, 457-464.
3. Belarbi A. and Acun B., "FRP systems in Shear Strengthening of Reinforced Concrete Structures". Procedia Engineering, 57, 2013, 2-8.
4. Branston J., Das S., Kenno S. Y., Taylor C., "Mechanical behaviour of basalt fiber reinforced concrete". Construction and Building Materials, 124, 2016, 878–886.
5. Branston J., Das S.,. Kenno S. Y, Taylor C., "Influence of basalt fibers on free and restrained plastic shrinkage". Cement and Concrete Composites, 74, 2016, 182-190.
6. Chen G. M., Teng J. G., Chen J. F. and Rosenboom O. A., "Interaction Between Steel Stirrups and Shear-Strengthening FRP Strips in Beams". ASCE- Journal of Composites for construction, Vol. 6, No. 9, 2010, 205-213.
7. Chen J. F. and Teng J. G., "Shear Capacity of Fiber Reinforced Polymer Strengthened Reinforced Concrete Beams: Fiber Reinforced polymer Rupture". ASCE- Journal of Structural Engineering, Vol. 3, No. 5, 2003, 195-203.
8. Colotti V., "Mechanical Shear Strength Model for Reinforced Concrete Beams Strengthened with FRP materials". Construction and Buildings Materials, 124, 2016, 855-865.
9. Dias D. P., Thaumaturgo C., "Fracture toughness of geopolymeric concretes reinforced with basalt fibers". Cement & Concrete Composites, 27, 2005, 49‑54.
10. Elgabbas F., Vincent P., Ahmed E. A. and Benmokrane B., "Experimental Testing of Basalt Fiber Reinforced Polymer bars in concrete beams". Composites part B, 91, 2016, 205-218.
11. Fiore V., Scalici T, Bella G. Di, Valenza A., "A review on basalt fiber and its composites". Composites Part B, 74, 2015, 74-94.

12. Gao Ma, Hui Li, “Experimental Study of the Seismic Behavior of predamaged reinforced concrete columns retrofitted with basalt fiber reinforced polymer”. ASCE-Journal of Composites for Construction, Vol. 7, No. 10, 2017, 195-203.
13. Garmendia L., San-José J.T., García D., Larrinaga P., “Rehabilitation of masonry arches with compatible advanced composite material”. Construction and Building Materials, 25, 2011, 4374–4385.
14. Hadi M.N.S., “Retrofitting of shear failed reinforced concrete beams”. Composite Structures, 62, 2003, 1-6.
15. High C., Hatem M. Seliem, El-Safty A. and Rizkalla S. H., “Use of basalt fibers for concrete structures”. Construction and Building Materials, 96, 2015, 37–46.
16. Http://www.compositesworld.com/articles/basalt-fibers-alternative-to-glass.
17. Http://theconstructor.org/wp-content/uploads/2010/10/Steel-Fiber-Reinforced-Concrete.
18. Http://www.bautech.eu/images/stories/oferta/produkty/wlokno-polimerowe-d.jpg.
19. Http://textilelearner.blogspot.in/2011/08/glass-fiber-types-of-glass-fiber_3834.html.
20. Http://www.singaporechaircane.com/images/natural-fiber-materials2.jpg.
21. Http://www.compositestoday.com/wp-content/uploads/2014/07/carbon-fibre.jpg.
22. Http://basalt.today/images/Basalt_fiber_reinforcement_concrete-basalttoday.jpg
23. Islam M. R., Mansur M. A. and Maalej M., “Shear Strengthening of RC deep beams using externally bonded FRP systems”. Cement and Concrete Composites, 27, 2005, 413-420.
24. Indian Standard: 456:2000 – Indian Standard Plain and Reinforced Concrete- Code of Practice.
25. Indian Road Congress: 44-2008 – Guidelines for Cement Concrete Mix Designs for Pavements with fibers.
26. Indian Road Congress: SP:76:2008- Guidelines for Ultra-Thin White Topping with fibers.
27. Jiang C., Fan K., Wu F., Chen D., “Experimental study on the mechanical properties and microstructure of chopped basalt fiber reinforced concrete”. Materials and Design, 58, 2014, 187–193.

28. Khalifa A., William J. Gold, Nanni A. and Abdel Aziz M.I., “Contribution of Externally Bonded FRP to Shear Capacity of Flexural Members”. ASCE- Journal of Composites for Construction, Vol. 2, No. 4, 1998, 195-203.
29. Lapko A., Urbanski M., “Experimental and theoretical analysis of deflections of concrete beams reinforced with basalt rebar”. Archives of Civil and Mechanical Engineering, 15, 2015, 223-230.
30. Larbi A. S., Agbossou A. and Hamelin P., “Experimental and numerical investigations about textile reinforced concrete and hybrid solutions for repairing and/or strengthening reinforced concrete beams”. Composite Structures, 99, 2013, 152-162.
31. Larrinaga P., Chastre C., Hugo C. Biscaia, San-José J. T., “Experimental and numerical modeling of basalt textile reinforced mortar behavior under uniaxial tensile stress”. Materials and Design, 55, 2014, 66–74.
32. Liang W. H. and Zhong Y. H., “Research status and proposals of Basalt Fiber Reinforced Concrete”. Advanced Materials Research,43, 2013, 55–64.
33. Li W. and Leung C. K.Y., “Effect of shear span-depth ratio on mechanical performance of RC beams strengthened in shear with U-wrapping FRP strips”. Composite Structures, 2017.
34. Liu D., Huang H., Yue Q., Xue Y. and Wang M., “Behaviour of tunnel lining strengthened by textile-reinforced concrete”. Construction and Building Materials, 100, 2015, 118–124.
35. Lorenzis D., Stafford L. T. J. and Hollway L.C., “Strengthening and rehabilitation of civil infrastructures using fiber reinforced polymer composites”. Construction and Building Materials, 75, 2013, 196-208.
36. Lu Z., Xian G., Hui Li, “Effects of elevated temperatures on the mechanical properties of basalt fibers and BFRP plates”. Construction and Building Materials,56, 2015, 154-160.
37. Majumdar A. J., “Fiber concrete materials”. Constructions,02, 1977, 15-24.
38. Monti G. and Liotta M. A., “Tests and Design Equations for FRP strengthening in shear”. Construction and Buildings Materials, 21, 2007, 799-809.
39. Mosallam A. S. and Banerjee S, “Shear enhancement of reinforced concrete beams strengthened with FRP composites laminates”. Composites Part B Engineering, 38, 2007, 781-793.

40. Mostofinejad D. and Shameli S. M, “Externally bonded reinforcement in grooves (EBRIG) technique to postpone debonding of FRP sheets in strengthened concrete beams”. Construction and Buildings Materials, 38, 2013, 751-758.
41. Pellegrino C. and Modena C., “Fiber Reinforced Polymer Shear Strengthening of Reinforced Concrete Beams: Experimental Study and Analytical Modeling”. ACI Structural Journal, Vol. 2, No. 5, 2007, 201-213.
42. Padanattil, Akhila, Karingamanna J. and Mini K. M, “Novel hybrid composites based on glass and sisal fiber for retrofitting of reinforced concrete structures”. Construction and Building Materials, 2017.
43. Parameswaran, V.S., "Fibre-reinforced concrete: a versatile construction material". Building and Environment, 1991.
44. Raftery G. M., Kelly F., “Basalt FRP rods for reinforcement and repair of timber”. Composites: Part B, 70, 2015, 9–19.
45. Shafiq N., Ayub T. and Khan S. U., “Investigating the performance of PVA and basalt fiber reinforced beams subjected to flexural action”. Composite Structures, 153, 2016, 30-41.
46. Sharaky I.A., Torres L. and Sallam H.E.M., “Experimental and analytical investigation into the flexure performance of the RC beams with partially and fully bonded NSM FRP bars/strips. Construction and Building Materials, 29, 2013, 4374–4385.
47. Shen D., Shi H., Yong Ji and Yin F., “Strain rate effect on effective bond length of basalt FRP sheet bonded to concrete”. Construction and Building Materials, 82, 2015, 206-218.
48. Shen D., Yang q., Jiao Y., Cui Z. and Zhang J., “Experimental investigations on RC specimens strengthened with basalt fiber reinforced polymer under cyclic loads”. Construction and Building Materials, 136, 2017, 217-229.
49. Shi J., Wang X., Wua Z., Zhu Z., “Creep behavior enhancement of a basalt fiber-reinforced polymer tendon”. Construction and Building Materials, 94, 2015, 750–757.
50. Sim J., Park C., Moon D. Y., “Characteristics of basalt fiber as a strengthening material for concrete structures”. Composites: Part B, 36, 2005, 504–512.
51. Sobuz H. R., “Use of carbon fiber laminates for strengthening reinforced concrete beams in bending”. International Journal of Civil and Structural Engineering Vol.2, No.1, 2011, 67-84.

52. Teng J. G. and Chen J. F., “Debonding Failures of RC Beams Strengthened with Externally Bonded FRP Reinforcement: Behavior and Modeling”. Asia-Pacific Conference on FRP in Structures, 2007.
53. Thorhallsson E. R., Hinriksson G. I., Snæbjornsson J. T., “Strength and stiffness of glulam beams reinforced with glass and basalt fibers”. Composites Part B, 2016, 1-8.
54. Wang X., Wanga Z., Wua Z., Cheng F., “Shear behavior of basalt fiber reinforced polymer (FRP) and hybrid FRP rods as shear resistance members”. Construction and Building Materials 73, 2014, 781–789.
55. Wei B., Cao H., Song S., “Tensile behavior contrast of basalt and glass fibers after chemical treatment”. Materials and Design 31, 2010, 4244–4250.
56. Yazdanbakhsh A. and Bank L. C., “The effect of shear strength on load capacity of FRP strengthened beams with recycled concrete aggregate”. Construction and Building Materials 102, 2016, 133-140.
57. Ye L. P., Lu X. Z. and Chen J. F., “Design Proposals for the Debonding Strengths of FRP Strengthened RC Beams in the Chinese Design Code”. Proceedings of International Symposium on Bond Behavior of FRP in Structures, 2005.
58. Yilmaz and Deniz N., “Agro-Residual fibers as potential reinforcement elements for biochemists”. Lignocellulosic Polymer Composites, 2014.
59. Z. Qu, X. Z. Lu, and L. P. Ye, “Size Effect of Shear Contribution of Externally Bonded FRP U-Jackets for RC Beams”. Proceedings of International Symposium on Bond Behavior of FRP in Structures, 2005.